

# DISCUSSION PAPER SERIES

DP15109  
(v. 5)

## **Modeling and Forecasting Macroeconomic Downside Risk**

Davide Delle Monache, Andrea De Polis and Ivan  
Petrella

**MONETARY ECONOMICS AND FLUCTUATIONS**

**CEPR**

# Modeling and Forecasting Macroeconomic Downside Risk

*Davide Delle Monache, Andrea De Polis and Ivan Petrella*

Discussion Paper DP15109  
First Published 30 July 2020  
This Revision 17 February 2022

Centre for Economic Policy Research  
33 Great Sutton Street, London EC1V 0DX, UK  
Tel: +44 (0)20 7183 8801  
[www.cepr.org](http://www.cepr.org)

This Discussion Paper is issued under the auspices of the Centre's research programmes:

- Monetary Economics and Fluctuations

Any opinions expressed here are those of the author(s) and not those of the Centre for Economic Policy Research. Research disseminated by CEPR may include views on policy, but the Centre itself takes no institutional policy positions.

The Centre for Economic Policy Research was established in 1983 as an educational charity, to promote independent analysis and public discussion of open economies and the relations among them. It is pluralist and non-partisan, bringing economic research to bear on the analysis of medium- and long-run policy questions.

These Discussion Papers often represent preliminary or incomplete work, circulated to encourage discussion and comment. Citation and use of such a paper should take account of its provisional character.

Copyright: Davide Delle Monache, Andrea De Polis and Ivan Petrella

# Modeling and Forecasting Macroeconomic Downside Risk

## Abstract

We model permanent and transitory changes of the predictive density of US GDP growth. A substantial increase in downside risk to US economic growth emerges over the last 30 years, associated with the long-run growth slowdown started in the early 2000s. Conditional skewness moves procyclically, implying negatively skewed predictive densities ahead and during recessions, often anticipated by deteriorating financial conditions. Conversely, positively skewed distributions characterize expansions. The modelling framework ensures robustness to tail events, allows for both dense or sparse predictor designs, and delivers competitive out-of-sample (point, density and tail) forecasts, improving upon standard benchmarks.

JEL Classification: E32, E44, C53

Keywords: Business cycle, Downside risk, Skewness, score driven models, financial conditions

Davide Delle Monache - [davide.dellemonache@bancaditalia.it](mailto:davide.dellemonache@bancaditalia.it)  
*Bank of Italy*

Andrea De Polis - [andrea.depolis.17@mail.wbs.ac.uk](mailto:andrea.depolis.17@mail.wbs.ac.uk)  
*University of Warwick*

Ivan Petrella - [ivan.petrella@wbs.ac.uk](mailto:ivan.petrella@wbs.ac.uk)  
*University of Warwick and CEPR*

## Acknowledgements

We thank Jesús Fernández-Villaverde for the thoughtful discussion and Domenico Giannone and Elmar Mertens for extensive comments on an earlier draft of the paper. We also thank Anastasia Allayioti, Daniele Bianchi, Scott Brave, Christian Brownlees, Andrew Butters, Andrea Carriero, Todd Clark, Gabriele Fiorentini, Ana Galvao, Martin Iseringhausen, Francesco Saverio Gaudio, Gary Koop, Francesca Loria, Andre' Lucas, Massimiliano Marcellino, Leonardo Melosi, James Mitchell, Mikkel Plagborg-Moller, Francesco Ravazzolo, Bernd Schwaab, Andreas Tryphonides, Fabrizio Venditti, Giorgio Vocalelli, Mark Watson and the participants at the Conference on Score-Driven and Nonlinear Time Series Models at University of Cambridge, the workshop "Vulnerable Growth in the Euro Area" at European Central Bank, the CFE-CMStatistics 2019 conference, the Conference on Real-Time Data Analysis, Methods, and Applications at the Philadelphia FED, the 2021 NBER NSF Seminar on Bayesian Inference in Econometrics and Statistics, and the participants of other workshops, conferences and seminars where the paper was presented for valuable feedback and suggestions. We are grateful to the Chicago FED for making the full panel of weighted contribution of the financial indicators available for this work. The views expressed in this manuscript are those of the authors and do not necessarily reflect the views of the Bank of Italy. Any errors and omissions are the sole responsibility of the authors.

# MODELING AND FORECASTING MACROECONOMIC DOWNSIDE RISK\*

Davide Delle Monache<sup>†</sup>      Andrea De Polis<sup>‡</sup>      Ivan Petrella<sup>§</sup>

This draft: February, 2022

## Abstract

We model permanent and transitory changes of the predictive density of US GDP growth. A substantial increase in downside risk to US economic growth emerges over the last 30 years, associated with the long-run growth slowdown started in the early 2000s. Conditional skewness moves procyclically, implying negatively skewed predictive densities ahead and during recessions, often anticipated by deteriorating financial conditions. Conversely, positively skewed distributions characterize expansions. The modelling framework ensures robustness to tail events, allows for both dense or sparse predictor designs, and delivers competitive out-of-sample (point, density and tail) forecasts, improving upon standard benchmarks.

**Keywords:** Business cycle, downside risk, skewness, score driven models, financial conditions.

**JEL codes:** C53, E32, E44

---

\*We thank Jesús Fernández-Villaverde for the thoughtful discussion and Domenico Giannone and Elmar Mertens for extensive comments on an earlier draft of the paper. We also thank Anastasia Allayioti, Daniele Bianchi, Scott Brave, Christian Brownlees, Andrew Butters, Andrea Carriero, Todd Clark, Gabriele Fiorentini, Ana Galvao, Martin Iseringhausen, Francesco Saverio Gaudio, Gary Koop, Francesca Loria, André Lucas, Massimiliano Marcellino, Leonardo Melosi, James Mitchell, Mikkel Plagborg-Møller, Francesco Ravazzolo, Bernd Schwaab, Andreas Tryphonides, Fabrizio Venditti, Giorgio Vocalelli, Mark Watson and the participants at the Conference on Score-Driven and Nonlinear Time Series Models at University of Cambridge, the workshop “Vulnerable Growth in the Euro Area” at European Central Bank, the CFE-CMStatistics 2019 conference, the Conference on Real-Time Data Analysis, Methods, and Applications at the Philadelphia FED, the 2021 NBER NSF Seminar on Bayesian Inference in Econometrics and Statistics, and the participants of other workshops, conferences and seminars where the paper was presented for valuable feedback and suggestions. We are grateful to the Chicago FED for making the full panel of weighted contribution of the financial indicators available for this work. The views expressed in this manuscript are those of the authors and do not necessarily reflect the views of the Bank of Italy. Any errors and omissions are the sole responsibility of the authors.

<sup>†</sup>Bank of Italy. [davide.dellemonache@bancaditalia.it](mailto:davide.dellemonache@bancaditalia.it)

<sup>‡</sup>University of Warwick. [andrea.depolis.17@mail.wbs.ac.uk](mailto:andrea.depolis.17@mail.wbs.ac.uk)

<sup>§</sup>University of Warwick & CEPR. [ivan.petrella@wbs.ac.uk](mailto:ivan.petrella@wbs.ac.uk)

# 1 Introduction

The Global Financial Crisis and the subsequent recession left policymakers with several new challenges. In a world of persistently sluggish growth, subject to infrequent but deep recessions, the idea of central bankers as ‘risk managers’ gained renewed popularity (see, e.g., [Cecchetti, 2008](#)). In this environment, policy makers pursuing a ‘*plan for the worst, hope for the best*’ approach, rely on downside risk measures to assess the distribution of risk around modal forecasts. Recently, the sharp contraction, and the subsequent recovery in 2020 provided a sound reminder of the importance of accounting for tail events when assessing macroeconomic risk. Yet, assessing the degree of asymmetry of business cycle fluctuations remains a challenging task, and even more so it is to reliably gauge the time variation of downside risk. In addition, sound economic policy should consider the evolution of secular macroeconomic trends in pursuing the long-run goals of price stability and sustainable economic growth. Failure to account for permanent shifts in the properties of GDP growth can, in turn, lead to ineffective policy (see, e.g., [Edge et al., 2007](#)). In this paper, we introduce a generalised, comprehensive framework fit to provide policy guidance on the developments of downside risks, tracking permanent and transitory changes in the conditional distribution of GDP growth.

We provide novel evidence in support of time-varying *conditional* asymmetry of GDP growth’s distribution. Despite *unconditional* asymmetry remains unsupported by the data, conditional skewness, and thus downside risk to economic growth, exhibits significant variation over time. Motivated by this evidence, we introduce a novel, flexible methodology that allows us to track and predict time-varying skewed Student-*t* (*Skew-t*) conditional densities. The time variation of the location, scale and asymmetry parameters is driven by the score of the predictive likelihood function ([Creal et al., 2013](#); [Harvey, 2013](#)), as well as by a set of observed predictors. The latter allow us to explore to what extent downside risk to economic growth reflects imbalances arising in financial markets ([Giglio et al., 2016](#); [Adrian et al., 2019](#)).

Our framework accommodates permanent and transitory components in the moments of GDP growth predictive densities. This allows us to provide novel evidence on the evolution of downside macroeconomic risk. Over the last 30 years, skewness has decreased steadily, implying a higher exposure to downside risk, which partially accounts for the slowdown in long-run growth observed since the early 2000s (see, e.g., [Antolin-Diaz et al., 2017](#)). In a similar fashion, we document that the fall in macroeconomic volatility since the mid-1980s, the so called Great Moderation ([McConnell and Perez-Quiros, 2000](#); [Stock and Watson, 2002](#)), reflects a significant reduction of upside volatility, with downside volatility remaining stable over the same period. Over the short-term, conditional skewness varies procyclically around a declining trend-skewness, so that at the onset of downturns, business cycle swings exhibit significant negative skewness, while expansions are characterized by positively skewed distributions. Therefore, the well-documented counter-cyclicity of GDP growth’s volatility (see [Jurado et al., 2015](#), among others) largely reflects increasing downside volatility during recessions.

Within our framework, the extreme realizations of the pandemic quarters are captured through move-

ments in volatility and skewness, allowing the model to remain remarkably stable, and suggesting that such outcomes were, to some extent, tail events. When assessed based on its out-of-sample performance, our model delivers well calibrated predictive densities, improving upon competitive benchmarks in terms of point, density and tail forecasts, as well as leading to timely predictions of the odds of forthcoming recessions.

Several measures of financial distress have been identified as relevant indicators for predicting economic downturns.<sup>1</sup> We show that the four subcomponents of the National Financial Condition Index (NFCI, [Brave and Butters, 2012](#)), capturing risk, credit, leverage and nonfinancial leverage developments, help predicting different features of the distribution of GDP growth. The slow building up of leverage emerges as a key determinant of the scale of distribution, whereas skewness relates to all the subindices. We document that financial deepening during the expansionary phase of the cycle is associated with positive GDP growth's skewness, whereas tightening of financial conditions, especially the build-up of household debt, consistently predicts downside risk episodes. Similarly, financial conditions significantly improve the out-of-sample forecasting accuracy of our model, in particular during recessions.

Although aggregate measures succeed in summarizing a large amount of data, concerns that information relevant for assessing risk can remain undetected persist (see, e.g., [Galvão and Owyang, 2018](#); [Carriero et al., 2020b](#)). We address this question by investigating whether different patterns of sparsity can arise in predicting different features of the conditional distribution of GDP growth. To this end, we follow the ‘*shrink-then-sparsify*’ approach of [Hahn and Carvalho \(2015\)](#), where sparsity is achieved by means of the *Signal Adaptive Variable Selector* (SAVS) of [Ray and Bhattacharya \(2018\)](#).<sup>2</sup> Indicators pertaining to the build up of leverage of financial institutions and households, as well as credit conditions, receive the least shrinkage over the full sample. During the latest financial crisis, the model selects indicators relating to developments in the shadow banking sector, credit spreads and mortgage-backed securities issuance. This highlights that information in the balance sheet of the intermediary sector ([Adrian and Shin, 2008](#)), and the growing imbalances in the housing market (see, e.g., [Gertler and Gilchrist, 2018](#)) provided considerable information about rising vulnerabilities in the economy, and thus about increasing downside risks ahead and during the financial crisis. We find that processing the signal from a large panel of financial predictors leads to substantial improvements in short-term predictions, and especially during the most recent pandemic quarters.

Our results highlight the importance of accounting for asymmetric business cycle fluctuations. These can emerge through nonlinearities in the transmission of Gaussian shocks (see, e.g., [Fernández-Villaverde and Guerrón-Quintana, 2020a](#)), or alternatively reflect conditionally skewed shocks hitting the economy (as in [Bekaert and Engstrom, 2017](#); [Salgado et al., 2019](#)). The procyclical skewness we document is found to be

---

<sup>1</sup>Among others, traditional spread measures (see, e.g., [Rudebusch and Williams, 2009](#)), credit and leverage growth ([Drehmann et al., 2010](#); [Jordà et al., 2013](#)), as well as the leverage position of financial intermediaries ([Adrian and Shin, 2008](#)) received particular attention.

<sup>2</sup>[Giannone et al. \(2021\)](#) warn that sparsity can arise as an artefact of strong *a priori* beliefs. We approach sparsity within the purely data-driven framework which is robust to this concern, as also argued in [Huber et al. \(2021\)](#).

associated with a dynamic correlation between the first and second moments, being positive in expansions, and turning negative in recessions. This further reinforces the necessity of distinguishing between “good” and “bad” uncertainty, which can potentially impact economic activity in opposite directions (Segal et al., 2015). Our findings also emphasise the need to account for the nonlinear relationship between financial conditions and credit availability, and the distribution of GDP growth (see, e.g., Fernández-Villaverde et al., 2019) for policy monitoring and stabilization policy design (Gadea Rivas et al., 2020). Lastly, the fall in trend-skewness of economic fluctuations and the associated increase of downside risk over the last three decades emerges as a salient feature of the data which needs to be accounted for by theoretical macroeconomic models (see, e.g., Jensen et al., 2020).

**Related literature:** This paper builds on the growing literature exploring the asymmetry characterizing business cycle fluctuations, and the relationship between real economic activity and financial conditions. Giglio et al. (2016) and Adrian et al. (2019) uncover a significant negative correlation between financial conditions and the lower quantiles of the conditional distribution of future economic growth by means of quantile regressions. We introduce a novel approach based on the modeling of the parameters of a *Skew-t* distribution. Our approach is based on a rich, yet parsimonious structure, and avoids the burdensome necessity to fit the estimated quantiles to a distribution. In particular, our model features persistence in the skewness of the distribution of GDP growth, in line with the term structure of the growth-at-risk displaying stronger asymmetry for the short- than for the medium-run (Adrian et al., 2022), and consistent with the pronounced skewness displayed by the Survey of Professional Forecasters’ short-term predictions (Ganics et al., 2020). Differently to other contributions (see, e.g., Plagborg-Møller et al., 2020), we model both permanent and transitory changes of the distribution of GDP growth. This is essential in order to recover well-known stylized facts, such as the Great Moderation period (McConnell and Perez-Quiros, 2000; Stock and Watson, 2002) and the fall in long-run GDP growth (Antolin-Diaz et al., 2017; Doz et al., 2020; Eo and Morley, 2022), as well as to uncover an increasingly negatively skewed business cycle in the last part of the sample.

A number of recent contributions have called into question the presence of asymmetry in business cycle fluctuations, and have suggested alternative ways of capturing time variation in downside risk (see, e.g., Carriero et al., 2020a). Our approach allows for, but does not impose, skewness in GDP growth. Yet, we document significant variation in the asymmetry of the conditional distribution of GDP growth, which is associated with substantial gains in out-of-sample forecasts and downside risk predictions over standard volatility models whose competitiveness has recently been highlighted by Brownlees and Souza (2021).

Existing models for conditional skewness rely on *ad hoc* law of motion for the time-varying parameters, and the asymmetry is updated as a function of higher-order powers of the residuals (Hansen, 1994; Harvey and Siddique, 1999). We, instead, rely on the score-driven framework put forward by Creal et al. (2013) and Harvey (2013), which has proven to be particularly suitable for accommodating parameters’ time variation

under different distributional assumptions (Koopman et al., 2016). Within our setting, parameters update according to (highly) nonlinear functions of past prediction errors, depending, among other, on the shape of the conditional distribution at the time of the update. Thus, not only the updating mechanism adapts to the local properties of the data, but it is also robust to the presence of extreme realizations, contrary to updates based on higher-order powers of the residuals. Within the score-driven setting, to the best of our knowledge, we are the first to rely on Bayesian estimation methods. This allows us to jointly tackle parameters' proliferation and incorporate estimation uncertainty when assessing the predictions of the model.

**Structure:** The remainder of the paper is organized as follows. [Section 2](#) provides evidence of time-varying business cycle asymmetry. [Section 3](#) presents the model, the estimation methodology and the forecasting procedure. [Section 4](#) illustrates the characteristics of the conditional distribution of GDP growth, and how these relate to financial predictors. [Section 5](#) reports the out-of-sample forecast and downside risk prediction evaluation. In [Section 6](#) we investigate the predictive ability of the large set of financial indicators. [Section 7](#) concludes.

## 2 Motivating evidence

Assessing the degree of skewness of GDP growth is notoriously challenging. When measured over the 1973-2020 (1973-2019) sample, we obtain a negative sample skewness of -2.58 (-0.42). Yet, due to the low precision of this estimate over the full sample, we cannot reject the null of symmetry using the [Bai and Ng \(2005\)](#) test. However, the absence of skewness in the unconditional distribution does not necessarily imply the conditional distribution being symmetric as well ([Carriero et al., 2020a](#)). The difficulty in obtaining significant skewness estimates can potentially reflect the dynamic nature of the asymmetry of economic fluctuations.<sup>3</sup>

[Harvey \(2013, Section 2.5\)](#) highlights that the Lagrange multiplier principle can be employed to construct appropriate test statistics for the time variation of parameters (see [Appendix A](#) for further details). Starting from the assumption that GDP growth follows an AR(2) process with *Skew-t* innovations, with a shape parameter pinning down the degree of asymmetry, we test for the time variation of this parameter considering both the case of constant volatility and the more realistic case of time-varying volatility. [Table 1](#) reports the statistics for the Portmanteau ( $Q$ ), Ljung-Box ( $Q^*$ ) and [Nyblom \(1989\)](#) ( $N$ ) tests. The null hypothesis of a constant shape parameter is strongly rejected, against the alternative of time variation. Moreover, the rejection of the Nyblom test, which under the alternative hypothesis assumes the parameter to follow a martingale process, suggests that the shape parameter is likely to be highly persistent.

---

<sup>3</sup>Using the [Bai and Ng \(2005\)](#) test over different rolling windows of 4 to 6 years, the test often rejects the null of symmetry, with periods of significant negative and positive skewness detected over the sample. See [Figure A.1](#) in [Appendix A](#), for a summary of these results.



**Table 1:** Score-based tests for time variation

|           | <i>time-varying location</i> |          |          | <i>time-varying location &amp; scale</i> |           |          |
|-----------|------------------------------|----------|----------|--|-----------|----------|
|           | $Q$                          | $Q^*$    | $N$      | $Q$                                      | $Q^*$     | $N$      |
| $Scale^2$ | 7.187***                     | 7.296*** | 0.979*** |  |           |          |
| $Shape$   | 8.497***                     | 8.626*** | 0.603**  | 22.608***                                | 22.951*** | 1.053*** |

*Note:*  $Q$  is the portmanteau test,  $Q^*$  is the Ljung-Box extension and  $N$  corresponds to the Nyblom test. The lag length for the Portmanteau and Ljung-Box tests are selected following Escanciano and Lobato (2009). The first two tests are distributed as a  $\chi^2$  distribution with 1 degree of freedom, and the Nyblom test statistics is instead distributed as a Cramer von-Mises distribution with 1 degree of freedom. \*  $p < 10\%$ , \*\*  $p < 5\%$ , \*\*\*  $p < 1\%$ .

Starting from this novel evidence, in the next Section we introduce a modeling framework that allows us to track the time-varying asymmetry in the conditional distribution of GDP growth.

### 3 A time-varying Skew-t model for GDP growth

Let  $y_t$  denote the annualized quarter-on-quarter GDP growth at time  $t$ . We assume its conditional distribution can be characterized by a *Skew-t* (Arellano-Valle et al., 2005; Gómez et al., 2007), with time-varying location  $\mu_t$ , scale  $\sigma_t$ , and shape  $\varrho_t$  parameters, and constant degrees of freedom  $\nu$ :

$$y_t = \mu_t + \varepsilon_t, \quad \varepsilon_t \sim Skt_\nu(0, \sigma_t, \varrho_t), \quad t = 1, \dots, T, \quad (1)$$

with  $\nu > 3$ ,  $\sigma_t > 0$ , and  $\varrho_t \in [-1, 1]$ . The shape parameter fully characterizes the asymmetry of the distribution, with  $\frac{1-\varrho_t}{1+\varrho_t}$  defining the ratio of the probability mass on the right, over the probability mass on the left of the mode,  $\mu_t$ . Therefore, positive (negative) values of  $\varrho_t$  imply negatively (positively) skewed distributions. The conditional log-likelihood function of the observation at time  $t$  is:

$$\ell_t = \log p(y_t | \theta, \mathcal{F}^{t-1}) = \log \mathcal{C}(\eta) - \frac{1}{2} \log \sigma_t^2 - \frac{1+\eta}{2\eta} \log \left[ 1 + \frac{\eta \varepsilon_t^2}{(1 - \text{sgn}(\varepsilon_t) \varrho_t)^2 \sigma_t^2} \right], \quad (2)$$

with  $\eta = \frac{1}{\nu}$  being the inverse of the degrees of freedom,  $\mathcal{C}(\eta) = \frac{\Gamma(\frac{1+\eta}{2\eta})}{\sqrt{\pi} \Gamma(\frac{1}{2\eta})}$ ,  $\Gamma(\cdot)$  is the Gamma function, and  $\text{sgn}(\cdot)$  is the sign function. The vector  $\theta$  collects all the static parameters of the model, and  $\mathcal{F}^{t-1}$  is the information set up to time  $t - 1$ . For  $\varrho_t = 0$  we have the symmetric Student-t distribution, for  $\eta \rightarrow 0$  we retrieve the epsilon-Skew-Gaussian distribution of Mudholkar and Hutson (2000), whereas the distribution collapses to a Gaussian density when both conditions hold.<sup>4</sup> Thus, we allow for, but do not impose, skewness in the conditional distribution of GDP growth.

We model the time-variation of the parameters within the score driven framework of Creal et al. (2013)

<sup>4</sup>As opposed to the *Skew-t* distribution of Azzalini and Capitanio (2003), the one of Gómez et al. (2007) retrieve an information matrix which is always non-singular, and can thus be inverted, provided that  $|\varrho_t| < 1$ .

and [Harvey \(2013\)](#). In order to ensure the scale  $\sigma_t$  to be positive and the shape  $\varrho_t$  to lie within the unit circle, we model  $\gamma_t = \log(\sigma_t)$  and  $\delta_t = \operatorname{arctanh}(\varrho_t)$ . Therefore, the vector of time-varying parameters is  $f_t = [\mu_t, \gamma_t, \delta_t]'$ , and the updating mechanism is given by the following process:<sup>5</sup>

$$f_{t+1} = A s_t + B f_t + C X_t, \quad t = 1, \dots, T, \quad (3)$$

where  $A$  collects the smoothing parameters adjusting the speed of the updating, driven by an appropriate function of the prediction error,  $s_t$ ,  $B$  contains autoregressive parameters governing the persistence of the updating, and  $C$  collects loadings on a potential set of covariates  $X_t$ . Specifically,  $s_t = \dot{\mathcal{S}}_t \dot{\nabla}_t$  is the scaled score, with  $\dot{\nabla}_t = \frac{\partial \ell_t}{\partial f_t} = J_t' \nabla_t$ , where  $\nabla_t = \left[ \frac{\partial \ell_t}{\partial \mu_t}, \frac{\partial \ell_t}{\partial \sigma_t^2}, \frac{\partial \ell_t}{\partial \varrho_t} \right]'$  is the gradient of the log-likelihood function with respect to the location, squared scale and shape parameter, and  $J_t$  is the Jacobian matrix associated to the nonlinear transformation of the time-varying parameters. Regarding the scaling matrix,  $\dot{\mathcal{S}}_t$ , we consider a smoothed version of the diagonal of the Information matrix:  $\dot{\mathcal{S}}_t = (1 - \chi) \dot{\mathcal{S}}_{t-1} + \chi (J_t' \operatorname{diag}(\mathcal{I}_t) J_t)^{-\frac{1}{2}}$ , where  $\mathcal{I}_t = \mathbb{E}[\nabla_t \nabla_t']$ , and the smoothing parameter  $0 < \chi < 1$  is estimated together with the static parameters  $\theta$ . As a consequence, each element of the score vector has (approximately) unit variance. Considering only the diagonal elements of the information matrix ensures that the update of each parameter is proportional to the respective gradient.<sup>6</sup> Smoothing the scaling matrix makes it less sensitive to a single observation, avoids possible instabilities when  $|\varrho_t| \rightarrow 1$ , and renders the filtering process more robust (see, e.g., [Creal et al., 2013](#)).

Hence, the direction and magnitude of the updating are dictated by the steepness and curvature of the likelihood function, to improve the local fit of the model. The resulting model (1)-(3) belongs to the class of observation-driven models, for which the trajectories of the time-varying parameters are perfectly predictable one-step-ahead, given past information, and the log-likelihood function is available in closed form ([Cox, 1981](#)). The following Proposition provides the closed form expressions for the gradient and the associated information matrix that are the key ingredients to compute the scaled score driving the parameter variation.

**Proposition 1.** *Given the model specification in [Equation \(1\)](#) and the likelihood in [Equation \(2\)](#), the elements of the gradient  $\nabla_t$ , with respect to location, squared scale and shape parameters, are:*

$$\nabla_{\mu,t} = \frac{1}{\sigma_t} w_t \zeta_t, \quad \nabla_{\sigma^2,t} = \frac{1}{2\sigma_t^2} (w_t \zeta_t^2 - 1), \quad \nabla_{\varrho,t} = -\frac{\operatorname{sgn}(\varepsilon_t)}{(1 - \operatorname{sgn}(\varepsilon_t) \varrho_t)} w_t \zeta_t^2, \quad (4)$$

where  $w_t = \frac{(1+\eta)}{(1 - \operatorname{sgn}(\varepsilon_t) \varrho_t)^2 + \eta \zeta_t^2}$  and  $\zeta_t = \frac{\varepsilon_t}{\sigma_t}$  denotes the standardized prediction error. The gradient vector

<sup>5</sup>In [Section 3.1](#) we allow the time-varying parameters to feature a permanent and a transitory component.

<sup>6</sup>Scaling the gradient by the diagonal of the information matrix ensures that negative (positive) prediction errors translate into negative (positive) updates of mode, skewness, and hence the mean, of the conditional distribution. This desirable property is not always guaranteed if one considers the full information matrix.

has zero mean,  $\mathbb{E}[\nabla_t] = 0$ , and the associated information matrix is:

$$\mathcal{I}_t = \mathbb{E}[\nabla_t \nabla_t'] = \begin{bmatrix} \frac{(1+\eta)}{\sigma_t^2(1-\varrho_t^2)(1+3\eta)} & 0 & -\frac{4\mathcal{C}(1+\eta)}{\sigma_t(1-\varrho_t^2)(1+3\eta)} \\ 0 & \frac{1}{2(1+3\eta)\sigma_t^4} & 0 \\ -\frac{4\mathcal{C}(1+\eta)}{\sigma_t(1-\varrho_t^2)(1+3\eta)} & 0 & \frac{3(1+\eta)}{(1-\varrho_t^2)(1+3\eta)} \end{bmatrix}. \quad (5)$$

Defining  $f_t = [\mu_t, \gamma_t, \delta_t]'$ , where  $\gamma_t = \log(\sigma_t)$  and  $\delta_t = \operatorname{arctanh}(\varrho_t)$ , the Jacobian matrix,  $J_t = \frac{\partial[\mu_t, \sigma_t^2, \varrho_t]}{\partial[\mu_t, \gamma_t, \delta_t]'}$ , is a diagonal matrix with elements  $[1, 2\sigma_t^2, 1 - \varrho_t^2]$ .

**Proof.** See [Appendix B](#). ■

**Proposition 1** highlights the central role of re-weighting the standardized prediction error (and its square values) for the updating of the time-varying parameters. Weights,  $w_t$ , penalize extreme standardized innovations depending on the thickness of the tails, as well as volatility and asymmetry estimated conditional on time  $t - 1$ . The top left panel of [Figure 1](#) displays the weights associated with the prediction error, for alternative model parametrizations. In a Gaussian setting (black line) weights are constant and equal to unity, implying no discounting. On the other hand, when the asymmetry parameter is zero (red line), the weights display the classic outlier-discounting typical of the Student-t distributions (see, e.g. [Delle Monache and Petrella, 2017](#)). When the distribution is positively (negatively) skewed, i.e., for  $\varrho_t < 0$  ( $\varrho_t > 0$ ), negative (positive) prediction errors are less likely in expectation, and as such command a larger update of the parameters. This asymmetric treatment of the signal of the prediction error is more pronounced as the skewness of the distribution grows larger (i.e.,  $|\varrho_t| \rightarrow 1$ ).

To illustrate how the information in the standardized prediction error translates into updates for the time-varying parameters, [Figure 1](#) plots the scaled scores for  $\chi = 1$  (i.e., no smoothing):

$$\begin{bmatrix} s_{\mu,t} \\ s_{\gamma,t} \\ s_{\delta,t} \end{bmatrix} = \begin{bmatrix} \sqrt{\frac{(1+3\eta)(1-\varrho_t^2)}{(1+\eta)}} w_t \zeta_t \\ \sqrt{\frac{(1+3\eta)}{2}} (w_t \zeta_t^2 - 1) \\ -\operatorname{sgn}(\varepsilon_t) \sqrt{\frac{(1+\operatorname{sgn}(\varepsilon_t)\varrho_t)(1+3\eta)}{3(1-\operatorname{sgn}(\varepsilon_t)\varrho_t)(1+\eta)}} w_t \zeta_t^2 \end{bmatrix}, \quad (6)$$

against the standardized innovations.<sup>7</sup> The location updates in the direction of the prediction error, and when the distribution is Gaussian the update is directly proportional to the prediction error as in traditional state-space models. The presence of heavy tails introduces an outlier discounting that gives rise to the typical S-shaped influence function (see, e.g. [Harvey and Luati, 2014](#)), which in our case adapts to the asymmetry of the conditional distribution. The shape updates in the opposite direction of the prediction error, such that for negative prediction errors (i.e.  $\zeta_t < 0$ ) the conditional distribution becomes more left skewed. On the contrary, updates of the scale do not depend on the sign of the innovations, but on their magnitude: the parameter increases for  $w_t \zeta_t^2 > 1$  and decreases otherwise. Notice that while the (scaled)

<sup>7</sup>[Figure 1](#) is akin to the news impact curves popularized by [Engle and Ng \(1993\)](#) in the context of GARCH models.

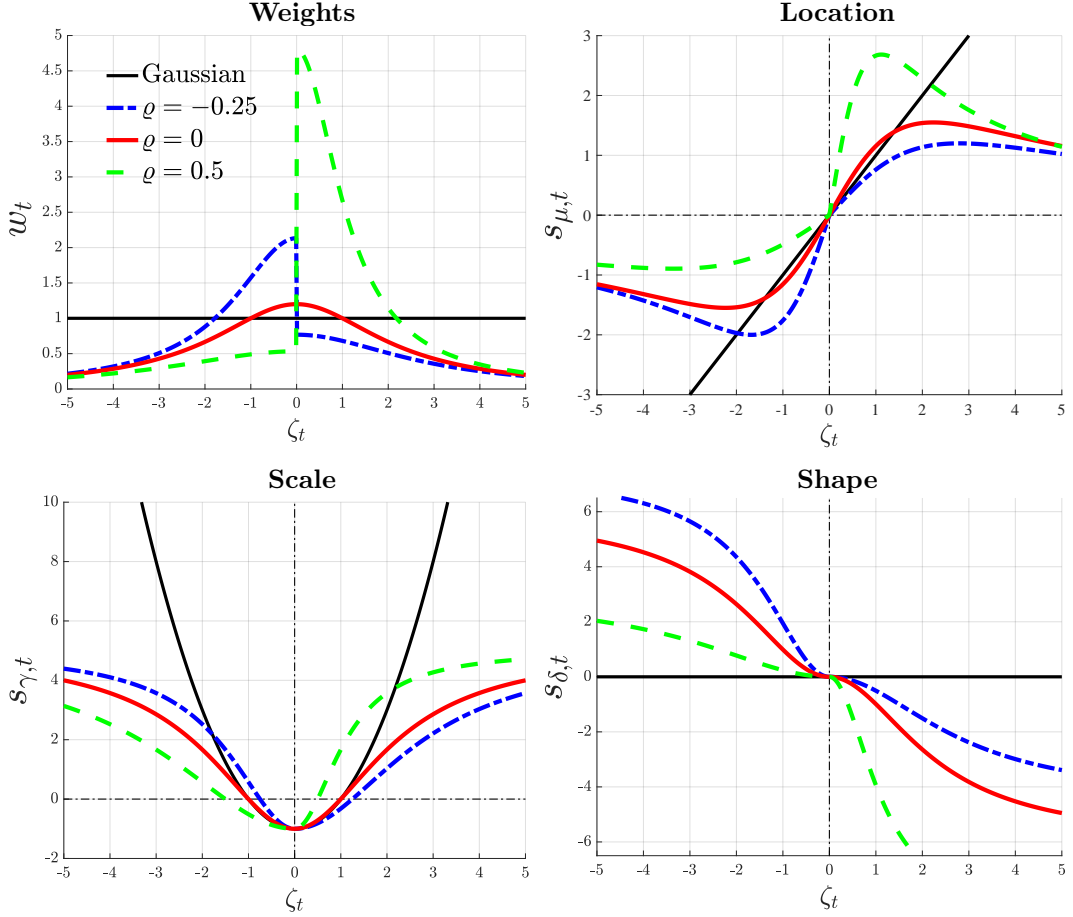


**Figure 1:** Prediction error and parameters' updating

*Note:* The figures plot the weighting scheme implied by  $w_t$ , and the scaled scores, for different values of the standardized prediction error  $\zeta_t = \frac{\varepsilon_t}{\sigma_t}$ . We consider three values of the asymmetry parameter: -0.5 (blue), 0 (red) and 0.7 (green). The Gaussian case is reported in black; for the Student- $t$  cases we set the degrees of freedom to 5.

scores for the location and shape parameters are negatively correlated ( $Corr(s_{\mu,t}, s_{\delta,t}) = -\frac{4C}{\sqrt{3}}$ ), updates of the scale are (unconditionally) uncorrelated with revisions of the other parameters, as suggested by the Information matrix in Equation (5). Yet, updates of the scale and shape parameters positively comove at the onset of recession: business cycle turning points are typically marked by large, negative prediction errors, such that the conditional distribution of GDP growth features negative shifts in the location, increasing dispersion and deepening negative skewness.

The updating mechanism associated with the score function in Equation (6) depends on the estimated parameters at time  $t$ , and thus varies over time. For a given prediction error, the magnitude of the updates is smaller when large errors are expected, i.e. when the conditional distribution features a large scale. Most importantly, the asymmetry of the distribution plays a key role in the translation of the standardized prediction error into a signal for the updates. When the distribution is left skewed (i.e.  $\rho_t > 0$ ) a positive (negative) prediction error leads to a more (less) pronounced update for the parameters, while the opposite is true in the case of a positively skew distribution. This property of the updating function is a direct consequence of the stark asymmetry in the weights. Hence, the model is faster to update the size and sign of the asymmetry of the distribution whenever there is evidence for a change of sign, like the occurrence

of a large, negative prediction error. In our application, this allows the model to promptly detect shifts in the skewness of GDP growth around business cycle turning points. In addition, the updating mechanism is robust to the presence of outliers. For extreme values of the (scaled) prediction errors, parameters' updates become inelastic to the standardized innovations (see [Appendix B.6](#)). As a consequence, our model remains well-behaved even in the face of extremely large realizations of the prediction error, as observed in the first quarters of 2020.

Existing models that account for time-varying conditional skewness and asymmetric  $t$  innovations are based on *ad hoc* updating mechanisms based on third-order powers of the prediction errors (see, e.g., [Hansen, 1994](#); [Harvey and Siddique, 1999](#)). This type of updating presents two main drawbacks. First, the implied mapping between prediction errors and time-varying parameters does not depend on current estimates of the conditional distribution and remains constant over time. For instance, this framework does not account for the higher probability of a negative prediction error when the conditional distribution of the data is negatively skewed. Instead, it updates the parameters regardless of the local properties of the distribution. Second, the introduction of higher-order powers of the innovations makes the time-varying parameters inherently sensitive to large prediction errors, thus becoming unstable in the presence of outliers. On the contrary, the score driven framework provides outlier robust and information theoretic optimal updates. In fact, [Blasques et al. \(2015\)](#) show that score-driven updates reduce the local Kullback-Leibler divergence between the true and the model-implied conditional density, even under severe misspecification.

### 3.1 Permanent and transitory variation of GDP growth's distribution

When modelling the conditional distribution of GDP growth, it is important to allow for both permanent and transitory movements of the central moments. Several papers have documented that, over the sample under analysis, GDP growth has experienced significant changes in the long run mean (see, e.g., [Antolin-Diaz et al., 2017](#); [Doz et al., 2020](#); [Eo and Morley, 2022](#)), as well as shifts in the volatility ([McConnell and Perez-Quiros, 2000](#); [Stock and Watson, 2002](#)), and skewness of the distribution ([Jensen et al., 2020](#)) since the late 1980s. At the same time, [Jurado et al. \(2015\)](#) show that the volatility of GDP growth is countercyclical, while [Giglio et al. \(2016\)](#) and [Adrian et al. \(2019\)](#) argue that the skewness of the cycle falls sharply during recessions. To account for these features, we postulate a two-component specification for the time-varying parameters, in the spirit of [Engle and Lee \(1999\)](#). We posit a random walk updating for the permanent components, where these are able to track both smooth variations and sudden breaks in the level of the parameters. Moreover, we allow a set of predictors,  $X_t$ , to have a transitory impact on the parameters of the distribution. Introducing a permanent and transitory decomposition of the time-varying parameters implies a linear transformation of the original parameters, hence leaving the scaled score unchanged.

The location parameter  $\mu_t$  is a linear combination of a permanent and transitory component:

$$\mu_{t+1} = \bar{\mu}_{t+1} + \tilde{\mu}_{t+1}, \quad (7)$$

$$\bar{\mu}_{t+1} = \bar{\mu}_t + \varsigma_\mu s_{\mu t}, \quad (8)$$

$$\tilde{\mu}_{t+1} = \phi_{\mu,1} \tilde{\mu}_t + \phi_{\mu,2} \tilde{\mu}_{t-1} + \beta'_\mu X_t + \kappa_\mu s_{\mu t}, \quad (9)$$

where the AR(2) specification for the transitory component is able to recover the characteristic hump shaped impulse response of the data (see, e.g. [Chauvet and Potter, 2013](#)). Following [Engle and Rangel \(2008\)](#), we assume a multiplicative specification for the scale parameter  $\sigma_t$ , therefore the log-scale  $\gamma_t = \log(\sigma_t)$  is modelled as

$$\gamma_{t+1} = \bar{\gamma}_{t+1} + \tilde{\gamma}_{t+1}, \quad (10)$$

$$\bar{\gamma}_{t+1} = \bar{\gamma}_t + \varsigma_\gamma s_{\gamma t}, \quad (11)$$

$$\tilde{\gamma}_{t+1} = \phi_\gamma \tilde{\gamma}_t + \beta'_\gamma X_t + \kappa_\gamma s_{\gamma t}. \quad (12)$$

Similarly, we posit an additive specification for the transformed shape parameter,  $\delta_t = \text{arctanh}(\varrho_t)$ :

$$\delta_{t+1} = \bar{\delta}_{t+1} + \tilde{\delta}_{t+1}, \quad (13)$$

$$\bar{\delta}_{t+1} = \bar{\delta}_t + \varsigma_\delta s_{\delta t}, \quad (14)$$

$$\tilde{\delta}_{t+1} = \phi_\delta \tilde{\delta}_t + \beta'_\delta X_t + \kappa_\delta s_{\delta t}. \quad (15)$$

Therefore, the resulting vector of time-varying parameters becomes  $f_t = (\bar{\mu}_t, \tilde{\mu}_t, \bar{\gamma}_t, \tilde{\gamma}_t, \bar{\delta}_t, \tilde{\delta}_t)'$  and its law of motion is described by a restricted specification of [Equation \(3\)](#), as we show in [Appendix B](#).

[Plagborg-Møller et al. \(2020\)](#) consider a time-varying *Skew-t* specification for GDP growth and specify the time-varying parameters (location, log-scale and shape) as linear functions of a set of predictors. In this case - which remains nested within our setting - the sole source of parameters' variation stems from the dynamics of the predictors. This modelling choice generates substantial variability in the underlying parameters, and thus uncertainty around the estimates. In contrast, our specification allows for both secular and transitory shifts in the parameters, where the autoregressive structure of the transitory components makes them functions of discounted values of all past predictors and scores (where these latter are themselves nonlinear functions of past data). Specifically,

$$\mu_{t+1} = \bar{\mu}_{t+1} + \sum_{j=0}^{t-1} \psi_{\mu,j} (\beta'_\mu X_{t-j} + \kappa_\mu s_{\mu t-j}), \quad (16)$$

$$\gamma_{t+1} = \bar{\gamma}_{t+1} + \sum_{j=0}^{t-1} \phi_\gamma^j (\beta'_\gamma X_{t-j} + \kappa_\gamma s_{\gamma t-j}), \quad (17)$$

$$\delta_{t+1} = \bar{\delta}_{t+1} + \sum_{j=0}^{t-1} \phi_{\delta}^j (\beta'_{\delta} X_{t-j} + \kappa_{\delta} s_{\delta t-j}), \quad (18)$$

where  $\psi_{\mu,j}$  is a convolution of the autoregressive parameters  $\phi_{\mu,1}$  and  $\phi_{\mu,2}$ , which decays to zero for  $j \rightarrow \infty$ , and the permanent components are proportional to the cumulative sum of past scores. As a result, the time-varying parameters we estimate are smoother and less affected by the noise in the data.<sup>8</sup>

## 3.2 Estimation

A feature of observation-driven models is the straightforward computation of the likelihood function (see, e.g., [Creal et al., 2013](#); [Harvey, 2013](#)). However, the optimization and computation of confidence intervals remain challenging, in particular when these models feature a rich parametrization. In this context, Bayesian estimators, which rely on Markov Chain Monte Carlo (MCMC) methods, represent a tractable and theoretically attractive alternative to the extremum-based estimation and inference.<sup>9</sup> In fact, under appropriate regularity conditions, asymptotic results guarantee that simulations from a Markov chain provide, after some burn-in period and sufficient iterations, samples from the posterior distribution of interest (for details, see [Smith and Roberts, 1993](#); [Besag et al., 1995](#)).<sup>10</sup> In addition, relying on MCMC provides a simple approach to compute any posterior summary of interest as a function of parameters, e.g. credible intervals for the time-varying moments of the distribution. Lastly, within a Bayesian setting we can easily incorporate parameter uncertainty when producing forecasts, which turns out to be critical for enhancing the reliability of the density forecasts, in particular if one focuses on downside risk predictions.

Taking a Bayesian perspective allows us to impose realistic priors on the static parameters,  $\pi(\theta)$ . Our choices encode the view that the transitory components of the time-varying parameters are smooth and stationary, while the permanent components capture slow-moving trends. We set Minnesota-type Normal priors for the AR coefficients ( $\phi$ ) of the transitory components, centered around high persistence values. For the location's AR parameters, we also introduce a prior on the sum of coefficients, in line with [Doan et al. \(1984\)](#). The prior distribution of the score loadings is inverse gamma, as we expect these parameters to be positive. Moreover, we expect the smoothing parameters of the transitory components ( $\kappa$ ) to be larger than those of the permanent components ( $\varsigma$ ), such that on impact the former react more to innovations with respect to the latter. This prior is reflected into a tighter scale for the inverse gamma prior of the smoothing coefficient of the permanent components.<sup>11</sup> We assume Normal priors for the loadings associated to the

<sup>8</sup>In addition, our framework allows for non-linearities through the (non-linear) mapping of the predictors into the scores, further down-weighting extreme fluctuations in the data. In [Appendix C](#) we highlight that these additional features turn out to be important to recover salient features of the distribution of GDP growth.

<sup>9</sup>See also [Vrontos et al. \(2000\)](#) for a discussion of the advantages of using a Bayesian approach in the estimation of observation driven models for time-varying volatility.

<sup>10</sup>Importantly, Bayesian estimators are not affected by local discontinuities, multiple local minima and flat areas of the likelihood, and they are often much easier to compute, particularly in the high-dimensional setting (see, e.g., [Tian et al., 2007](#); [Belloni and Chernozhukov, 2009](#)).

<sup>11</sup>Introducing priors for the smoothing coefficients effectively circumvents the ‘pile-up’ problem, which often arises where the variation of time-varying parameters is small (see, e.g., [Stock and Watson, 1998](#)). At the same time these

explanatory variables ( $\beta$ ). These coefficients are centered around zero, with tight scales in order to avoid overfitting of the parameters, in the fashion of  $L_2$  (Ridge) regularization. We assume an inverse gamma prior for  $\eta$ . Lastly, we also estimate the initial values of the permanent components assuming independent Gaussian priors centered around historical average values for the three parameters, and with reasonably small variance.

Draws from the posteriors are generated using an Adaptive Random-Walk Metropolis-Hastings (AR-WMH) algorithm (Haario et al., 1999), with the chain initialized at the Maximum likelihood estimates. For each draw  $\theta^j$ , using equations (1)-(5) we compute the time-varying parameters  $\{f_1, \dots, f_T|\theta^j\}$  and the log-likelihood  $\ell(y|\theta^j) = \sum_{t=1}^T \ell_t$ . We accept the current draw with probability  $p = \min\{1, \exp(\pi(\theta^j|y) - \pi(\theta'|y))\}$ , where  $\pi(\theta^j|y) \propto \pi(\theta^j)\ell(y|\theta^j)$  is the posterior distribution of  $\theta^j$ ; when accepted, we set  $\theta' = \theta^j$ . Credible sets for both static and time-varying parameters are obtained from the empirical distribution functions arising from the resampling. Appendix D provides an extensive description of the sampling algorithm, as well as the details on the exact prior specification for the parameters and convergence diagnostics.

**Monte Carlo exercise** Appendix E investigates the small sample properties of the model through a Monte Carlo analysis. The model successfully tracks parameters' time variation for a variety of different data generating processes. When the distribution is symmetric throughout the entire sample, the model quickly estimates a null shape parameter, with limited variability over time. In particular, the model does not confound any correlation between the time variation of the location and the scale (known to generate unconditional skewness) for the presence of conditional asymmetry. We also simulate a model with a one-time break in the shape parameter: the model correctly captures the break in the asymmetry, and the two-component specification properly disentangles long- and short-lived fluctuations, so that the break is tracked by the permanent component whereas the transitory component features low variability.

### 3.3 Forecasts

For any draw of the model parameters,  $\theta$ , the last step of the the observation driven filter in Equation (3) provides the optimal one-step-ahead prediction of the parameters of interest (Cox, 1981). These values can then be used to retrieve the one-step-ahead prediction density for GDP growth,  $p(y_{T+1}|\theta) = skt_\nu(f_{T+1}(\theta))$ , which allows us to draw the forecast of interest as  $p(y_{T+1}) = \int p(y_{T+1}|\theta)d\theta$ .

For multiple-steps forecasts additional complications arise from the necessity to sample the score, and the dependence of the forecasts on the predicted values of the conditioning variables. In Section 5, due to the high persistence of the predictors, we produce forecasts keeping these fixed to their last observations, akin to assuming a random walk specification for their law of motion.<sup>12</sup> As for the score vector, we follow Koopman et al. (2018) and adopt a “bootcasting” algorithm to sample multiple  $h - 1$  dimensional vectors

---

priors are quite conservative, implying that any evidence in favour of the time variation of permanent components reflects strong evidence in the data.

<sup>12</sup>As an alternative, one could feed predictions for the explanatory variables into the model. The latter approach produces results very similar to the ones reported here.



of scores from the (scaled) score vector obtained in the estimation, thus avoiding any assumption on the distribution of the score. Therefore, for a given (bootstrapped) draw of the score, and assuming  $X_{T+h} = X_T$ , the score filter (3) can be used to obtain  $f_{T+h}$ , and thus compute  $p(y_{T+h}|\theta, X_{T+h} = X_T)$ . The  $h$ -step ahead forecast reads  $p(y_{T+h}) = \int p(y_{T+h}|\theta, X_{T+h} = X_T)d\theta$ .

### 3.4 Data and alternative model specifications

We use US quarterly data over the period 1973Q1 to 2020Q4 on economic activity and financial conditions. For the latter we consider the broad NFCI and its four subindices, tracking developments in the credit, risk, leverage and non-financial leverage markets (Brave and Butters, 2012). We will consider alternative models with either the NFCI or the disaggregated components. While the risk and credit components closely track the dynamics of the NFCI, the leverage indicators, in particular the nonfinancial leverage, are often regarded as an “early warning” signal for economic downturns (Mian and Sufi, 2010).<sup>13</sup>

The modeling framework we propose can accommodate several features of the conditional distribution of economic growth. Specifically, our framework encompasses a wide spectrum of specifications: from a simpler Gaussian AR(2) with time-varying volatility, to the full-blown two-component specification outlined above. In Appendix G we report the Deviance Information Criterion (Spiegelhalter et al., 2002) and the log Marginal Likelihood for different model specifications. According to these measures: i) modelling non-Gaussian features improves upon a Normal benchmark, ii) allowing for an additional low-frequency variation in the parameters (two-component specification) better fits the data compared to a version of the model that only allows for transitory variation of the parameters (one-component specification), and iii) including financial variables improves the model fit. Therefore, we set as our baseline specification a Skew-t model with a permanent and transitory component for the time-varying parameters and with (two lags of) the four subcomponent of the NFCI as exogenous predictors (*Sk-t -4DFI*).

## 4 Time variation in the distribution of GDP growth

Our model allows us to study the characteristics of the conditional distribution of GDP growth. Figure 2 reports the time-varying first and second moments of the distribution of GDP growth. The mean moves along the business cycle and displays sharp contractions during recessions. Volatility features a marked countercyclical behaviour, with peaks occurring during recessions. Focusing on the last year of the sample, the model features a sharp increase in volatility and a quickly rebounding mean. Yet, these movements are not as sharp as the ones observed over the Great Recession, suggesting that through the lenses of the model Covid-quarters are, at least partially, characterized as tail events. On the same charts, we also report in red the low-frequency components. That is, the moments of the distribution that would prevail in the absence of any transitory variation of the parameters. The model neatly captures a fall in long-run growth, with

<sup>13</sup>See Appendix F for a detailed discussion on the data.

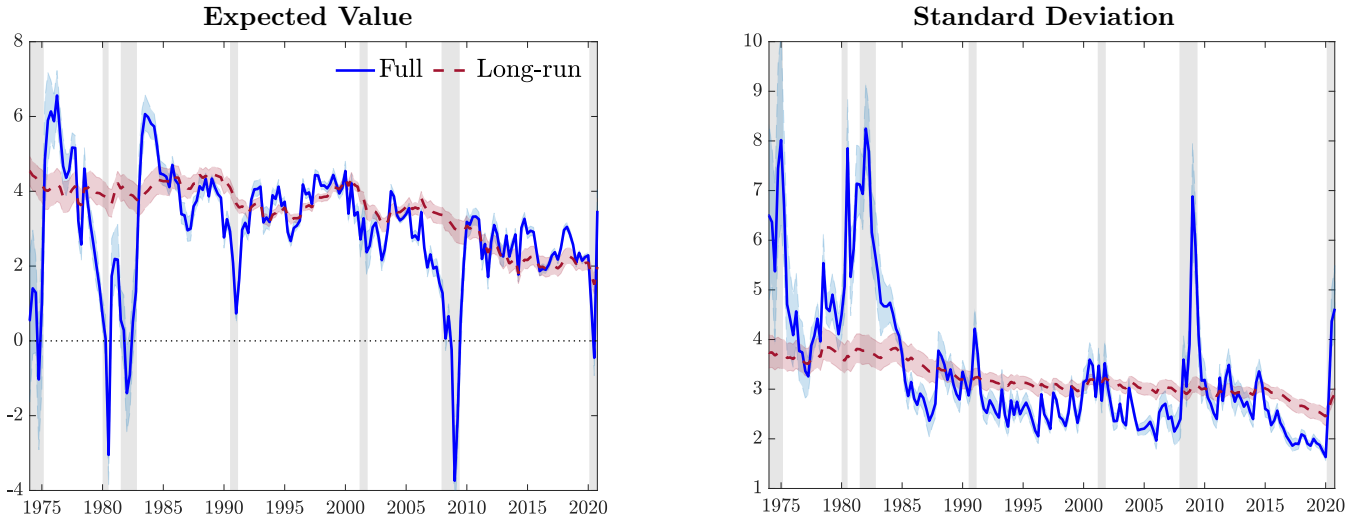


**Figure 2:** Time-varying mean and variance

*Note:* The plots illustrate the estimated time-varying mean and standard deviation (blue), along with the respective long-run components, in red, and 90% credible intervals. Shaded bands represent NBER recessions.

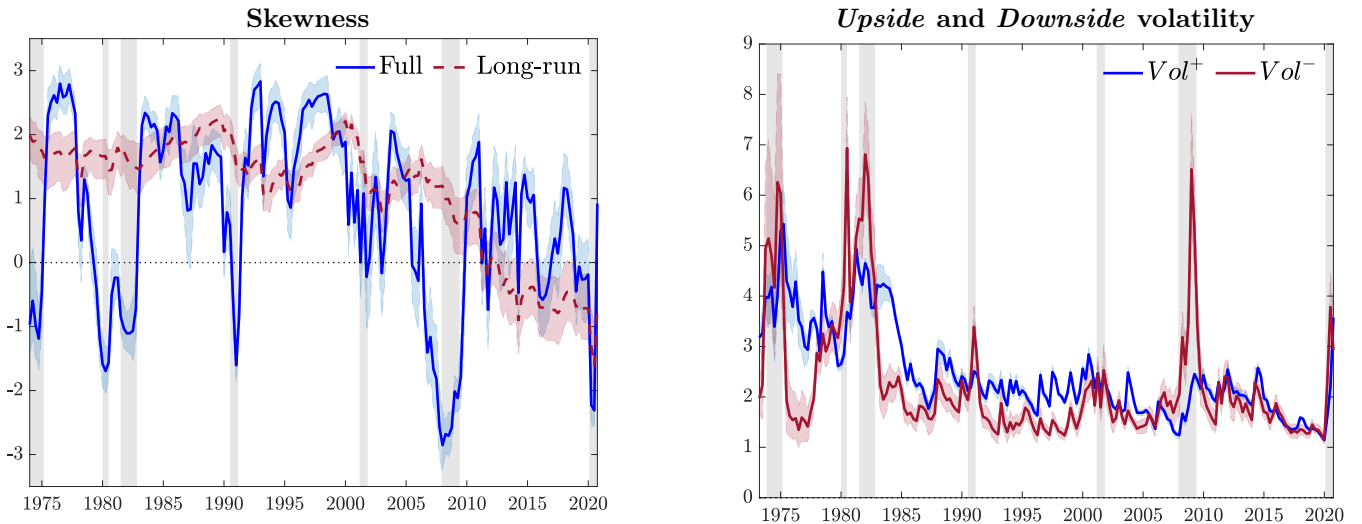


**Figure 3:** Time-varying asymmetry

*Note:* The left panel illustrates the estimated time-varying skewness (blue), along with its long-run component (red). The right panel reports the upside and downside volatilities, in blue and red, respectively. Shadings correspond to 90% credible intervals. Shaded bands represent NBER recessions.

the expected value falling from roughly 4% in the 1970s, to roughly 2.3% at the end of the sample, in line with the evidence in [Antolin-Diaz et al. \(2017\)](#).<sup>14</sup> The Great Moderation is reflected in a visible reduction in GDP growth's volatility: starting in the mid-1980s, transitory fluctuations in volatility dampen down as the impact of the consecutive recessions of the 1970s and 1980s fades away, and the long-run volatility is revised downward by roughly 30%.

Time-varying skewness is reported in the left panel of [Figure 3](#). This evolves in a distinctively procyclical pattern, such that substantially negative skewness characterizes recessions, whereas expansions are marked

<sup>14</sup>Similarly, [Doz et al. \(2020\)](#) and [Eo and Morley \(2022\)](#) document a downward trend in US economic growth starting in the early 2000s.

by positively skewed distributions. Interestingly, skewness tends to decrease in anticipation of recessions, a feature which we show to be related to the information contained in the financial indicators, suggesting that downside risk dominates ahead of, and during downturns. Over the long-run, skewness displays a downward trend starting in the late 1980s, and falling markedly in the post-2000 sample. As a result, business cycle fluctuations are characterized by decreasing, but positive, trend-skewness until the onset of the financial crisis in 2007. In the aftermath of the subsequent recession, this long-term trend turns to negative values, implying negatively skewed long-run conditional distributions. This signals the build-up of vulnerabilities, resulting in the economy being increasingly exposed to downside risk episodes.

**Upside and downside volatility** Arellano-Valle et al. (2005) highlight that the *Skew-t* distribution can be easily rewritten as a two-piece density by reweighting the scale by a function of the asymmetry parameter (see Appendix B). In line with the “good” and “bad” volatility decomposition proposed by Bekaert and Engstrom (2017), one can define “*upside*” ( $Vol^+ = \sqrt{\text{Var}(y_t|y_t \geq \mu_t)}$ ) and “*downside*” ( $Vol^- = \sqrt{\text{Var}(y_t|y_t < \mu_t)}$ ) volatility as:

$$Vol^+ = \frac{1 - \rho_t}{2} \sqrt{\text{Var}(y_t|\theta, \mathcal{F}^{t-1})}, \quad Vol^- = \frac{1 + \rho_t}{2} \sqrt{\text{Var}(y_t|\theta, \mathcal{F}^{t-1})}. \quad (19)$$

These two volatility components are reported in the right panel of Figure 3. Downside volatility spikes during recessions, whereas upside volatility displays only modest (pro-)cyclicality. Therefore, the marked countercyclicality of aggregate volatility (see, e.g., Jurado et al., 2015) is largely a reflection of countercyclical downside risk. Whereas the financial crisis of 2007-2008 appears as an episode of purely downside volatility, the more recent Covid-recession is characterized by a spike in downside volatility in the first half of 2020 quickly receding in favor of upside volatility in the second half. Over the long-run, upside volatility features a steep decline starting in the mid-1980s with small cyclical variations. On the other hand, downside volatility has remained stable at around the same values observed in the aftermath of mid-1970s recession, with sudden spikes occurring during recessions.

**Expected value and variance decomposition** The estimated model suggests that conditional skewness fluctuations are a prominent feature of the predictive distribution of GDP growth, playing an important role in determining the dynamics of the first and second moments.<sup>15</sup> To see that, it is worth noting that in our model:

$$\mathbb{E}[y_t|\theta, \mathcal{F}^{t-1}] = \mu_t - g(\eta)\sigma_t\rho_t, \quad g(\eta) = \frac{4\mathcal{C}(\eta)}{1 - \eta}, \quad (20)$$

$$\text{Var}(y_t|\theta, \mathcal{F}^{t-1}) = \sigma_t^2 \left( \frac{1}{1 - 2\eta} + h(\eta)\rho_t^2 \right), \quad h(\eta) = \frac{3}{1 - 2\eta} - g(\eta)^2. \quad (21)$$

<sup>15</sup>Although an expression for the skewness is not available in closed form, a Taylor expansion of the skewness function attributes almost all of the variation to movements of the shape parameter, while remaining relatively insensitive to location and scale.

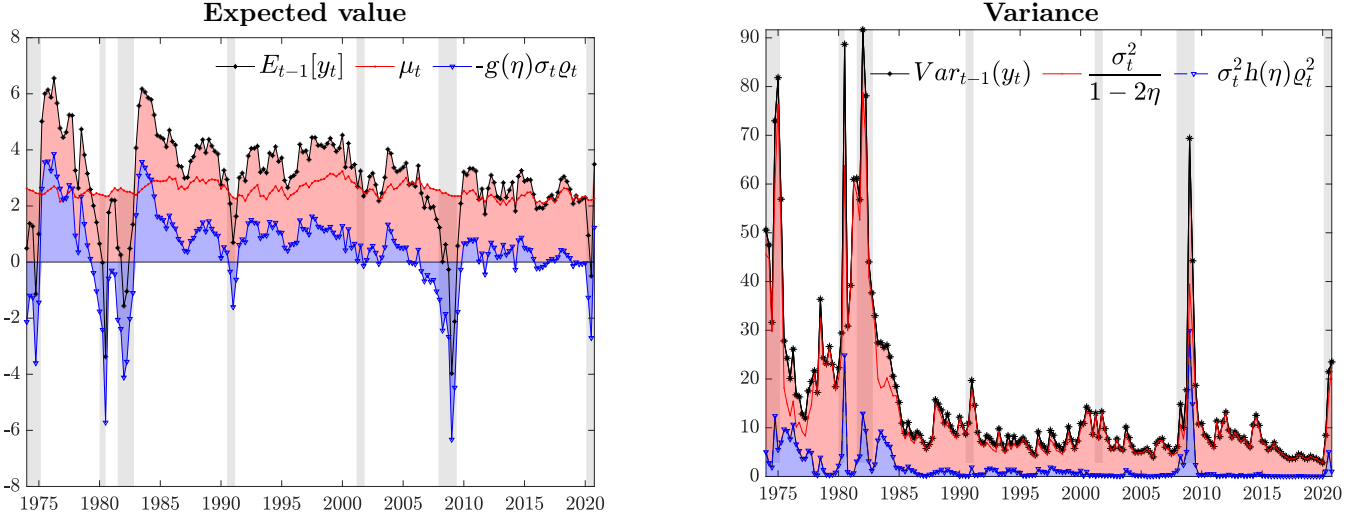


**Figure 4:** Expected value and variance decomposition

*Note:* The plot shows the decomposition of the expected value and variance of GDP growth. We report in red the contribution of the moment estimator (e.g. location and scale), whereas the blue area identifies the contribution of higher order moments. Central moments (black lines) are computed as in Equation (20)-(21). Shaded bands represent NBER recessions.

Thus, the (time-varying) expected value and variance are equal to the mean and variance of a standard Student-t distribution, plus a component which is a function of the shape parameter. The latter is magnified by larger values of  $\sigma_t$ , while it disappears from both moments when  $\varrho_t$  is equal to 0.

Figure 4 isolates the contribution of the asymmetry for both the first and second moments. The expected value decomposition highlights how the location parameter (red line) is remarkably stable over the sample, while most of the fluctuations reflect shifts in the shape of the distribution (blue line), with expansions characterized by positive skewness and contractions associated with negative skewness. Interestingly, the contribution of the asymmetry for positive expected values becomes more muted during the Great Moderation, whereas the negative drag from the asymmetry remains of substantial importance during recessions. In contrast, the effect of the shape parameter on the second moment is less pervasive, despite deepening skewness during recessions accounts for a non-trivial share of the increase in variance.

Equations (20) and (21) also highlight that procyclical variations of skewness are reflected into a time-varying correlation between the mean and the volatility of GDP growth. While the mean is always negatively affected by shifts of the shape parameter (i.e.  $\frac{\partial \mathbb{E}(y_t|\theta, \mathcal{F}^{t-1})}{\partial \varrho_t} < 0, \forall \varrho_t$ ), an increase of the latter is associated with an increase in the variance when the distribution is negatively skewed, and a decrease in the variance when the distribution is positively skewed, in that  $\frac{\partial \text{Var}(y_t|\theta, \mathcal{F}^{t-1})}{\partial \varrho_t} = 2h(\eta)\sigma_t^2\varrho_t$ . Since  $h(\eta) > 0$  for  $\nu > 3$ , changes of the asymmetry are associated with changes of the variance of the same sign as that of the shape parameter (and thus of opposite sign to that of conditional skewness). The procyclicality of skewness reduces volatility during expansions, whereas dispersion increases as skewness plummets to negative values. This is reflected into a procyclicality in the correlation between mean and variance, which is in line with findings in [Carriero et al. \(2020a\)](#). These nonlinearities in the interaction between uncertainty

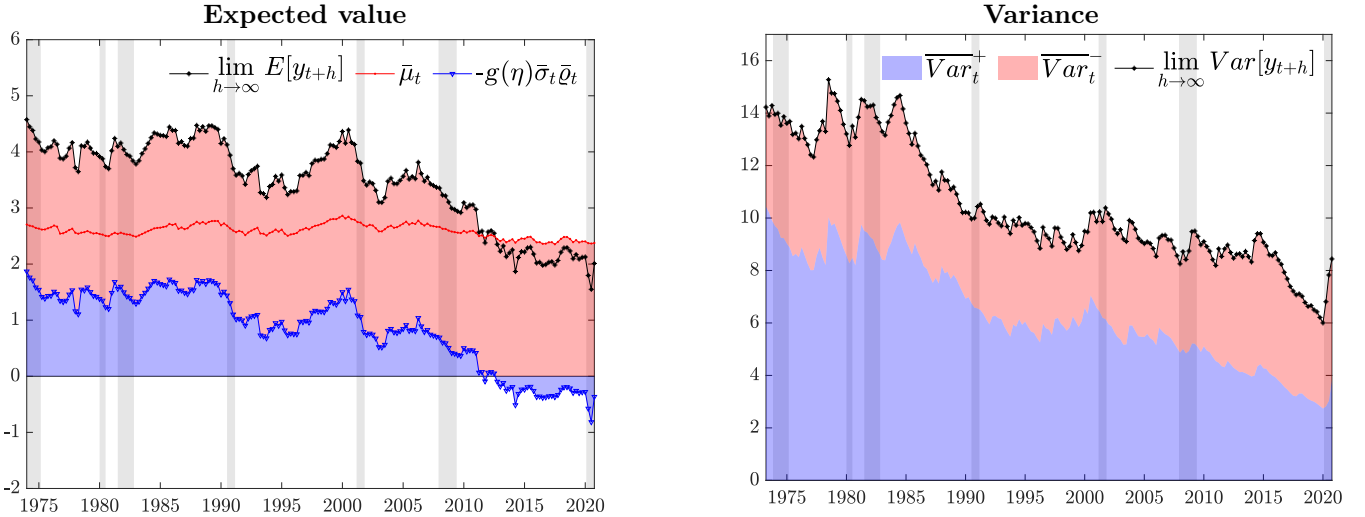


**Figure 5:** Long-run GDP growth and volatility

*Note:* The plot shows the decomposition of the long-run expected value (black lines), akin to taking  $\lim_{h \rightarrow \infty} \mathbb{E}[y_{t+h}]$ . We report in red the contribution of the long-run location component  $\bar{\mu}_t$ , whereas the blue area identifies the contribution of higher order moments.  $\bar{\sigma}_t$  and  $\bar{\varrho}_t$  refers to the secular components of scale and shape, respectively. Shaded bands represent NBER recessions.

and aggregate economic activity are consistent with findings in Segal et al. (2015), which highlight how “positive uncertainty” (i.e. volatility in the procyclical phases of the business cycle) tends to be associated with positive expected growth, whereas this correlation turns negative during contractions.<sup>16</sup>

**Accounting for the slowdown in long-run growth and the Great Moderation.** Making use of the expected value decomposition in Equation (20), we can assess to what extent shifts in long-run growth that we observe over the sample reflect a reassessment of (long-run) risk in GDP growth. Starting in the late 1980s, the distribution of GDP growth featured decreasing positive skewness. This increase in downside risk maps into a decline of the long-run growth, as shown in Figure 5, so that roughly two thirds of the slowdown reflect a reassessment of risk. The downward trend in long-run growth is temporarily reversed in correspondence of the IT productivity boom of the mid-1990s, when long-run growth is revised upward by roughly 0.5%. Interestingly, we find that this upward revision reflects, to a large extent, a shift in the risk of the upside, rather than the central tendency, of GDP growth’s distributions. Over the post-2000 sample, the slowdown in long-run growth accelerates, and it is associated with a rebalancing of risks towards the downside. In the aftermath of the Great Recession, the long-run component displays a pronounced left tail, thus becoming a negative drag to long-term growth.

Similarly, we decompose long-run variance into the contributions of long-run upside (blue) and downside (red) variance in the right panel of Figure 5. Upside variance decreases quite markedly over the Great Moderation period, and by the end of the sample upside variance is half the level estimated for the 70s. On the contrary, the downside component of the long-run variance has remained quite stable throughout

<sup>16</sup>Fernández-Villaverde and Guerrón-Quintana (2020b) discuss a possible rationale for the presence of an expansionary impact of increases in in uncertainty.

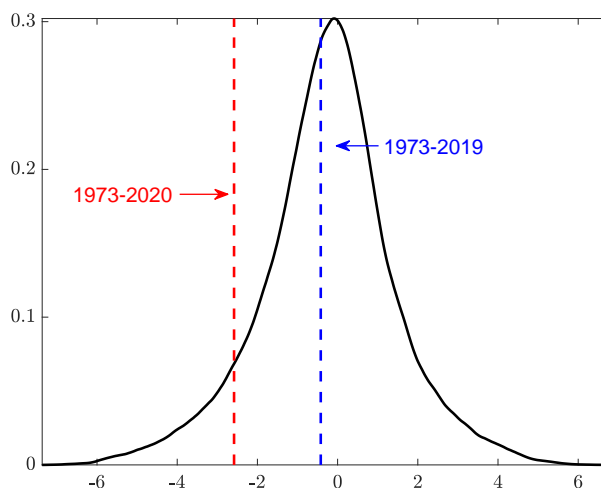


**Figure 6:** *Unconditional* skewness

*Note:* The figure reports the distribution of unconditional skewness, along with its sample value, in red, and the sample value excluding the last year of data, in blue

the sample. This evidence supports the findings in [Jensen et al. \(2020\)](#) and highlights that the Great Moderation reflects a reduction of the upside risk not matched by an equal fall in downside risk.

**Conditional vs. Unconditional skewness** [Figure 3](#) highlights that the skewness of the conditional distribution displays a marked procyclicality: expansions are characterized by right-skewed distributions, whereas contractions are associated with deepening asymmetry, leading to negatively-skewed conditional distributions during recessions. What does this mean for the unconditional distribution of GDP growth? To answer this question, we use the estimated model to draw inference on the unconditional (a)symmetry of the data. Specifically, we simulate 10000 alternative paths of GDP growth from the model, and for each of them we compute the associated (unconditional) skewness. The results of this exercise are summarized in [Figure 6](#). Negative skewness estimates of the unconditional distribution turn out to be 20% more likely than positive estimates, despite conditional distributions displaying positive skewness for a large part of the sample. As shown in the left panel of [Figure 3](#), during expansions upside volatility is, on average, 15% higher than downside volatility, while downside volatility is almost double the upside volatility during recessions. Thus, despite expansions being typically characterized by right-skewed conditional distributions, the occurrence of tail events is impaired by lower dispersion. On the contrary, recessions are characterized by more downside uncertainty, resulting in large negative observations being more likely. Excluding the last year of observations, the sample skewness value of -0.42 lies close to the expected value of the empirical distribution. However, the sample skewness of -2.58 due to the Pandemic-recession still lies well within the 95% interval.<sup>17</sup> Performing the [Bai and Ng \(2005\)](#) test for unconditional skewness on simulated data fails to find evidence of any degree of asymmetry, not rejecting the null of symmetry about 90% of the times. Therefore, despite conditional skewness largely varying over the sample, this does not prevent the model

<sup>17</sup>Repeating the same exercise leaving out the post 2019 sample would leave the distribution of the unconditional skewness unchanged.

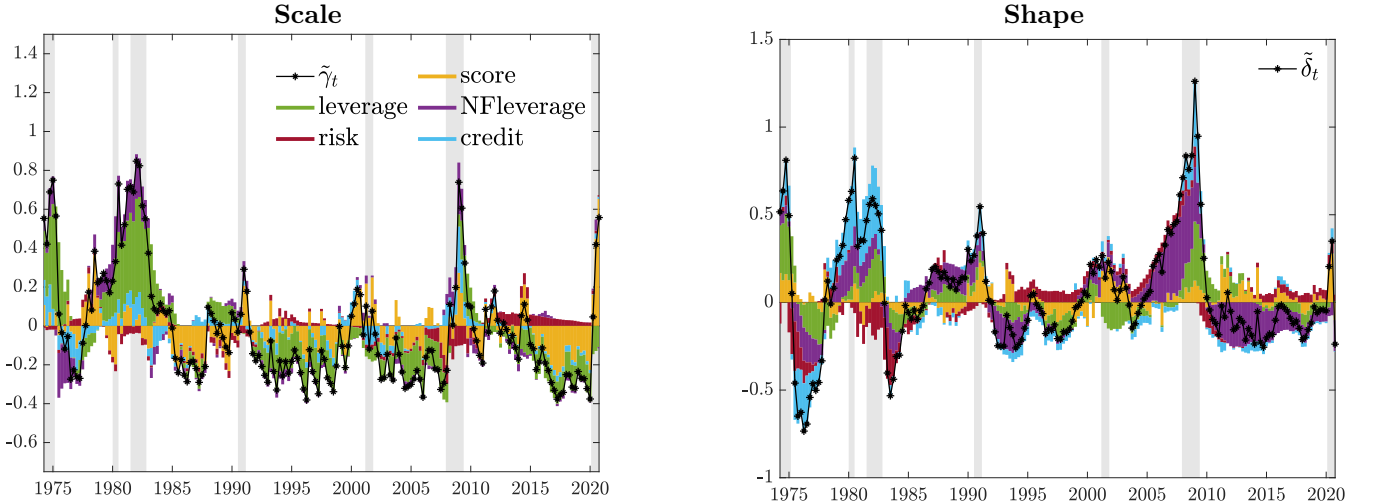


**Figure 7:** Predictive financial conditions

*Note:* The figures plot the decomposition of the “untransformed” transitory component of the time-varying parameters (in black) into a “Score-driven” (yellow) and a “Predictor-driven” component, for which we highlight all the subcomponents. Shaded bands represent NBER recessions.

from generating unconditional symmetry in the sample distribution of GDP growth, consistent with what we find in the data.

**The contribution of financial predictors** To gauge the contribution of financial indicators to the overall variation of the parameters, we exploit the moving average representation of the transitory components in Equations (17) and (18). In Figure 7, we decompose  $\tilde{\gamma}_t$  and  $\tilde{\delta}_t$  into a “score-driven” component,  $\kappa_\gamma \sum_{j=0}^{t-1} \phi_\gamma^j s_{\gamma t-j}$  and  $\kappa_\delta \sum_{j=0}^{t-1} \phi_\delta^j s_{\delta t-j}$ , respectively, and a component reflecting the share of variation driven by the predictors  $\beta'_\gamma \sum_{j=0}^{t-1} \phi_\gamma^j X_{t-j}$  and  $\beta'_\delta \sum_{j=0}^{t-1} \phi_\delta^j X_{t-j}$ . These latter components are further decomposed so as to highlight the contribution of each financial index, separately. Leverage is the largest contributor to the variation of the scale parameter. Increases in leverage during expansions are associated with a reduction of the overall dispersion of the conditional distribution of GDP growth, whereas deleveraging during recessions maps into higher uncertainty. Leverage is also an important determinant of the dynamics of the shape parameter, and thus of the skewness of the conditional distribution. However, in this case it is nonfinancial leverage that drives most of asymmetry’s variation. Consistent with the leverage-cycle narrative of Mian and Sufi (2010) and Jordà et al. (2013), the build-up of the household leverage is identified as the main contributor to the increase in downside risk in the first half of the 2000s, and the deleveraging associated with a substantial fall in downside risk. In contrast, indicators of credit spread and credit risk mainly seem to be good indicators of the sharp increase in downside risk at the height of major recessions. Lower credit spreads before the crash impaired a sharp increase of the asymmetry parameter, while as the crisis unfolded their higher values pushed the parameter towards further positive values, as argued by Krishnamurthy and Muir (2017), thereby contributing to determining the amount of asymmetry recessions are characterized by. The contribution of financial indicators is muted during the dot-com recession, in line

with the weak link between that recession and financial predictors, as highlighted by [Stock and Watson \(2003\)](#).

## 5 Out-of-sample evaluation

In this Section we explore the out-of-sample forecasting performance of the model. We re-estimate the model every quarter over the period 1980Q1-2020Q4, and produce one-quarter and one-year horizon forecasts. For the one-year ahead predictions, results are reported as cumulated output growth over the next four quarters. Forecasts are obtained from real-time GDP vintages and evaluated using the latest available release. We compare the performance of the models for the entire out-of-sample period, as well as for the post-2000s, and for the recessive periods in the forecasting sample.<sup>18</sup>

We assess the point forecast accuracy via the mean square forecast error (MSFE). Density forecast accuracy is evaluated via the predictive log-score and quantile scores. The latter, put forward by [Gneiting and Ranjan \(2011\)](#), reads as  $wQS_{t+h} = \int_0^1 QS(\alpha)\omega(\alpha)d\alpha$ , where  $\alpha$  represents the quantiles,  $QS(\alpha) = 2(I(y_{t+h} < F^{-1}(\alpha)) - \alpha)(F^{-1}(\alpha) - y_{t+h})$ , with  $F^{-1}(\alpha)$  being the empirical quantile function of the density forecast, and  $\omega(\alpha)$  is a weighting function. We consider two versions of this measure: i) the Continuously Ranked Probability Score (CRPS, [Gneiting and Raftery, 2007](#)), which assigns equal weight to each quantile of the empirical distribution function (i.e.  $\omega(\alpha) = 1$ ) and ii) a scoring rule with  $\omega(\alpha) = (1 - \alpha)^2$  that assigns higher weights to the lower quantiles of the distribution function, thus emphasising the accuracy in predicting the left tail of the distribution. The latter assesses the ability of the model to correctly characterize downside risk predictions. Similarly, when we evaluate the calibration of the predictive densities by means of the probability integral transforms (PITs) ([Diebold et al., 1998](#)), we explicitly consider the calibration of the left side of the distribution. Lastly, we investigate the use of the model in producing measures of downside risk and predicting recessions.

### 5.1 Point, density and downside risk forecasts

**Asymmetry and the value of financial predictors.** As a first step into our analysis, we aim at evaluating the importance of accounting for the skewness of the distribution of GDP growth, as well as assessing whether conditioning on financial predictors leads to forecast improvements. We consider a Gaussian autoregressive model with GARCH innovations as a benchmark, which has been shown to deliver competitive out-of-sample forecasts for GDP growth ([Clark and Ravazzolo, 2015](#)) and GDP growth-at-risk ([Brownlees and Souza, 2021](#)). [Table 2](#) reports the predictive performance of alternative Skew-t models against the Gaussian benchmark, for one-quarter and one-year ahead predictions. In particular, we produce forecasts from (a) a Skew-t model without any financial predictors, (b) a Skew-t model that includes as

---

<sup>18</sup>We do not include the pandemic-quarters within the recession sample to avoid predictive statistics being dominated by a single event.



**Table 2:** Forecasting performance

|                          | <i>Sk</i>               | <i>Sk</i><br><i>NFCI</i> | <i>Sk</i><br><i>4DFI</i> | <i>Sk</i>               | <i>Sk</i><br><i>NFCI</i> | <i>Sk</i><br><i>4DFI</i> |
|--------------------------|-------------------------|--------------------------|--------------------------|-------------------------|--------------------------|--------------------------|
| <i>One-quarter ahead</i> |                         |                          |                          |                         |                          |                          |
|                          | MSFE                    |                          |                          | logS                    |                          |                          |
| <i>Full</i>              | <b>0.842</b><br>(0.000) | <b>0.817</b><br>(0.000)  | <b>0.812</b><br>(0.000)  | <b>0.122</b><br>(0.000) | <b>0.140</b><br>(0.000)  | <b>0.060</b><br>(0.084)  |
| <i>Post '00</i>          | <b>0.809</b><br>(0.000) | <b>0.804</b><br>(0.000)  | <b>0.793</b><br>(0.000)  | <b>0.181</b><br>(0.000) | <b>0.211</b><br>(0.000)  | <b>0.167</b><br>(0.001)  |
| <i>Rec.</i>              | <b>0.831</b><br>(0.000) | <b>0.807</b><br>(0.000)  | <b>0.795</b><br>(0.000)  | <b>0.227</b><br>(0.034) | <b>0.265</b><br>(0.056)  | <b>0.148</b><br>(0.269)  |
|                          | CRPS                    |                          |                          | wQS                     |                          |                          |
| <i>Full</i>              | <b>0.964</b><br>(0.047) | <b>0.941</b><br>(0.005)  | <b>0.952</b><br>(0.025)  | <b>0.960</b><br>(0.064) | <b>0.926</b><br>(0.006)  | <b>0.926</b><br>(0.009)  |
| <i>Post '00</i>          | <b>0.934</b><br>(0.000) | <b>0.912</b><br>(0.000)  | <b>0.918</b><br>(0.000)  | <b>0.919</b><br>(0.000) | <b>0.894</b><br>(0.000)  | <b>0.891</b><br>(0.002)  |
| <i>Rec.</i>              | <b>0.961</b><br>(0.191) | <b>0.945</b><br>(0.135)  | <b>0.938</b><br>(0.112)  | <b>0.925</b><br>(0.030) | <b>0.907</b><br>(0.030)  | <b>0.868</b><br>(0.019)  |
| <i>One-year ahead</i>    |                         |                          |                          |                         |                          |                          |
|                          | MSFE                    |                          |                          | logS                    |                          |                          |
| <i>Full</i>              | <b>0.720</b><br>(0.000) | <b>0.716</b><br>(0.002)  | <b>0.694</b><br>(0.003)  | <b>0.486</b><br>(0.000) | <b>0.585</b><br>(0.000)  | <b>0.518</b><br>(0.001)  |
| <i>Post '00</i>          | <b>0.720</b><br>(0.000) | <b>0.696</b><br>(0.000)  | <b>0.718</b><br>(0.002)  | <b>0.849</b><br>(0.000) | <b>0.978</b><br>(0.000)  | <b>0.970</b><br>(0.000)  |
| <i>Rec.</i>              | <b>0.743</b><br>(0.063) | <b>0.764</b><br>(0.163)  | <b>0.656</b><br>(0.044)  | <b>1.071</b><br>(0.004) | <b>1.209</b><br>(0.007)  | <b>1.238</b><br>(0.015)  |
|                          | CRPS                    |                          |                          | wQS                     |                          |                          |
| <i>Full</i>              | <b>0.912</b><br>(0.003) | <b>0.902</b><br>(0.002)  | <b>0.883</b><br>(0.003)  | <b>0.778</b><br>(0.001) | <b>0.747</b><br>(0.001)  | <b>0.766</b><br>(0.005)  |
| <i>Post '00</i>          | <b>0.843</b><br>(0.000) | <b>0.826</b><br>(0.000)  | <b>0.820</b><br>(0.000)  | <b>0.725</b><br>(0.000) | <b>0.703</b><br>(0.000)  | <b>0.711</b><br>(0.000)  |
| <i>Rec.</i>              | <b>0.942</b><br>(0.193) | <b>0.957</b><br>(0.316)  | <b>0.890</b><br>(0.099)  | <b>0.725</b><br>(0.008) | <b>0.737</b><br>(0.028)  | <b>0.668</b><br>(0.016)  |

*Note:* The table reports the average forecast metrics relative to the Gaussian model. We use ratios for the MSFE, CRSP and wQS, and differences for the logS. Ratios smaller than 1, and positive values of the log-score differences indicate that the column-specific model performs better than the Gaussian benchmark. The p-values for [Diebold and Mariano \(1995\)](#) tests, augmented with the small sample correction of [Harvey et al. \(1997\)](#), are in parentheses. Values in **bold** are significant at the 10% level; gray shaded cells highlight the best score.

predictor only the NFCI and (c) our baseline Skew-t model, including the four disaggregate financial indices (*4DFI*). For all measures, we report ratios with respect to the Gaussian benchmark, except for the log-score (logS) for which we report differences. Values in parentheses report the p-values of the [Diebold and Mariano \(1995\)](#) test for equal predictive accuracy with the small sample correction proposed by [Harvey et al. \(1997\)](#). Simply introducing fat tails and time-varying asymmetry improves the forecast accuracy of the model with respect to the benchmark Gaussian specification, under all loss functions. Further predictive accuracy is gained when conditioning on financial information. Using the four subcomponents leads to additional gains, in particular during recessions. This is true for both the one-quarter and one-year ahead forecasts, for which the improvements are generally larger. The gains over the benchmark Gaussian model are substantial: the baseline *Sk* -*4DFI* model produces roughly 20% (30%) improvement in MSFE, and 5% (12%) and 10% (25%) improvements in the CRPS and wQS, respectively, for the one-quarter (one-year) ahead forecasts. Gains become generally even larger if one focuses on the post-2000s sample, or only considers recessions.

**Table 3:** Forecast performance with respect to Adrian et al. (2019)

|                 | <i>One-quarter ahead</i> |                         |                         |                         | <i>One-year ahead</i>   |                         |                         |                  |
|-----------------|--------------------------|-------------------------|-------------------------|-------------------------|-------------------------|-------------------------|-------------------------|------------------|
|                 | MSFE                     | logS                    | CRPS                    | wQS                     | MSFE                    | logS                    | CRPS                    | wQS              |
| <i>Full</i>     | <b>0.890</b><br>(0.000)  | <b>2.473</b><br>(0.000) | 0.983<br>(0.221)        | 1.006<br>(0.599)        | 1.014<br>(0.562)        | <b>0.571</b><br>(0.000) | 0.989<br>(0.425)        | 1.026<br>(0.672) |
| <i>Post '00</i> | <b>0.837</b><br>(0.000)  | <b>4.499</b><br>(0.000) | <b>0.920</b><br>(0.000) | <b>0.941</b><br>(0.006) | <b>0.894</b><br>(0.098) | <b>0.436</b><br>(0.000) | <b>0.902</b><br>(0.046) | 0.944<br>(0.224) |
| <i>Rec.</i>     | <b>0.877</b><br>(0.000)  | <b>8.567</b><br>(0.000) | 0.962<br>(0.111)        | 0.966<br>(0.197)        | 1.073<br>(0.649)        | <b>1.407</b><br>(0.015) | 0.948<br>(0.332)        | 0.975<br>(0.425) |

*Note:* The table reports the average forecast metrics from the *Skt* -4DFI model relative to Adrian et al. (2019). We use ratios for the MSFE, CRSP and wQS, and differences for the logS. Ratios smaller than 1, and positive values of the log-score differences indicate that the *Skt* 4DFI model performs better than Adrian et al. (2019). The p-values for Diebold and Mariano (1995) tests, augmented with the small sample correction of Harvey et al. (1997), are in parentheses. Values in **bold** are significant at the 10% level.

**Comparison with Adrian et al. (2019)** In Table 3 we report the comparison of the baseline specification against the model of Adrian et al. (2019).<sup>19</sup> Our baseline model specification is associated with better point and density forecasts, and with significant improvements arising especially in the post-2000s sample. In particular, it is worth noticing that the forecast gains that we document during recessions stem from the adaptiveness of the score filter. This, as explained in Section 3, is due to the shape parameter reacting promptly to turning points, thus implying timely and marked movements of the skewness of the predictive distributions. As a consequence, forecast densities are characterized by longer left tails during recessions as compared to those implied by the Skew-t model of Adrian et al. (2019).<sup>20</sup>

**Density calibration** Table 4 evaluates the calibration of the density forecasts looking at the properties of the PITs.<sup>21</sup> Berkowitz (2001) highlights that if the PITs are uniformly distributed (0,1), then the normal transform of the PITs should be a standard normal random variable, and at the one-step ahead the series should also be independent. The upper part of Table 4 reports the estimate of the mean and variance of the normal transforms of the PITs, their autocorrelation coefficient for the one-quarter ahead, and the p-values associated with the relevant null hypotheses. Both the Gaussian specification and the model of Adrian et al. (2019) deliver densities that are too wide on the right side of the distribution, corresponding to a strongly negative unconditional mean of the normalized forecast errors for the one-quarter ahead forecast, therefore overestimating, on average, upside risk. The same models also produce overly disperse densities, hence overpredicting both upside and downside risk for the one-year ahead forecasts. The baseline model, on the other hand, does not display any sign of miscalibration. The remainder of Table 4 reports test statistics for the correct calibration of the forecast densities of Rossi and Sekhposyan (2019). Since the correct specification of the left part of the density is fundamental to any assessment of downside risk, we also

<sup>19</sup>For comparability, we follow exactly the procedure of Adrian et al. (2019), but re-estimating the model using real-time vintages of GDP growth.

<sup>20</sup>Compared to the model of Adrian et al. (2019), the *Skt* -4DFI specification appears to be faster and more precise in capturing increases (decreases) in downside (upside) risk ahead of recessions, and it adapts to the subsequent rebounds in GDP growth in a more timely manner. See Figure H1 in Appendix H.

<sup>21</sup>A plot of the PITs is available in Appendix H.2.

**Table 4:** Density calibration tests

|                  | <i>AR(2)</i>             | <i>ABG</i>               | <i>Sk</i><br><i>t</i><br><i>4DFI</i> | <i>AR(2)</i>             | <i>ABG</i>              | <i>Sk</i><br><i>t</i><br><i>4DFI</i> |
|------------------|--------------------------|--------------------------|--------------------------------------|--------------------------|-------------------------|--------------------------------------|
|                  | <i>One-quarter ahead</i> |                          |                                      | <i>One-year ahead</i>    |                         |                                      |
| <i>Mean</i>      | <b>-0.352</b><br>(0.000) | <b>-0.238</b><br>(0.028) | 0.030<br>(0.755)                     | <b>-0.941</b><br>(0.000) | -0.225<br>(0.248)       | 0.011<br>(0.951)                     |
| <i>Var</i>       | 0.963<br>(0.801)         | 0.983<br>(0.904)         | 1.041<br>(0.745)                     | <b>2.009</b><br>(0.007)  | <b>2.071</b><br>(0.001) | 1.290<br>(0.125)                     |
| <i>AR(1)</i>     | -0.026<br>(0.742)        | <b>0.171</b><br>(0.028)  | 0.120<br>(0.126)                     |                          |                         |                                      |
| <i>RS test:</i>  |                          |                          |                                      |                          |                         |                                      |
| <i>Full</i>      | <b>2.102</b>             | <b>1.925</b>             | 0.883                                | <b>4.865</b>             | <b>2.306</b>            | 1.162                                |
| <i>Left-half</i> | <b>1.798</b>             | <b>1.415</b>             | 0.805                                | <b>4.865</b>             | <b>2.306</b>            | 1.162                                |
| <i>Left tail</i> | <b>1.074</b>             | <b>1.166</b>             | 0.501                                | <b>4.757</b>             | <b>2.306</b>            | 1.162                                |

*Note:* The table reports the properties of the normal transform of the PITs (upper panel), as well as the Kolmogorov-Smirnov statistics for the Rossi and Sekhposyan (2019) tests of correct specification of the density forecast (*RS test*, lower panel). For each model we report the mean and variance of  $\Phi^{-1}(z_t)$ , where  $z_t$  denotes the PIT of the one-quarter and one-year ahead forecast error, with  $\Phi^{-1}(\cdot)$  being the inverse of the standard normal distribution function; for the one-quarter ahead forecasts we also report the estimated coefficient of an AR(1) model on  $\Phi^{-1}(z_t)$ . We test the null hypotheses of unbiasedness and unit variance of the normalized forecast error; for the one-step ahead we also test the null of no persistence. The p-values, computed with HAC variance, are reported in parentheses. For the calibration tests we consider the full density support (*Full*), the *left-half*, defined over the  $[0, 0.5]$  support, and the *left-tail*, computed over the support  $[0, 0.25]$ . Values in **bold** indicate the rejection of the null hypothesis at the 10% confidence level. Critical values for the tests are obtained by 1000 bootstrap simulations.

report the test statistics for the correct calibration of the left-half and the left tail of the density. The test rejects the null hypothesis of correct specification of the density forecast at the 10% critical value for both the Gaussian benchmark and for the model of Adrian et al. (2019), for the one-quarter and one-year ahead forecasts. In contrast, for our baseline model the test fails to reject the null of well calibrated forecasts for the entire density, as well as for the left part of the predictive distributions capturing movements in downside risk.

## 5.2 Tail risk predictions

We now turn to the assessment of tail risk predictions, placing particular focus on the ability of the model to anticipate the build up in downside risk ahead of the 2008 financial crisis, and its reduction during the subsequent recovery. Measures such as Value at Risk (VaR), as well as the Expected Shortfall (ES), are readily obtained within our framework.  $ES_{t+h}^\alpha = \alpha^{-1} \int_0^\alpha VaR_{t+h|t}^a da$  describes the expected growth level for  $y_{t+h} < VaR_{t+h}^\alpha$ , corresponding to the  $(100\alpha)^{\text{th}}$  percentile of the h-step ahead predictive distribution, whereas the Expected Longrise ( $EL_{t+h}^{1-\alpha} = \alpha^{-1} \int_{1-\alpha}^1 VaR_{t+h|t}^a da$ ) is the upper counterpart of the ES. In order to highlight the different risk assessments associated to the models, the left hand panel of Figure 8 contrasts the 5% expected shortfall and the 95% expected longrise for the Gaussian model, the Skew-t model without financial predictors and our baseline model, considering 10 years around the financial crisis.

The Gaussian model fails to capture the building-up of risk ahead of the Great Recession, predicting an expected shortfall around zero as the economy enters the recession. In addition, assuming a symmetric distribution implies that a fall in the ES is often associated with peaks in the EL. Precisely, the minimum

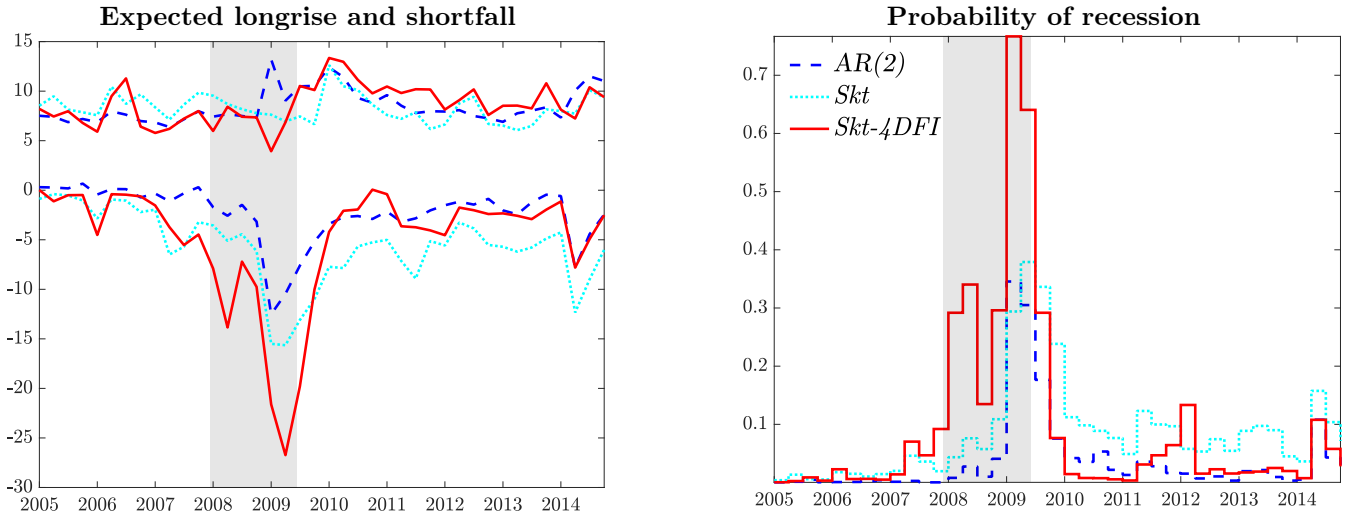


**Figure 8:** Expected Shortfall and Expected Longrise

*Note:* We report the ES and EL for  $\alpha = 0.05$ . Probabilities of recessions are computed as the probability of observing two consecutive negative growth forecasts over the next four quarters. Shaded bands represent NBER recessions.

ES corresponds to the maximum EL in 2009Q2. Allowing for *Skew-t* innovations alleviates both problems, delivering more conservative risk measures with less erratic longrise figures, and anticipating the build-up of downside risk ahead of the recession. Conditioning the forecasts on the available subindices of financial conditions increases the timeliness of the prediction of risk, due to the prompt discounting of financial overheating. The prediction of the ES falls to roughly  $-5\%$  in the first quarter of the recessions, and decreases consistently until the first quarter of recovery, when it is sharply revised upwards. Moreover, during the recession, the model delivers a downward longrise, predicting modest gains even for the most optimistic scenario. The longrise is sharply revised upward already for the first post-trough quarter. These results are mainly due to the fast updating of the asymmetry parameter, especially when the economy hits a turning point. This induces a reduction in the mean and an increase in downside risk.<sup>22</sup>

Brownlees and Souza (2021) argue that a GARCH model provides competitive out-of-sample forecasts for the lower quantiles of the GDP growth distribution. Evaluating the accuracy of the VaR and ES for  $\alpha = 0.05$  using the metric proposed by Fissler et al. (2016) highlights that allowing for time-varying skewness produces large and significant gains with respect to the Gaussian model. During recession the baseline model produces improvements of 35% at the one-quarter ahead horizon, and up to 70% at the one-year ahead. In Table 5 we document similar gains in tail risk prediction using different scores, such as the Asymmetric Laplace Score of Taylor (2019), or the tick loss function for the VaR, proposed by Giacomini and Komunjer (2005).

Last, we investigate the ability of the model to predict recessions. The NBER Business Cycle Dating Committee (BCDC) defines a recession as “[...] a significant decline in activity spread across the economy,

<sup>22</sup>In Q1 of 2009, the *Skt-4DFI* model predicts a negative mean and substantial downside risk, whereas the Gaussian model only predicts a slightly negative growth, with a roughly symmetric assessment of the risk surrounding this prediction; see Figure J2, in Appendix J.

**Table 5:** Tail risk scores

|                 | <i>Skt</i><br><i>no-X</i> | <i>Skt</i><br><i>4DFI</i> | <i>Skt</i><br><i>no-X</i> | <i>Skt</i><br><i>4DFI</i> | <i>Skt</i><br><i>no-X</i> | <i>Skt</i><br><i>4DFI</i> |
|-----------------|---------------------------|---------------------------|---------------------------|---------------------------|---------------------------|---------------------------|
|                 | FZG                       |                           | ALS                       |                           | TLF                       |                           |
|                 | <i>One-quarter ahead</i>  |                           |                           |                           |                           |                           |
| <i>Full</i>     | <b>0.831</b><br>(0.040)   | <b>0.819</b><br>(0.028)   | 0.959<br>(0.111)          | <b>0.948</b><br>(0.028)   | 0.978<br>(0.246)          | <b>0.900</b><br>(0.003)   |
| <i>Post '00</i> | <b>0.693</b><br>(0.002)   | <b>0.720</b><br>(0.003)   | <b>0.912</b><br>(0.012)   | <b>0.926</b><br>(0.038)   | <b>0.943</b><br>(0.066)   | <b>0.915</b><br>(0.040)   |
| <i>Rec.</i>     | <b>0.741</b><br>(0.014)   | <b>0.651</b><br>(0.013)   | <b>0.880</b><br>(0.030)   | <b>0.850</b><br>(0.044)   | <b>0.925</b><br>(0.072)   | <b>0.821</b><br>(0.012)   |
|                 | <i>One-year ahead</i>     |                           |                           |                           |                           |                           |
| <i>Full</i>     | <b>0.241</b><br>(0.000)   | <b>0.310</b><br>(0.001)   | <b>0.397</b><br>(0.000)   | <b>0.424</b><br>(0.000)   | <b>0.692</b><br>(0.002)   | <b>0.622</b><br>(0.002)   |
| <i>Post '00</i> | <b>0.246</b><br>(0.001)   | <b>0.371</b><br>(0.003)   | <b>0.361</b><br>(0.000)   | <b>0.398</b><br>(0.001)   | <b>0.727</b><br>(0.003)   | <b>0.600</b><br>(0.003)   |
| <i>Rec.</i>     | <b>0.192</b><br>(0.000)   | <b>0.300</b><br>(0.000)   | <b>0.263</b><br>(0.000)   | <b>0.308</b><br>(0.000)   | <b>0.551</b><br>(0.000)   | <b>0.495</b><br>(0.003)   |

*Note:* The table reports the average downside tail risk scores, expressed as ratios relative to the Gaussian model. Ratios smaller than 1 indicate that the column-specific model performs better than the benchmark. The p-values for Diebold and Mariano (1995) tests, augmented with the small sample correction of Harvey et al. (1997), are reported in parentheses. Values in **bold** are significant at the 10% level; gray shaded cells highlight the best score. FZG: Fissler et al. (2016) loss function; ALS: Taylor (2019) loss function; TLF: Giacomini and Komunjer (2005) tick loss function.

*lasting more than a few months [...]".* Therefore, we define the one-year-ahead probability of recession as the probability of observing any two consecutive negative forecasts in the next four quarters. The right panel of Figure 8 highlights that combining the information on financial conditions and allowing for asymmetry in the forecast densities produces a realistic assessment of recession risk. The implied probability of recession starts picking up earlier compared to the other measures, warning against an imminent output contraction. Moreover, the probability of observing a recession within the forthcoming year recedes sharply when the recession ends and is already below 5% just a quarter after the end of the recession, as dated by the BCDC. In contrast, the Gaussian model, as well as the Skew-t model without conditioning information, produces a reasonable probability of recession only toward the end of the recession period, and they continue to perceive a substantial treat of recession many quarters after the formal end of it. We evaluate the ability of the model to time recessions over the sample 1980-2020, using the Brier score. Deviating from the Gaussian assumption provides gains of around 10%, and an additional 20% gain can be directly ascribed to the inclusion of financial predictors.

Overall, these results underline the importance of allowing for time variation in the skewness of the conditional distribution of GDP growth for predicting downside risk, both in terms of magnitude and timing.

### 5.3 Robustness

In this Section, we provide a summary of additional analysis regarding the forecasting performances of the model. Detailed results are provided in Appendix H.

**Lagged GDP growth as additional predictor** Comparing the forecast performance of the baseline model with the same version of the model augmented with past lags of GDP growth as predictors, we find a generally weaker predictive ability in terms of point and density forecasts (see [Table H1](#)). These results confirm that parameter updates driven by the scaled score appropriately summarizes the necessary information provided by past realizations of the dependent variable, making the explicit use of lagged GDP growth redundant.

**How important is parameters' uncertainty?** To answer this question we produce forecasts from our baseline model fixing the parameters to the (recursively re-estimated) modal estimates, and we compare their performance with the baseline model's (which integrate parameter uncertainty). Explicitly accounting for parameter uncertainty leads to significant gains in terms of both point and density forecast, while, forecasts produced with the modal estimates are found to understate downside risk (see [Tables H2](#) and [H3](#)).

**Excluding 2020 from the forecast evaluation sample** We evaluate the forecasting performances of the specifications taking out the last year of data and find that the results are generally in line with those presented above. This highlights that i) gains in forecasting performance are associated with the time variation of conditional asymmetry, and ii) the information of financial indicators are not specific to the events in 2020 (see [Tables H4–H6](#)).

**Conditional vs. unconditional skewness** We compare the predictive ability of our models with respect to an AR(2) model with time-varying volatility and *Skew-t* innovations with constant skewness (i.e., with a constant asymmetry parameter re-estimated every time we produce a new forecast). This model performs similarly with the Gaussian benchmark, reflecting the weak evidence in favour of unconditional skewness over the sample. This underlines that the substantial gains in forecast accuracy are to be attributed to the time variation in the conditional skewness (see [Tables H7](#) and [H8](#)).

**Predicting GDP vintage releases** GDP growth undergoes substantial revisions, in particular over the first releases, and even more so around turning points (see, e.g, [Croushore, 2011](#)). In the previous section we have assessed the ability of different models to forecast the latest release.<sup>23</sup> In a real-time setting, it is common to target the first or the second releases of GDP. [Tables H9](#) and [H10](#) show that time-varying skewness is key to increase the predictive accuracy of the model, at both horizons, also when targeting earlier releases of the data.

**NFCI: last vintage vs. real time data** The pseudo-out-of-sample forecasting exercise presented above relies on the latest vintages of the NFCI and its subcomponents. Real time vintages of these financial indicators are only available from 2013, and have historically only experienced few, limited revisions. To

---

<sup>23</sup>This choice implies that the forecast error produced by our models also accounts for a 'measurement error' component, induced by possible GDP measurement redefinitions, that took place over the considered forecast sample (for further discussion, see [Croushore, 2011](#)).

evaluate whether the latest vintages provide an unfair advantage to the models, we compare our baseline forecasting performances to those from a pure real-time out-of-sample exercise, starting in 2013. Results point at some marginal improvements associated to the use of real time vintages, suggesting that the evaluation based on the latest releases does not advantage our model (see [Table H11](#)).

## 6 Dissecting the Financial Condition Index

In the previous Section we have documented that the predictive accuracy of a simple *Skt* model could be improved by considering financial condition indices as predictors of the time-varying parameters. Here we investigate whether the predictive power of the model can be further improved by considering the whole set of data that feeds into the NFCI, and allowing for different patterns of sparsity for each time-varying parameter.

We consider the full set of 105 (smoothed) indicators of financial activity that constitute the NFCI. We start our forecasting exercise at the beginning of the 2000s, and at each point in time, we only consider indicators for which at least four years of data are available. Hence, the first forecast we produced relies on about 70% of the total available indicators, and we reach approximately 85% about the 2007-2009 recession.<sup>24</sup>

### 6.1 Variables selection: “*shrink-then-sparsify*”

A potential concern of this exercise lies in the steep increase in the number of parameters our model needs to accommodate. We tackle this dimensionality problem through a “*shrink-then-sparsify*” strategy (see, e.g., [Hahn and Carvalho, 2015](#)).<sup>25</sup> Shrinkage is achieved by means of Horseshoe (HS) priors ([Carvalho et al., 2010](#)):  $b_i \sim \mathcal{N}(0, \lambda_i \tau)$ , where the hyperparameters  $\lambda_i$  and  $\tau$  control the local and the global shrinkage of the predictor loadings, respectively. Specifically,  $\lambda_i \sim HC^+(0, 1)$  and  $\tau \sim HC^+(0, 1)$ , where  $HC^+(0, 1)$  denotes the standard Half-Cauchy distribution. Unlike other common shrinkage priors (e.g. Ridge, Lasso), HS priors are free of exogenous inputs, implying a fully adaptive shrinkage procedure. We then apply the Signal Adaptive Variable Selector (SAVS) algorithm of [Ray and Bhattacharya \(2018\)](#) in order to reduce the estimation uncertainty associated with the near-zero shrinkage coefficients. This data-driven procedure specifies the sparsification tuning parameter as  $m_i = |\hat{b}_i|^{-2}$  such that each predictor  $i$  receives a penalization “*ranked in inverse-squared order of magnitude of the corresponding coefficient*” ([Ray and](#)

<sup>24</sup>As these data are not available in real-time, we assume that at time  $t$  the set of predictors corresponds to the quarterly average of the financial indicators from the third week of the previous quarter to the second week of the current quarter. This approach mimics the information set available to the econometrician in real-time, and avoids dealing with overlapping quarters. Once a new indicator enters the model, missing observations are set to 0, while the Euclidean norm required for the sparsification step is computed only on the part of data available (scaled by the a factor  $\sqrt{T/T^*}$  where  $T^*$  represent the length of the available sample).

<sup>25</sup>Further details on this approach are provided in [Appendix D.2](#).

**Table 6:** *Sparse* forecast performance

|                 | <i>One-quarter ahead</i> |                         |                         |                         | <i>One-year ahead</i> |                         |                  |                  |
|-----------------|--------------------------|-------------------------|-------------------------|-------------------------|-----------------------|-------------------------|------------------|------------------|
|                 | MSFE                     | logS                    | CRPS                    | wQS                     | MSFE                  | logS                    | CRPS             | wQS              |
| <i>Full</i>     | <b>0.900</b><br>(0.000)  | <b>0.327</b><br>(0.000) | <b>0.896</b><br>(0.000) | <b>0.883</b><br>(0.000) | 1.003<br>(0.214)      | <b>0.239</b><br>(0.075) | 0.954<br>(0.160) | 0.943<br>(0.310) |
| <i>Pre-2020</i> | <b>0.899</b><br>(0.012)  | <b>0.100</b><br>(0.001) | <b>0.915</b><br>(0.003) | <b>0.907</b><br>(0.010) | 0.940<br>(0.518)      | 0.082<br>(0.355)        | 0.964<br>(0.348) | 0.965<br>(0.648) |
| <i>Rec.</i>     | <b>0.906</b><br>(0.000)  | <b>0.716</b><br>(0.000) | <b>0.897</b><br>(0.000) | <b>0.890</b><br>(0.002) | 0.935<br>(0.968)      | 0.312<br>(0.807)        | 1.011<br>(0.896) | 1.005<br>(0.972) |

*Note:* The table reports the average forecast metrics from the *sparse* model relative to *Skt* 4DFI. We use ratios for the MSFE, CRPS and wQS, and differences for the logS. Ratios smaller than 1, and positive values of the log-score differences indicate that the big data model performs better than *Skt* 4DFI. The p-values for Diebold and Mariano (1995) tests, augmented with the small sample correction of Harvey et al. (1997), are in parentheses. Values in **bold** are significant at the 10% level.

Bhattacharya, 2018). Therefore,

$$b_i^* = \text{sgn}(\hat{b}_i) \|X_j\|^{-2} \max \{ |\hat{b}_i| \cdot \|X_j\|^2 - m_i, 0 \}, \quad (22)$$

where  $\|\cdot\|$  represents the Euclidean norm of the vector  $X_j$ . Note that by applying the sparsification step at each draw of the MCMC algorithm, the approach fully accounts for model uncertainty, akin to the idea of Bayesian model averaging (Huber et al., 2021).

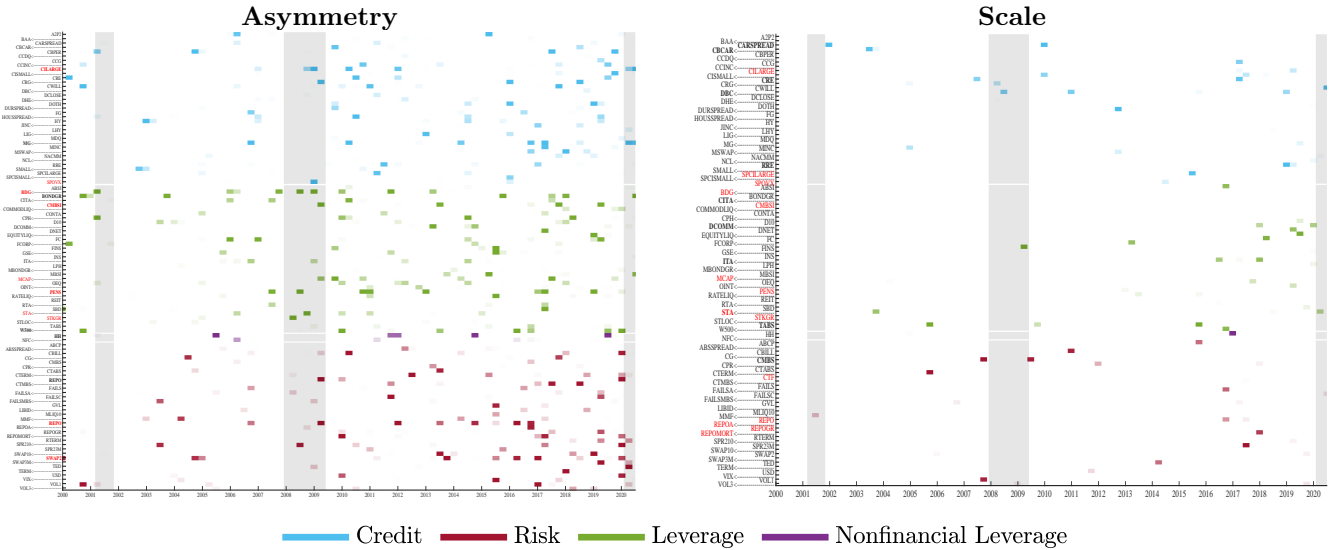
## 6.2 On the importance of financial indicators

Table 6 reports the forecasting performance of the *sparse* model, based on the  $b_j^*$  coefficients, against our baseline specification (*Skt* -4DFI), over three different samples: the full sample (2000-2020), the same sample excluding the quarters of 2020, and the 2000, 2007-2009 and 2020 recessions.

Over the full sample, the *sparse* model realizes gains of up to 10% (12%) in point (density) forecast accuracy, at the one-quarter-ahead; these translate into gains up to 25% (20%) with respect to the Gaussian benchmark. Interestingly, these performances are only slightly affected by 2020, suggesting the model is well suited to cope with such extraordinary realizations. Looking at the cumulative sums of the relative forecast scores it emerges that the *sparse* model gains advantage over the *Skt* -4DFI throughout the entire sample and, especially, during the second quarter of 2020, where the model is able to timely capture the fall in GDP and the surrounding uncertainty (see Appendix I). Largest improvements in density forecasting are documented during the main recession periods, indicating that closely monitoring signals of distress in financial markets can drastically affect the assessment of macroeconomic (downside) risk ahead and during times of crisis, in line with the insights of Alessi et al. (2014).

We further investigate the importance of sparsity when relying on a large number of predictors. Specifically, we compare the *sparse* model to a “dense” specification, where the SAVS step is omitted. The *sparse* model is associated with large gains in forecasting performance under any loss function and over all the forecasting samples we consider, pointing at the importance of reducing estimation uncertainty relative to





**Figure 9:** Sparsity

*Note:* The top panel reports the evolution of the financial predictors selected for the asymmetry parameter; the bottom panel reports those for the scale parameter. Names in red indicate the 10 predictors with the highest posterior probability ( $pip$ ) of inclusion; names in bold indicates predictors with the highest  $pip$  around the Global Financial Crisis.

the predictors' loadings in a large data setting.<sup>26</sup>

To highlight the different predictor designs arising from the *sparse* specification, in [Figure 9](#) we illustrate the evolution of sparsity in the financial information set over time, for the asymmetry and scale parameters. Financial information appears to be more informative for capturing the time variation of the asymmetry parameter, rather than the scale, and for both we observe a decreasing pattern in sparsity. On average, about 7.5% of the predictors feed into the prediction of the asymmetry parameter, while only about 2% contribute to the scale; towards the end of the sample, more than 10% of the indicators inform the asymmetry parameter, while only 5% relate to the scale. Moreover, during the financial crisis we document a decrease in the sparsity of the asymmetry parameter, highlighting the importance of monitoring developments in financial markets to gauge the severity of the Great Recession.

By ranking predictors by their average posterior probability of inclusion, it emerges that indicators pertaining to leverage markets provide most of the information relevant to predict the evolution of the asymmetry parameter, along with credit conditions indicators and household debt. Credit spreads, instead, appear most informative for the scale parameter. If we focus on the Global Financial Crisis, the size of the shadow-banking sector (as highlighted by [Adrian and Shin, 2008](#)), as well as the issuance of commercial mortgage-backed securities, provide useful signals to gauge the increasing downside risk associated with the crisis outburst.

<sup>26</sup>See [Table II](#) in [Appendix I](#).

## 7 Conclusions

The severity of the latest financial crisis and the ensuing recession has spurred the interest of both academics and practitioners in developing models that allow us to better understand and predict downside risk to economic growth. In this paper, we introduce a framework to capture permanent and transitory variation in the conditional distribution of GDP growth. Procyclical asymmetry is a strong feature of the data, with business cycle fluctuations characterized by positive skewness in expansions and negative skewness in recessions. As a result, the correlation between the mean and the variance of the conditional distribution varies over business cycle phases, turning negative during recessions. These features become even more prominent after we allow measures of financial conditions to drive time variation in the parameters. When financial markets are overheating, future economic growth becomes more uncertain, and downside risk arises, reflecting the negative skewness of the predictive distributions of GDP growth. Leverage and credit are important signals when assessing downside risk in GDP growth. In particular, non financial leverage measures anticipate a fall in economic growth, driving the rising negative asymmetry of the 2007-2009 recession. Overall, our results point to the paramount importance of nonlinearities and non-Gaussianity in capturing the dynamics of downside risk to economic growth, and for improving prediction accuracy. Conditioning on large financial information sets further improves forecasts, accurately characterizing the left tail of the predictive distribution, both at short- and medium-term projections.

Our model highlights how the statistical properties of GDP growth have dramatically changed over the last 50 years. The fall in volatility observed since the mid-1980s is reflected into a substantial fall in upside volatility, with downside volatility remaining relatively stable over the entire sample. The slowdown in long-run growth observed over the last two decades largely reflects a reassessment of risk, pointing to an increase in downside risk in the conditional distribution. We document that, since the Great Recession, the long-run predictions of the distribution of GDP growth display a marked negative skewness. This suggests that in the last 10 years, the slow economic recovery took place in an environment characterized by increasing downside risk to economic activity, well before the COVID-19 crisis.

## References

- ADRIAN, T., N. BOYARCHENKO, AND D. GIANNONE (2019): “Vulnerable Growth,” *American Economic Review*, 109, 1263–89.
- ADRIAN, T., F. GRINBERG, N. LIANG, S. MALIK, AND J. YU (2022): “The Term Structure of Growth-at-Risk,” *American Economic Journal: Macroeconomics*, Forthcoming.
- ADRIAN, T. AND H. S. SHIN (2008): “Financial intermediaries, financial stability and monetary policy,” *Proceedings - Economic Policy Symposium - Jackson Hole*, 287–334.
- ALESSI, L., E. GHYSELS, L. ONORANTE, R. PEACH, AND S. POTTER (2014): “Central bank macroeconomic forecasting during the global financial crisis: the european central bank and federal reserve bank of new york experiences,” *Journal of Business & Economic Statistics*, 32, 483–500.

- ANTOLIN-DIAZ, J., T. DRECHSEL, AND I. PETRELLA (2017): “Tracking the slowdown in long-run GDP growth,” *Review of Economics and Statistics*, 99, 343–356.
- ARELLANO-VALLE, R. B., H. W. GÓMEZ, AND F. A. QUINTANA (2005): “Statistical inference for a general class of asymmetric distributions,” *Journal of Statistical Planning and Inference*, 128, 427–443.
- AZZALINI, A. AND A. CAPITANIO (2003): “Distributions generated by perturbation of symmetry with emphasis on a multivariate skew t-distribution,” *Journal of the Royal Statistical Society: Series B (Statistical Methodology)*, 65, 367–389.
- BAI, J. AND S. NG (2005): “Tests for skewness, kurtosis, and normality for time series data,” *Journal of Business & Economic Statistics*, 23, 49–60.
- BEKAERT, G. AND E. ENGSTROM (2017): “Asset Return Dynamics under Habits and Bad Environment-Good Environment Fundamentals,” *Journal of Political Economy*, 125, 713–760.
- BELLONI, A. AND V. CHERNOZHUKOV (2009): “On the Computational Complexity of MCMC-Based Estimators in Large Samples,” *The Annals of Statistics*, 37, 2011–2055.
- BERKOWITZ, J. (2001): “Testing Density Forecasts, With Applications to Risk Management,” *Journal of Business & Economic Statistics*, 19, 465–474.
- BESAG, J., P. GREEN, D. HIGDON, AND K. MENGENSEN (1995): “Bayesian Computation and Stochastic Systems,” *Statistical Science*, 10, 3–41.
- BLASQUES, F., S. J. KOOPMAN, AND A. LUCAS (2015): “Information-theoretic optimality of observation-driven time series models for continuous responses,” *Biometrika*, 102, 325–343.
- BRAVE, S. AND R. A. BUTTERS (2012): “Diagnosing the Financial System: Financial Conditions and Financial Stress,” *International Journal of Central Banking*, 8, 191–239.
- BROWNLEES, C. AND A. B. SOUZA (2021): “Backtesting Global Growth-at-Risk,” *Journal of Monetary Economics*, 118, 312–330.
- CARRIERO, A., T. E. CLARK, AND M. MARCELLINO (2020a): “Capturing Macroeconomic Tail Risks with Bayesian Vector Autoregressions,” Working Paper 20-02, Federal Reserve Bank of Cleveland.
- (2020b): “Nowcasting Tail Risks to Economic Activity with Many Indicators,” Working Papers WP 20-13, Federal Reserve Bank of Cleveland.
- CARVALHO, C. M., N. G. POLSON, AND J. G. SCOTT (2010): “The horseshoe estimator for sparse signals,” *Biometrika*, 97, 465–480.
- CECCHETTI, S. G. (2008): “Measuring the Macroeconomic Risks Posed by Asset Price Booms,” in *Asset Prices and Monetary Policy*, University of Chicago Press, NBER Chapters, 9–43.
- CHAUVET, M. AND S. POTTER (2013): “Forecasting output,” in *Handbook of Economic Forecasting*, Elsevier, vol. 2, 141–194.
- CLARK, T. E. AND F. RAVAZZOLO (2015): “Macroeconomic Forecasting Performance under Alternative Specifications of Time-Varying Volatility,” *Journal of Applied Econometrics*, 30, 551–575.
- COX, D. R. (1981): “Statistical analysis of time series: Some recent developments,” *Scandinavian Journal of Statistics*, 93–115.
- CREAL, D., S. J. KOOPMAN, AND A. LUCAS (2013): “Generalized autoregressive score models with applications,” *Journal of Applied Econometrics*, 28, 777–795.
- CROUSHORE, D. (2011): “Frontiers of real-time data analysis,” *Journal of Economic Literature*, 49, 72–100.

- DELLE MONACHE, D. AND I. PETRELLA (2017): “Adaptive models and heavy tails with an application to inflation forecasting,” *International Journal of Forecasting*, 33, 482–501.
- DIEBOLD, F. X., T. A. GUNTHER, AND A. TAY (1998): “Evaluating density forecasts, with Applications to Financial Risk Management,” *International Economic Review*, 39, 863–883.
- DIEBOLD, F. X. AND R. S. MARIANO (1995): “Comparing predictive accuracy,” *Journal of Business & Economic Statistics*, 20, 134–144.
- DOAN, T., R. LITTERMAN, AND C. SIMS (1984): “Forecasting and conditional projection using realistic prior distributions,” *Econometric Reviews*, 3, 1–100.
- DOZ, C., L. FERRARA, AND P.-A. PIONNIER (2020): “Business cycle dynamics after the Great Recession: An extended Markov-Switching Dynamic Factor Model,” OECD Statistics Working Papers 2020/01.
- DREHMANN, M., C. E. BORIO, L. GAMBACORTA, G. JIMENEZ, AND C. TRUCHARTE (2010): “Counter-cyclical capital buffers: exploring options,” Working Paper 317, Bank for International Settlement.
- EDGE, R. M., T. LAUBACH, AND J. C. WILLIAMS (2007): “Learning and shifts in long-run productivity growth,” *Journal of Monetary Economics*, 54, 2421–2438.
- ENGLE, R. F. AND G. LEE (1999): “A permanent and transitory component model of stock return volatility,” in *Causality, and Forecasting: A Festschrift in Honor of Clive W. J. Granger*, ed. by R. F. Engle and H. White, Oxford: Oxford University Press, chap. 20, 475–497.
- ENGLE, R. F. AND V. K. NG (1993): “Measuring and Testing the Impact of News on Volatility,” *Journal of Finance*, 48, 1749–1778.
- ENGLE, R. F. AND J. G. RANGEL (2008): “The spline-GARCH model for low-frequency volatility and its global macroeconomic causes,” *The Review of Financial Studies*, 21, 1187–1222.
- EO, Y. AND J. MORLEY (2022): “Why has the U.S. economy stagnated since the Great Recession?” *The Review of Economics and Statistics*.
- ESCANCIANO, J. C. AND I. N. LOBATO (2009): “An automatic portmanteau test for serial correlation,” *Journal of Econometrics*, 151, 140–149.
- FERNÁNDEZ-VILLAVERDE, J. AND P. GUERRÓN-QUINTANA (2020a): “Estimating DSGE Models: Recent Advances and Future Challenges,” NBER Working Papers 27715, National Bureau of Economic Research.
- (2020b): “Uncertainty Shocks and Business Cycle Research,” *Review of Economic Dynamics*, 37, 118–166.
- FERNÁNDEZ-VILLAVERDE, J., S. HURTADO, AND G. NUÑO (2019): “Financial Frictions and the Wealth Distribution,” NBER Working Papers 26302, National Bureau of Economic Research.
- FISSLER, T., J. F. ZIEGEL, AND T. GNEITING (2016): “Expected shortfall is jointly elicitable with value-at-risk: implications for backtesting.” *Risk.net* ([www.risk.net/2439862](http://www.risk.net/2439862)).
- GADEA RIVAS, M. D., L. LAEVEN, AND G. PÉREZ-QUIRÓS (2020): “Growth-and-Risk Trade-off,” CEPR Discussion Papers 14492, Center for Economic Policy and Research.
- GALVÃO, A. B. AND M. T. OWYANG (2018): “Financial stress regimes and the macroeconomy,” *Journal of Money, Credit and Banking*, 50, 1479–1505.
- GANICS, G., B. ROSSI, AND T. SEKHOSYAN (2020): “From Fixed-event to Fixed-horizon Density Forecasts: Obtaining Measures of Multi-horizon Uncertainty from Survey Density Forecasts,” CEPR Discussion Papers 14267, Centre for Economic Policy Research.

- GERTLER, M. AND S. GILCHRIST (2018): “What happened: Financial factors in the great recession,” *Journal of Economic Perspectives*, 32, 3–30.
- GIACOMINI, R. AND I. KOMUNJER (2005): “Evaluation and combination of conditional quantile forecasts,” *Journal of Business & Economic Statistics*, 23, 416–431.
- GIANNONE, D., M. LENZA, AND G. E. PRIMICERI (2021): “Economic predictions with big data: The illusion of sparsity,” *Econometrica*, 89, 2409–2437.
- GIGLIO, S., B. KELLY, AND S. PRUITT (2016): “Systemic risk and the macroeconomy: An empirical evaluation,” *Journal of Financial Economics*, 119, 457–471.
- GNEITING, T. AND A. E. RAFTERY (2007): “Strictly proper scoring rules, prediction, and estimation,” *Journal of the American Statistical Association*, 102, 359–378.
- GNEITING, T. AND R. RANJAN (2011): “Comparing density forecasts using threshold-and quantile-weighted scoring rules,” *Journal of Business & Economic Statistics*, 29, 411–422.
- GÓMEZ, H. W., F. J. TORRES, AND H. BOLFARINE (2007): “Large-sample inference for the epsilon-skew-t distribution,” *Communications in Statistics—Theory and Methods*, 36, 73–81.
- HAARIO, H., E. SAKSMAN, AND J. TAMMINEN (1999): “Adaptive proposal distribution for random walk Metropolis algorithm,” *Computational Statistics*, 14, 375–396.
- HAHN, P. R. AND C. M. CARVALHO (2015): “Decoupling shrinkage and selection in Bayesian linear models: a posterior summary perspective,” *Journal of the American Statistical Association*, 110, 435–448.
- HANSEN, B. E. (1994): “Autoregressive Conditional Density Estimation,” *International Economic Review*, 35, 705–730.
- HARVEY, A. AND A. LUATI (2014): “Filtering With Heavy Tails,” *Journal of the American Statistical Association*, 109, 1112–1122.
- HARVEY, A. C. (2013): *Dynamic models for volatility and heavy tails: with applications to financial and economic time series*, vol. 52, Cambridge University Press.
- HARVEY, C. R. AND A. SIDDIQUE (1999): “Autoregressive conditional skewness,” *Journal of Financial and Quantitative Analysis*, 34, 465–487.
- HARVEY, D., S. LEYBOURNE, AND P. NEWBOLD (1997): “Testing the equality of prediction mean squared errors,” *International Journal of forecasting*, 13, 281–291.
- HUBER, F., G. KOOP, AND L. ONORANTE (2021): “Inducing sparsity and shrinkage in time-varying parameter models,” *Journal of Business & Economic Statistics*, 39, 669–683.
- JENSEN, H., I. PETRELLA, S. H. RAVN, AND E. SANTORO (2020): “Leverage and Deepening Business-Cycle Skewness,” *American Economic Journal: Macroeconomics*, 12, 245–81.
- JORDÀ, Ò., M. SCHULARICK, AND A. M. TAYLOR (2013): “When credit bites back,” *Journal of Money, Credit and Banking*, 45, 3–28.
- JURADO, K., S. C. LUDVIGSON, AND S. NG (2015): “Measuring uncertainty,” *American Economic Review*, 105, 1177–1216.
- KOOPMAN, S. J., A. LUCAS, AND M. SCHARTH (2016): “Predicting time-varying parameters with parameter-driven and observation-driven models,” *Review of Economics and Statistics*, 98, 97–110.
- KOOPMAN, S. J., A. LUCAS, AND M. ZAMOJSKI (2018): “Dynamic term structure models with score-driven time-varying parameters: estimation and forecasting,” Working Papers 258, Narodowy Bank Polski.

- KRISHNAMURTHY, A. AND T. MUIR (2017): “How credit cycles across a financial crisis,” Working Paper 23850, National Bureau of Economic Research.
- MCCONNELL, M. M. AND G. PEREZ-QUIROS (2000): “Output fluctuations in the United States: What has changed since the early 1980’s?” *American Economic Review*, 90, 1464–1476.
- MIAN, A. AND A. SUFI (2010): “Household Leverage and the Recession of 2007–09,” *IMF Economic Review*, 58, 74–117.
- MUDHOLKAR, G. S. AND A. D. HUTSON (2000): “The epsilon–skew–normal distribution for analyzing near-normal data,” *Journal of Statistical Planning and Inference*, 83, 291–309.
- NYBLOM, J. (1989): “Testing for the constancy of parameters over time,” *Journal of the American Statistical Association*, 84, 223–230.
- PLAGBORG-MØLLER, M., L. REICHLIN, G. RICCO, AND T. HASENZAGL (2020): “When is Growth at Risk?” *Brookings Papers on Economic Activity*, 2020, 167–229.
- RAY, P. AND A. BHATTACHARYA (2018): “Signal Adaptive Variable Selector for the Horseshoe Prior,” *arXiv preprint arXiv:1810.09004*.
- ROSSI, B. AND T. SEKHOSYAN (2019): “Alternative tests for correct specification of conditional predictive densities,” *Journal of Econometrics*, 208, 638–657.
- RUDEBUSCH, G. D. AND J. C. WILLIAMS (2009): “Forecasting Recessions: The Puzzle of the Enduring Power of the Yield Curve,” *Journal of Business & Economic Statistics*, 27, 492–503.
- SALGADO, S., F. GUVENEN, AND N. BLOOM (2019): “Skewed business cycles,” Working Paper 26565, National Bureau of Economic Research.
- SEGAL, G., I. SHALIASTOVICH, AND A. YARON (2015): “Good and bad uncertainty: Macroeconomic and financial market implications,” *Journal of Financial Economics*, 117, 369–397.
- SMITH, A. F. M. AND G. O. ROBERTS (1993): “Bayesian Computation Via the Gibbs Sampler and Related Markov Chain Monte Carlo Methods,” *Journal of the Royal Statistical Society. Series B (Methodological)*, 55, 3–23.
- SPIEGELHALTER, D. J., N. G. BEST, B. P. CARLIN, AND A. VAN DER LINDE (2002): “Bayesian measures of model complexity and fit,” *Journal of the Royal Statistical Society: Series B (Statistical Methodology)*, 64, 583–639.
- STOCK, J. H. AND M. W. WATSON (1998): “Median Unbiased Estimation of Coefficient Variance in a Time-Varying Parameter Model,” *Journal of the American Statistical Association*, 93, 349–358.
- (2002): “Has the business cycle changed and why?” *NBER Macroeconomics Annual Report*, 17, 159–218.
- (2003): “How did leading indicator forecasts perform during the 2001 recession?” *FRB Richmond Economic Quarterly*, 89, 71–90.
- TAYLOR, J. W. (2019): “Forecasting value at risk and expected shortfall using a semiparametric approach based on the asymmetric Laplace distribution,” *Journal of Business & Economic Statistics*, 37, 121–133.
- TIAN, L., J. S. LIU, AND L. J. WEI (2007): “Implementation of Estimating Function-Based Inference Procedures with Markov Chain Monte Carlo Samplers,” *Journal of the American Statistical Association*, 102, 881–900.
- VRONTOS, I. D., P. DELLAPORTAS, AND D. N. POLITIS (2000): “Full Bayesian Inference for GARCH and EGARCH Models,” *Journal of Business & Economic Statistics*, 18, 187–198.

# MODELING AND FORECASTING MACROECONOMIC DOWNSIDE RISK: SUPPLEMENTARY MATERIAL

Davide Delle Monache\*      Andrea De Polis†      Ivan Petrella‡

This draft: February, 2022

---

\*Bank of Italy. [davide.dellemonache@bancaditalia.it](mailto:davide.dellemonache@bancaditalia.it)

†University of Warwick. [andrea.depolis.17@mail.wbs.ac.uk](mailto:andrea.depolis.17@mail.wbs.ac.uk)

‡University of Warwick & CEPR. [ivan.petrella@wbs.ac.uk](mailto:ivan.petrella@wbs.ac.uk)

# Contents

|          |  |           |
|----------|--|-----------|
| <b>A</b> | <b>Testing for time-varying asymmetry</b>                    | <b>2</b>  |
| <b>B</b> | <b>Skew-t score derivations</b>                              | <b>5</b>  |
| B.1      | Score vector   | 5         |
| B.2      | The <i>Skew-t</i> distribution                               | 6         |
| B.3      | Unbiasedness of the scores                                   | 8         |
| B.4      | Fisher information matrix                                    | 10        |
| B.5      | Nonlinear transformation of the parameters                   | 13        |
| B.6      | Robustness to outliers                                       | 13        |
| B.7      | Matrix representation  | 14        |
| <b>C</b> | <b>On the importance of dynamic conditional moments</b>      | <b>14</b> |
| <b>D</b> | <b>Bayesian estimation</b>                                   | <b>16</b> |
| D.1      | Prior specification  | 16        |
| D.2      | Horseshoe priors and SAVS                                    | 17        |
| D.3      | Adaptive Metropolis-Hastings                                 | 18        |
| D.4      | MCMC Convergence Diagnostics                                 | 20        |
| D.5      | Sensitivity to priors  | 23        |
| <b>E</b> | <b>Monte Carlo Exercise</b>                                  | <b>26</b> |
| <b>F</b> | <b>Data</b>  | <b>32</b> |
| F.1      | Main data sources and mnemonics                              | 34        |
| F.2      | Additional details on the disaggregated financial indicators | 34        |
| <b>G</b> | <b>Model fit diagnostics</b>                                 | <b>39</b> |
| G.1      | Deviance Information Criterion and Marginal Likelihood       | 39        |
| G.2      | Model fit diagnostics  | 39        |
| <b>H</b> | <b>Additional forecast results</b>                           | <b>41</b> |
| H.1      | Comparison with Adrian et al. (2019)                         | 41        |
| H.2      | Additional details on density forecast calibration           | 42        |
| H.3      | Lagged GDP growth as additional predictor                    | 42        |
| H.4      | How important is parameters' uncertainty?                    | 43        |
| H.5      | Excluding 2020 from the forecast evaluation sample           | 43        |
| H.6      | Conditional vs. unconditional skewness                       | 45        |
| H.7      | Predicting GDP vintage releases                              | 46        |
| H.8      | NFCI: last vintage vs. real time data                        | 49        |
| <b>I</b> | <b>Additional results on the <i>Sparse</i> model</b>         | <b>49</b> |
| <b>J</b> | <b>Additional material</b>                                   | <b>52</b> |
| J.1      | Additional tables  | 52        |
| J.2      | Additional plots   | 53        |



## A Testing for time-varying asymmetry

Testing for the presence of time-varying asymmetry of economic growth has always been a daunting task. One way to obtain a preliminary gauge of this time variation is to estimate skewness recursively over smaller windows of data. In [Figure A.1](#) we report the time series of [Bai and Ng \(2005\)](#) test statistics over different rolling windows of 4 to 6 years. The null of symmetry is often rejected, with periods of significant

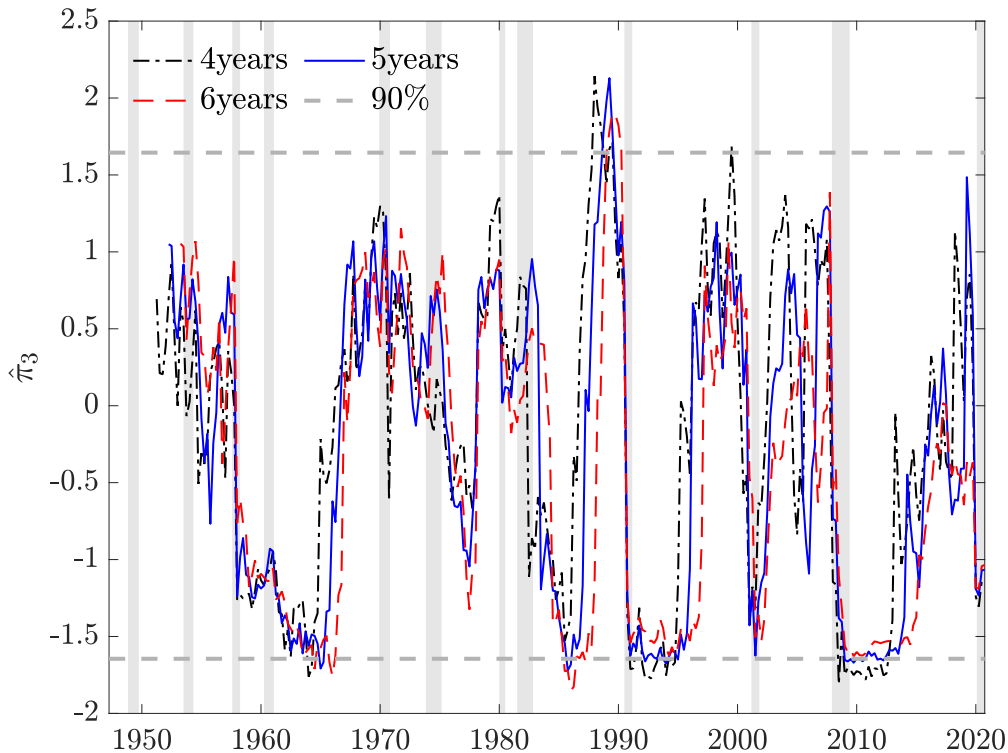


**Figure A.1:** [Bai and Ng \(2005\)](#) test for skewness

*Note:* We report the [Bai and Ng \(2005\)](#) test for skewness' test statistic  $\hat{\pi}_3$ , for different rolling windows sizes of 4, 5 and 6 years. The gray lines represent 90% (dotted) critical values. Shaded bands represent NBER recessions.

negative and positive skewness detected over the sample.

Score driven models provide a framework for testing for time-varying asymmetry. As highlighted by [Harvey \(2013, Section 2.5\)](#), the score incorporates information about the level of time variation of the respective parameter. Specifically, the dynamics of any generic time-varying parameter of interest,  $f_{t+1}$ , can be approximated by  $f_{t+1} = \bar{f} + \sum_{i=0}^{\infty} \psi_i s_{t-i}$ , where  $s_t$  is the associated conditional score. Therefore, by looking at the autocorrelation properties of the score, the Lagrange Multiplier (LM) principle can be employed to formally test for the time variation of the parameter of interest (see also, [Calvori et al., 2017](#)).

Assume the conditional distribution of GDP growth being the Skew-t of [Gómez et al. \(2007\)](#) with fixed scale and shape parameters,  $y_t | \theta, \mathcal{F}^{t-1} \sim Skt_{\nu}(\mu_t, \sigma, \rho)$ , with log-likelihood given in [Equation \(2\)](#).<sup>1</sup> The

<sup>1</sup>[Horswell and Looney \(1993\)](#) show that, when testing for skewness, omitting the presence of kurtosis might deliver misleading results. Repeating the tests with Skew-Normal innovations delivers similar evidence.

gradient associated with  $\gamma = \log \sigma$  and  $\delta = \operatorname{arctanh} \varrho$  reads as:<sup>2</sup>

$$\begin{bmatrix} \nabla_{\gamma,t} \\ \nabla_{\delta,t} \end{bmatrix} = \begin{bmatrix} (w_t \zeta_t^2 - 1) \\ -\frac{\operatorname{sgn}(\varepsilon_t)(1-\varrho^2)}{(1-\operatorname{sgn}(\varepsilon_t)\varrho)} w_t \zeta_t^2 \end{bmatrix}, \quad (\text{A.1})$$

where  $w_t = \frac{(1+\eta)}{(1-\operatorname{sgn}(\varepsilon_t))\varrho + \eta\zeta_t^2}$ ,  $\zeta_t = \frac{\varepsilon_t}{\sigma}$ , and  $\varepsilon_t = y_t - \mu_t$ . Alternatively, assuming time-varying location and scale, and fixed shape parameters, that is  $y_t|\theta, \mathcal{F}^{t-1} \sim \operatorname{Skt}_\nu(\mu_t, \sigma_t, \varrho)$ , the gradient associated with the transformed shape parameter reads as

$$\nabla_{\delta,t} = -\frac{\operatorname{sgn}(\varepsilon_t)(1-\varrho^2)}{(1-\operatorname{sgn}(\varepsilon_t)\varrho)} w_t \zeta_t^2, \quad (\text{A.2})$$

with  $\zeta_t = \frac{\varepsilon_t}{\sigma_t}$ . Tests for the time variation of these parameters can then be carried out using the score's autocorrelation function,  $r_s(\tau)$ . The Portmanteau,  $Q$ , and the Ljung-Box,  $Q^*$ , test for the null hypothesis of no time variation of the parameter of interest can be computed as:

$$Q(P) = T \sum_{\tau=1}^P r_s(\tau)^2, \quad (\text{A.3})$$

and

$$Q(P)^* = T(T+2) \sum_{\tau=1}^P (T-\tau)^{-1} r_s(\tau)^2. \quad (\text{A.4})$$

For both tests, the optimal lag-length,  $P$ , is selected following the methodology of [Escanciano and Lobato \(2009\)](#). As highlighted by [Harvey and Thiele \(2016\)](#) following this model selection procedure should select an increasing number of lags as the (first) partial autocorrelation of the score goes to unity. Therefore, under the null hypothesis, in large samples only the first lag is selected with probability one, and the asymptotic distribution of the test is  $\chi_1^2$ .

[Nyblom \(1989\)](#) introduces a general test for constant parameters against a random walk alternative based on the LM principle. In our case, the test statistics reads:

$$N = \sigma_{\nabla}^{-2} T^{-2} \sum_{j=1}^T \left( \sum_{k=j}^T \nabla_{i,k} \right)^2 \quad (\text{A.5})$$

where  $\nabla_{i,k}$ , for  $i = \{\gamma, \delta\}$  denotes the score of the distribution at time  $k$ . Under the null hypothesis of no time variation, the statistic follows a Cramer-von Mises distribution with a 5% critical value of 0.462. Although the Nyblom test is usually regarded as a test against a random walk alternative, it can also be interpreted as a test against a very persistent, but stationary, alternative, as in [Harvey and Streibel \(1998\)](#).

We apply the testing procedure to three different specifications for the dynamics of the location of the conditional distribution of GDP growth,  $\mu_t$ :

**S1:**  $\mu_t = 0$  and  $y_t \sim \operatorname{AR}(2)$  with  $\operatorname{skt}_\nu(0, \sigma, \varrho)$  innovations (see [Section 2](#)).

**S2:**  $\mu_t \sim \operatorname{GAS}(1, 1)$  with a unit root (RW);

**S3:**  $\mu_t \sim \operatorname{RW} + \operatorname{GAS}(1, 2)$  with stationary roots;

---

<sup>2</sup>Following [Harvey \(2013\)](#), we only use the gradient to construct the tests. Results are robust to using scores scaled by the square root of the diagonal elements of the Information matrix.

**Table A.1:** Score-based tests for time variation

|                           | <i>time-varying location</i> |           |          | <i>time-varying location &amp; scale</i> |           |          |
|---------------------------|------------------------------|-----------|----------|--|-----------|----------|
|                           | $Q$                          | $Q^*$     | $N$      | $Q$                                      | $Q^*$     | $N$      |
|                           | <b>S2</b>                    |           |          |  |           |          |
| <i>Scale</i> <sup>2</sup> | 33.221***                    | 33.724*** | 1.189*** |  |           |          |
| <i>Shape</i>              | 24.238***                    | 24.606*** | 0.803*** | 11.565***                                | 11.740*** | 1.468*** |
|                           | <b>S3</b>                    |           |          |  |           |          |
| <i>Scale</i> <sup>2</sup> | 48.028***                    | 48.755*** | 0.982*** |  |           |          |
| <i>Shape</i>              | 38.668***                    | 39.254*** | 1.009*** | 22.761***                                | 23.106*** | 1.529*** |

*Note:*  $Q$  is the portmanteau test,  $Q^*$  is the Ljung-Box extension and  $N$  corresponds to the Nyblom test. The lag length for the Portmanteau and Ljung-Box tests are selected following Escanciano and Lobato (2009). The first two tests are distributed as a  $\chi^2$  distribution with 1 degree of freedom, and the Nyblom test statistics is distributed as a Cramer von-Mises distribution with 1 degree of freedom. \*  $p < 10\%$ , \*\*  $p < 5\%$ , \*\*\*  $p < 1\%$ .

**Table A.2:** Score-based tests for time variation, 1973-2019 sample

|                           | <i>time-varying location</i> |           |          | <i>time-varying location &amp; scale</i> |           |          |
|---------------------------|------------------------------|-----------|----------|--|-----------|----------|
|                           | $Q$                          | $Q^*$     | $N$      | $Q$                                      | $Q^*$     | $N$      |
|                           | <b>S1</b>                    |           |          |  |           |          |
| <i>Scale</i> <sup>2</sup> | 3.432***                     | 3.485***  | 1.489    |  |           |          |
| <i>Shape</i>              | 5.199**                      | 5.280**   | 0.559**  | 31.705***                                | 32.196*** | 0.800*** |
|                           | <b>S2</b>                    |           |          |  |           |          |
| <i>Scale</i> <sup>2</sup> | 37.416***                    | 37.995*** | 1.796*** |  |           |          |
| <i>Shape</i>              | 31.987***                    | 32.482*** | 0.827*** | 33.737***                                | 34.258*** | 1.642*** |
|                           | <b>S3</b>                    |           |          |  |           |          |
| <i>Scale</i> <sup>2</sup> | 48.937***                    | 49.694*** | 1.536*** |  |           |          |
| <i>Shape</i>              | 52.172***                    | 52.979*** | 0.727**  | 32.743***                                | 33.249*** | 1.458*** |

*Note:*  $Q$  is the portmanteau test,  $Q^*$  is the Ljung-Box extension and  $N$  corresponds to the Nyblom test. The lag length for the Portmanteau and Ljung-Box tests are selected following Escanciano and Lobato (2009). The first two tests are distributed as a  $\chi^2$  distribution with 1 degree of freedom, and the Nyblom test statistics is distributed as a Cramer von-Mises distribution with 1 degree of freedom. \*  $p < 10\%$ , \*\*  $p < 5\%$ , \*\*\*  $p < 1\%$ .

For each case, we consider a specification with constant  $\gamma = \log \sigma$ , and another with time-varying  $\gamma_t = \log \sigma_t$ , following a  $GAS(1, 1)$  process. Tests' results, using data on GDP growth from 1973 to 2020, are reported in Table 1 (Section 2) for **S1**, while Table A.1 reports the results for **S2** and **S3**. For all cases and specifications we reject the null hypothesis of constant shape at the 1% confidence level.

To make sure that statistical significance is not induced by the Covid-related observations, we also report the same test over the 1973-2019 sample. Table A.2 confirms that the evidence in favor of the shape parameter being time-varying is robust to the inclusion of outliers.

## B Skew-t score derivations

In this Appendix we provide details on the Skew-t model introduced in [Section 3](#). We derive the score vector in [Appendix B.1](#). In [Appendix B.2](#) we propose a general treatment of the *Skew-t* distribution and we introduce several tools necessary for the proof of the unbiasedness of the score vector ([Appendix B.3](#)) and the derivation of the information matrix ([Appendix B.4](#)). We discuss the impact of the nonlinear transformation of the scale and shape parameters on the score in [Appendix B.5](#). We highlight how the model deals with extreme outliers ([Appendix B.6](#)). Lastly, in [Appendix B.7](#) we provide a matrix representation of the model put forward in [Section 3.1](#).

### B.1 Score vector

Let  $y_t$  be distributed as a *Skew-t* with location  $\mu_t$ , scale  $\sigma_t$ , shape  $\varrho_t$ , and degrees of freedom  $\nu$ ,  $y_t|\theta, \mathcal{F}^{t-1} \sim Skt_\nu(\mu_t, \sigma_t, \varrho_t)$ , as in [Gómez et al. \(2007\)](#). The log-likelihood function in [Equation \(2\)](#) of [Section 3](#) can be expressed as:

$$\ell_t = \log p(y_t|\theta, \mathcal{F}^{t-1}) = \log \mathcal{C}(\eta) - \frac{1}{2} \log \sigma_t^2 - \frac{1+\eta}{2\eta} \log g(\mu_t, \sigma_t, \varrho_t),$$

where  $\eta = \frac{1}{\nu}$ ,  $g(\mu_t, \sigma_t, \varrho_t) = \left(1 + \frac{\eta \zeta_t^2}{h_t^2}\right)$ ,  $\zeta_t = \frac{\varepsilon_t}{\sigma_t}$ ,  $\varepsilon_t = (y_t - \mu_t)$ ,  $h_t = (1 - \text{sgn}(\varepsilon_t)\varrho_t)$ ,  $\text{sgn}(\cdot)$  is the sign function,  $\log \mathcal{C}(\eta) = \log \Gamma\left(\frac{\eta+1}{2\eta}\right) - \log \Gamma\left(\frac{1}{2\eta}\right) - \frac{1}{2} \log\left(\frac{1}{\eta}\right) - \frac{1}{2} \log \pi$ , and  $\Gamma(\cdot)$  is the Gamma function. The time-varying parameters,  $\mu_t$ ,  $\sigma_t$  and  $\varrho_t$ , are non-stochastic conditional on the static parameters,  $\theta$ , and past information,  $\mathcal{F}^{t-1}$ , and the sole source of randomness comes from the prediction error  $\varepsilon_t$ . Let us also define  $w_t = \frac{(1+\eta)}{(1 - \text{sgn}(\varepsilon_t)\varrho_t)^2 + \eta \zeta_t^2} = \frac{1+\eta}{h_t^2 + \eta \zeta_t^2}$ , a set of weights, common to all the gradients, that downplay the effect of outliers.

**Location** The gradient with respect to the location parameter reads:

$$\nabla_{\mu,t} = \frac{1}{\sigma_t} w_t \zeta_t.$$

*Proof.*

$$\begin{aligned} \nabla_{\mu,t} &= \frac{\partial \ell_t}{\partial \mu_t} = - \left(\frac{1+\eta}{2\eta}\right) \frac{1}{g(\mu_t, \sigma_t, \varrho_t)} \frac{\partial g(\mu_t, \sigma_t, \varrho_t)}{\partial \mu_t} \\ &= \left(\frac{1+\eta}{2\eta}\right) \frac{h_t^2}{h_t^2 + \eta \zeta_t^2} \frac{2\eta \zeta_t}{h_t^2 \sigma_t} \\ &= \frac{1}{\sigma_t} w_t \zeta_t. \end{aligned}$$

■

**Squared scale** The gradient with respect to the squared scale parameter reads:

$$\nabla_{\sigma^2,t} = \frac{1}{2\sigma_t^2} (w_t \zeta_t^2 - 1).$$

*Proof.*

$$\nabla_{\sigma^2,t} = \frac{\partial \ell_t}{\partial \sigma_t^2} = - \frac{1}{2\sigma_t^2} - \left(\frac{1+\eta}{2\eta}\right) \frac{1}{g(\mu_t, \sigma_t^2, \varrho_t)} \frac{\partial g(\mu_t, \sigma_t^2, \varrho_t)}{\partial \sigma_t^2}$$

$$\begin{aligned}
&= -\frac{1}{2\sigma_t^2} + \left(\frac{1+\eta}{2\eta}\right) \frac{h_t^2}{h_t^2 + \eta\zeta_t^2} \frac{\eta\zeta_t^2}{h_t^2\sigma_t^2} \\
&= \frac{1}{2\sigma_t^2} \left[ \frac{(1+\eta)\zeta_t^2}{h_t^2 + \eta\zeta_t^2} - 1 \right] \\
&= \frac{1}{2\sigma_t^2} (w_t\zeta_t^2 - 1)
\end{aligned}$$

■

**Shape** The gradient with respect to the shape parameter reads:

$$\nabla_{\varrho,t} = -\frac{\text{sgn}(\varepsilon_t)}{(1 - \text{sgn}(\varepsilon_t)\varrho_t)} w_t\zeta_t^2$$

*Proof.*

$$\begin{aligned}
\nabla_{\varrho,t} = \frac{\partial \ell_t}{\partial \varrho_t} &= -\left(\frac{1+\eta}{2\eta}\right) \frac{1}{g(\mu_t, \sigma_t, \varrho_t)} \frac{\partial g(\mu_t, \sigma_t, \varrho_t)}{\partial \varrho_t} \\
&= -\left(\frac{1+\eta}{2\eta}\right) \frac{h_t^2}{h_t^2 + \eta\zeta_t^2} \frac{2\eta\zeta_t^2 \text{sgn}(\varepsilon_t)}{h_t^3} \\
&= -\frac{(1+\eta)}{h_t^2 + \eta\zeta_t^2} \frac{\text{sgn}(\varepsilon_t)}{h_t} \zeta_t^2 \\
&= -\frac{\text{sgn}(\varepsilon_t)}{(1 - \text{sgn}(\varepsilon_t)\varrho_t)} w_t\zeta_t^2
\end{aligned}$$

■

## B.2 The *Skew-t* distribution

In order to prove the unbiasedness of the score vector and to derive the associated information matrix, we will exploit (i) the *two-piece representation* of the *Skew-t* distribution of [Gómez et al. \(2007\)](#), and (ii) the relationship that links the *t* and the *Beta* distributions. To simplify the notation, from this point onward we drop the time subscript from all parameters.

### B.2.1 Two-piece representation

Let us denote with  $t_\nu$  a symmetric *Student-t* density with  $\nu$  degrees of freedom ([Johnson et al., 1995](#)),  $y \sim Skt_\nu(\mu, \sigma, \varrho)$  is a *Skew-t* random variable with density function of the form:

$$p(y|\mu, \sigma, \varrho, \nu) = \frac{2}{\sigma(a(\varrho) + b(\varrho))} \left[ t_\nu \left( \frac{y - \mu}{\sigma a(\varrho)} \right) I\{y \geq \mu\} + t_\nu \left( \frac{y - \mu}{\sigma b(\varrho)} \right) I\{y < \mu\} \right], \quad (\text{B.1})$$

with location parameter  $\mu$ , scale  $\sigma$ , and  $\varrho$  being the parameter regulating the asymmetry of the distribution with respect to the mode ([Arellano-Valle et al., 2005](#)). When  $a(\varrho) = 1 - \varrho$  and  $b(\varrho) = 1 + \varrho$ , we obtain the *Skew-t* distribution proposed by [Gómez et al. \(2007\)](#) which is the distribution we adopt throughout the paper:

$$p(y|\mu, \sigma, \varrho, \nu) = \frac{\mathcal{C}}{\sigma} \left[ 1 + \frac{1}{\nu} \left( \frac{y - \mu}{\sigma(1 - \text{sgn}(y - \mu)\varrho)} \right)^2 \right]^{-\frac{1+\nu}{2}}, \quad (\text{B.2})$$

where  $\mathcal{C} = \frac{\Gamma(\frac{\nu+1}{2})}{\sqrt{\nu\pi}\Gamma(\frac{\nu}{2})}$ .

Since any symmetric density on  $\mathbb{R}$  can be uniquely determined from a density on  $\mathbb{R}^+$ , the *Skt* distribution can be defined in terms of strictly positive densities (Arellano-Valle et al., 2005), and it is often convenient to express this as a two-piece distribution (Fernández and Steel, 1998). Specifically, we can re-parametrize the density in Equation (B.2) as:

$$p(y|\mu, \sigma, \varrho, \nu) = \begin{cases} \frac{\underline{c}}{\sigma} \left[ 1 + \frac{1}{\nu} \left( \frac{y-\mu}{\sigma_+} \right)^2 \right]^{-\frac{1+\nu}{2}}, & y \geq \mu \\ \frac{\underline{c}}{\sigma} \left[ 1 + \frac{1}{\nu} \left( \frac{y-\mu}{\sigma_-} \right)^2 \right]^{-\frac{1+\nu}{2}}, & y < \mu \end{cases} \quad (\text{B.3})$$

where  $\sigma_+ = (1 - \varrho)\sigma$  and  $\sigma_- = (1 + \varrho)\sigma$  are the scale parameters of the two *Half-t* densities on each side, and

$$P(y \geq \mu) = \frac{\sigma_+}{\sigma_+ + \sigma_-} = \frac{1 - \varrho}{2}, \quad P(y < \mu) = \frac{\sigma_-}{\sigma_+ + \sigma_-} = \frac{1 + \varrho}{2}. \quad (\text{B.4})$$

Taking the log of Equation (B.3) one obtains the log-likelihood function in Equation (2) of Section 3. Recalling that  $\varepsilon = y - \mu$ , we denote the positive (negative) prediction error as  $\varepsilon_+$  ( $\varepsilon_-$ ), and the corresponding positive (negative) standardized version as  $\zeta_+ = \frac{\varepsilon_+}{\sigma_+}$  ( $\zeta_- = \frac{\varepsilon_-}{\sigma_-}$ ). Moreover,  $h = (1 - \text{sgn}(\varepsilon)\varrho)$ , with  $h_+ = (1 - \varrho)$  and  $h_- = (1 + \varrho)$ , thus  $h_+\zeta_+ = \frac{\varepsilon_+}{\sigma}$ , and  $h_-\zeta_- = \frac{\varepsilon_-}{\sigma}$ .

The two-piece formulation allows us to consider separately the two halves of the distribution when taking expectations: for  $y = \mu + \sigma\zeta$ , where  $\zeta \sim \text{Skt}_\nu(0, 1, \varrho)$ , the moments of  $y$  are weighted averages of the moments of  $|\zeta|$ , where  $|\zeta| \sim \text{Ht}_\nu$ , is an *Half-t* distribution (see, e.g., Gómez et al., 2007).<sup>3</sup> Specifically:

$$\mathbb{E}[\zeta^r] = \mu_r = \frac{1}{2} [(1 - \varrho)^{r+1} + (-1)^r(1 + \varrho)^{r+1}] d_r(\nu),$$

where  $d_r(\nu) = \int_{-\infty}^{\infty} |\zeta|^r p(\zeta) d\zeta < \infty$  is the  $r^{\text{th}}$  moment of the *Half-t* distribution (Johnson et al., 1995).

## B.2.2 Useful relationships between the *t* and the *Beta* distribution

In the following sections of this Appendix we will extensively use the following results:

**Corollary 1.** *Given a beta distributed variable,  $b \sim \mathcal{B}(\alpha, \beta)$ , then*

$$\mathbb{E}[b^h(1-b)^k] = \frac{B(\alpha + h, \beta + k)}{B(\alpha, \beta)},$$

where  $B(\alpha, \beta)$  is the beta function (Harvey, 2013, pag. 23).

**Corollary 2.** *Let  $T \sim t_{1/\eta}$  be a *t*-distributed random variable with  $\frac{1}{\eta}$  degrees of freedom. We can define*

$$b = \frac{\eta T^2}{1 + \eta T^2} \sim \mathcal{B}\left(\frac{1}{2}, \frac{1}{2\eta}\right),$$

and

$$1 - b = \frac{1}{1 + \eta T^2} \sim \mathcal{B}\left(\frac{1}{2\eta}, \frac{1}{2}\right),$$

(Harvey, 2013, pag. 25).

**Corollary 3.** *Let  $T \sim t_{1/\eta}$  be a *t*-distributed random variable with  $\frac{1}{\eta}$  degrees of freedom. Then,*

$$\frac{\sqrt{\eta}T}{1 + \eta T^2} = \frac{\sqrt{\eta}T}{\sqrt{1 + \eta T^2}} \frac{1}{\sqrt{1 + \eta T^2}} = b^{\frac{1}{2}}(1-b)^{\frac{1}{2}}.$$

<sup>3</sup>Notice that the *Half-t* distribution is a special case of the *folded-t* distribution (Psarakis and Panaretos, 1990).

**Notable results** Following the result in [Corollary 1](#), we can compute some notable expectations of the form  $\mathbb{E}[b^h(1-b)^k]$ , where  $b$  is defined as in [Corollary 2](#):

$$\mathbb{E}[b] = \frac{B\left(\frac{3}{2}, \frac{1}{2\eta}\right)}{B\left(\frac{1}{2}, \frac{1}{2\eta}\right)} = \frac{\frac{1}{2}\Gamma\left(\frac{1}{2}\right)\Gamma\left(\frac{1}{2\eta}\right)}{\Gamma\left(\frac{1+3\eta}{2\eta}\right)} \frac{\Gamma\left(\frac{1+\eta}{2\eta}\right)}{\Gamma\left(\frac{1}{2}\right)\Gamma\left(\frac{1}{2\eta}\right)} = \frac{\eta}{1+\eta}, \quad (\text{B.5})$$

$$\mathbb{E}[b^2] = \frac{B\left(\frac{5}{2}, \frac{1}{2\eta}\right)}{B\left(\frac{1}{2}, \frac{1}{2\eta}\right)} = \frac{\frac{3}{4}\Gamma\left(\frac{1}{2}\right)\Gamma\left(\frac{1}{2\eta}\right)}{\Gamma\left(\frac{1+5\eta}{2\eta}\right)} \frac{\Gamma\left(\frac{1+\eta}{2\eta}\right)}{\Gamma\left(\frac{1}{2}\right)\Gamma\left(\frac{1}{2\eta}\right)} = \frac{3\eta^2}{(1+3\eta)(1+\eta)}, \quad (\text{B.6})$$

$$\mathbb{E}[b^{\frac{1}{2}}(1-b)^{\frac{1}{2}}] = \frac{B\left(1, \frac{1+\eta}{2\eta}\right)}{B\left(\frac{1}{2}, \frac{1}{2\eta}\right)} = \frac{\Gamma(1)\Gamma\left(\frac{1+\eta}{2\eta}\right)}{\Gamma\left(\frac{1+\eta}{2\eta}+1\right)} \frac{\Gamma\left(\frac{1+\eta}{2\eta}\right)}{\Gamma\left(\frac{1}{2}\right)\Gamma\left(\frac{1}{2\eta}\right)} = \frac{2\eta}{1+\eta} \frac{\Gamma\left(\frac{1+\eta}{2\eta}\right)}{\sqrt{\pi}\Gamma\left(\frac{1}{2\eta}\right)} = \frac{2\sqrt{\eta}}{1+\eta} \mathcal{C}, \quad (\text{B.7})$$

$$\mathbb{E}[b(1-b)] = \frac{B\left(\frac{3}{2}, \frac{1+2\eta}{2\eta}\right)}{B\left(\frac{1}{2}, \frac{1}{2\eta}\right)} = \frac{\frac{1}{2}\Gamma\left(\frac{1}{2}\right)\frac{1}{2\eta}\Gamma\left(\frac{1}{2\eta}\right)}{\Gamma\left(\frac{1+5\eta}{2\eta}\right)} \frac{\Gamma\left(\frac{1+\eta}{2\eta}\right)}{\Gamma\left(\frac{1}{2}\right)\Gamma\left(\frac{1}{2\eta}\right)} = \frac{\eta}{(1+3\eta)(1+\eta)}, \quad (\text{B.8})$$

$$\mathbb{E}[b^{\frac{3}{2}}(1-b)^{\frac{1}{2}}] = \frac{B\left(2, \frac{1+\eta}{2\eta}\right)}{B\left(\frac{1}{2}, \frac{1}{2\eta}\right)} = \frac{\Gamma\left(\frac{1+\eta}{2\eta}\right)}{\Gamma\left(\frac{1+5\eta}{2\eta}\right)} \frac{\Gamma\left(\frac{1+\eta}{2\eta}\right)}{\Gamma\left(\frac{1}{2}\right)\Gamma\left(\frac{1}{2\eta}\right)} = \frac{4\mathcal{C}\sqrt{\eta}\eta}{(1+3\eta)(1+\eta)}, \quad (\text{B.9})$$

recognizing that  $B(a, b) = \frac{\Gamma(a)\Gamma(b)}{\Gamma(a+b)}$ , and  $\Gamma\left(\frac{1+3\eta}{2\eta}\right) = \frac{(1+\eta)\Gamma\left(\frac{1+\eta}{2\eta}\right)}{2\eta}$ ,  $\Gamma\left(\frac{1+5\eta}{2\eta}\right) = \frac{1+3\eta}{2\eta}\Gamma\left(\frac{1+3\eta}{2\eta}\right) = \frac{(1+3\eta)(1+\eta)}{4\eta^2}\Gamma\left(\frac{1+\eta}{2\eta}\right)$ ,  $\Gamma(2) = \Gamma(1) = 1$ , and  $\Gamma\left(\frac{1}{2}\right) = \sqrt{\pi}$ . We will extensively use these results in the following derivations.

### B.3 Unbiasedness of the scores

Following [Equation \(B.3\)](#), we can rewrite the gradient as the sum of the semi-gradients computed over the positive and negative semi-support,  $\nabla_+$  and  $\nabla_-$  respectively (see also, [Harvey, 2013](#), Sec. 3.11.2):

$$\nabla = \nabla_+ I(y \geq \mu) + \nabla_- I(y < \mu), \quad (\text{B.10})$$

where  $I(\cdot)$  is the indicator function. It follows that the expectation of the gradient can be computed as:

$$\mathbb{E}[\nabla] = \mathbb{E}[\nabla_+] P(y \geq \mu) + \mathbb{E}[\nabla_-] P(y < \mu),$$

where the probabilities are defined in [Equation \(B.4\)](#). In addition, recall that the (time-varying) parameters,  $\mu$ ,  $\sigma$  and  $\varrho$  are conditionally non-stochastic, and thus the sole source of randomness comes from the prediction errors.

**Location.** The gradient with respect to the location is:

$$\nabla_\mu = \frac{1}{\sigma} w\zeta.$$

Taking advantage of the two-piece representation in [Equation \(B.10\)](#) and given the definition in [\(B.4\)](#):

$$\begin{aligned} \mathbb{E}[\nabla_\mu] &= P(y \geq \mu) \mathbb{E}[\nabla_{\mu,+}] + P(y < \mu) \mathbb{E}[\nabla_{\mu,-}] \\ &= \frac{1}{\sigma} (P(y \geq \mu) \mathbb{E}[(w\zeta)_+] + P(y < \mu) \mathbb{E}[(w\zeta)_-]) \\ &= \frac{1}{\sigma} \mathbb{E}[w\zeta]. \end{aligned}$$

Notice that:

$$w\zeta = \frac{1+\eta}{\sqrt{\eta}} \frac{\sqrt{\eta}\zeta}{h^2 + \eta\zeta^2} = \frac{1+\eta}{\sqrt{\eta}} \frac{\sqrt{\eta}\sigma\varepsilon}{\sigma^2 h^2 + \eta\varepsilon^2},$$

and evaluating over the positive (negative) semi-support we have:

$$(w\zeta)_+ = \frac{1}{1-\varrho} \frac{1+\eta}{\sqrt{\eta}} \frac{\sqrt{\eta}\zeta_+}{1+\eta\zeta_+^2}, \quad (w\zeta)_- = -\frac{1}{1+\varrho} \frac{1+\eta}{\sqrt{\eta}} \frac{\sqrt{\eta}|\zeta_-|}{1+\eta\zeta_-^2},$$

for  $\zeta_- = -|\zeta_-|$  and  $|\zeta_-|^2 = \zeta_-^2$ . Using [Corollaries 1](#) and [3](#) and [Equation \(B.7\)](#) we have that:

$$\begin{aligned} \mathbb{E}[(w\zeta)_+] &= \frac{1}{1-\varrho} \frac{1+\eta}{\sqrt{\eta}} \mathbb{E}[b^{\frac{1}{2}}(1-b)^{\frac{1}{2}}] = \frac{2\mathcal{C}}{1-\varrho}, \\ \mathbb{E}[(w\zeta)_-] &= -\frac{1}{1+\varrho} \frac{1+\eta}{\sqrt{\eta}} \mathbb{E}[b^{\frac{1}{2}}(1-b)^{\frac{1}{2}}] = -\frac{2\mathcal{C}}{1+\varrho}, \end{aligned}$$

and thus,

$$\mathbb{E}[\nabla_{\mu}] = \frac{1}{\sigma} \mathbb{E}[w\zeta] = 0. \tag{B.11}$$

■

**Squared scale.** The score with respect to the squared scale is:

$$\nabla_{\sigma^2} = \frac{1}{2\sigma^2} (w\zeta^2 - 1).$$

Taking advantage of the two-piece representation and given the definition in [\(B.4\)](#):

$$\begin{aligned} \mathbb{E}[\nabla_{\sigma^2}] &= P(y \geq \mu) \mathbb{E}[\nabla_{\sigma^2,+}] + P(y < \mu) \mathbb{E}[\nabla_{\sigma^2,-}] \\ &= \frac{1}{2\sigma^2} (P(y \geq \mu) \mathbb{E}[(w\zeta^2)_+] + P(y < \mu) \mathbb{E}[(w\zeta^2)_-] - 1) \\ &= \frac{1}{2\sigma^2} (\mathbb{E}[(w\zeta^2)] - 1). \end{aligned}$$

Notice that:

$$w\zeta^2 = \frac{1+\eta}{\eta} \frac{\eta\zeta^2}{h^2 + \eta\zeta^2} = \frac{1+\eta}{\eta} \frac{\eta\varepsilon^2}{\sigma^2 h^2 + \eta\varepsilon^2},$$

and evaluating over the positive (negative) support we have:

$$(w\zeta^2)_+ = \frac{1+\eta}{\eta} \frac{\eta\zeta_+^2}{1+\eta\zeta_+^2}, \quad (w\zeta^2)_- = \frac{1+\eta}{\eta} \frac{\eta\zeta_-^2}{1+\eta\zeta_-^2}.$$

Using [Corollaries 1](#) and [2](#) and [Equation \(B.5\)](#):

$$\mathbb{E}[(w\zeta^2)_+] = \mathbb{E}[(w\zeta^2)_-] = \frac{1+\eta}{\eta} \mathbb{E}[b] = 1, \tag{B.12}$$

thus  $\mathbb{E}[(w\zeta^2)] = 1$  and

$$\mathbb{E}[\nabla_{\sigma^2}] = 0.$$

■

**Shape.** The score with respect to the shape is:

$$\nabla_{\varrho} = -\frac{\text{sgn}(\varepsilon)}{h} w\zeta^2.$$



Taking advantage of the two-piece representation, given the definition in (B.4) and Equation (B.12):

$$\begin{aligned}\mathbb{E}[\nabla_{\varrho}] &= P(y \geq \mu) \mathbb{E}[\nabla_{\varrho,+}] + P(y < \mu) \mathbb{E}[\nabla_{\varrho,-}] \\ &= -\frac{P(y \geq \mu)}{1 - \varrho} \mathbb{E}[(w\zeta^2)_+] + \frac{P(y < \mu)}{1 + \varrho} \mathbb{E}[(w\zeta^2)_-] = 0.\end{aligned}$$

■

## B.4 Fisher information matrix

Provided  $\mathbb{E}[\nabla] = 0$ , we can compute the information matrix as the outer product of the gradients,  $\mathcal{I} = \mathbb{E}[\nabla\nabla']$ . In what follows, we will show that the information matrix is equal to:<sup>4</sup>

$$\mathcal{I} = \begin{bmatrix} \mathcal{I}_{\mu,\mu} & \mathcal{I}_{\mu,\sigma^2} & \mathcal{I}_{\mu,\varrho} \\ \mathcal{I}_{\sigma^2,\mu} & \mathcal{I}_{\sigma^2,\sigma^2} & \mathcal{I}_{\sigma^2,\varrho} \\ \mathcal{I}_{\varrho,\mu} & \mathcal{I}_{\varrho,\sigma^2} & \mathcal{I}_{\varrho,\varrho} \end{bmatrix} = \begin{bmatrix} \frac{(1+\eta)}{\sigma^2(1+3\eta)(1-\varrho^2)} & 0 & -\frac{4\mathcal{C}(1+\eta)}{\sigma(1+3\eta)(1-\varrho^2)} \\ 0 & \frac{1}{2\sigma^4(1+3\eta)} & 0 \\ -\frac{4\mathcal{C}(1+\eta)}{\sigma(1+3\eta)(1-\varrho^2)} & 0 & \frac{3(1+\eta)}{(1+3\eta)(1-\varrho^2)} \end{bmatrix}.$$

In the same fashion as above, we can take advantage of the two-piece representation, and write:

$$\mathbb{E}[\nabla\nabla'] = P(y \geq \mu) \mathbb{E}[\nabla_+\nabla'_+] + P(y < \mu) \mathbb{E}[\nabla_-\nabla'_-]. \quad (\text{B.13})$$

where (B.4) defines  $P(y \geq \mu)$  and  $P(y < \mu)$ .

$\mathcal{I}_{\mu,\mu}$ .

$$\mathcal{I}_{\mu,\mu} = \mathbb{E}[\nabla_{\mu}\nabla'_{\mu}] = \frac{1}{\sigma^2} \mathbb{E}[w^2\zeta^2],$$

taking advantage of Equation (B.13) we get:

$$\begin{aligned}\mathcal{I}_{\mu,\mu} &= P(y \geq \mu) \mathbb{E}[\nabla_{\mu,+}\nabla_{\mu,+}] + P(y < \mu) \mathbb{E}[\nabla_{\mu,-}\nabla_{\mu,-}] \\ &= \frac{1}{\sigma^2} (P(y \geq \mu) \mathbb{E}[(w^2\zeta^2)_+] + P(y < \mu) \mathbb{E}[(w^2\zeta^2)_-]) \\ &= \frac{1}{\sigma^2} \mathbb{E}[w^2\zeta^2].\end{aligned}$$

Notice that:

$$w^2\zeta^2 = \frac{(1+\eta)^2}{\eta} \frac{\eta\zeta^2}{h^2 + \eta\zeta^2} \frac{1}{h^2 + \eta\zeta^2} = \frac{(1+\eta)^2\sigma^2}{\eta} \frac{\eta\varepsilon^2}{\sigma^2h^2 + \eta\varepsilon^2} \frac{1}{\sigma^2h^2 + \eta\varepsilon^2};$$

evaluating over the positive (negative) semi-support:

$$(w^2\zeta^2)_+ = \frac{(1+\eta)^2}{\eta(1-\varrho)^2} \frac{\eta\zeta_+^2}{1 + \eta\zeta_+^2} \frac{1}{1 + \eta\zeta_+^2}, \quad (w^2\zeta^2)_- = \frac{(1+\eta)^2}{\eta(1+\varrho)^2} \frac{\eta\zeta_-^2}{1 + \eta\zeta_-^2} \frac{1}{1 + \eta\zeta_-^2}.$$

Using Corollaries 1 and 2 and Equation (B.8) we have:

$$\mathbb{E}[(w^2\zeta^2)_+] = \frac{(1+\eta)}{(1+3\eta)(1-\varrho)^2}, \quad \mathbb{E}[(w^2\zeta^2)_-] = \frac{(1+\eta)}{(1+3\eta)(1+\varrho)^2},$$

and thus,

$$\mathcal{I}_{\mu,\mu} = \frac{(1+\eta)}{\sigma^2(1+3\eta)} \left( \frac{P(y \geq \mu)}{(1-\varrho)^2} + \frac{P(y < \mu)}{(1+\varrho)^2} \right)$$

<sup>4</sup>Notice that Gómez et al. (2007) derive the same expression using the expectation of the negative Hessian matrix.

$$= \frac{(1 + \eta)}{\sigma^2(1 + 3\eta)(1 - \varrho^2)}.$$

$\mathcal{I}_{\sigma^2, \sigma^2}$ .

$$\begin{aligned} \mathcal{I}_{\sigma^2, \sigma^2} &= \mathbb{E}[\nabla_{\sigma^2} \nabla'_{\sigma^2}] = \frac{1}{4\sigma^4} \mathbb{E}[(w\zeta^2 - 1)^2] \\ &= \frac{1}{4\sigma^4} \mathbb{E}[1 - 2w\zeta^2 + w^2\zeta^4] \\ &= \frac{1}{4\sigma^4} (\mathbb{E}[w^2\zeta^4] - 1), \end{aligned}$$

as per [Equation \(B.12\)](#). Using the two-piece representation:

$$\begin{aligned} \mathcal{I}_{\sigma^2, \sigma^2} &= P(y \geq \mu) \mathbb{E}[\nabla_{\sigma^2, +} \nabla'_{\sigma^2, +}] + P(y < \mu) \mathbb{E}[\nabla_{\sigma^2, -} \nabla'_{\sigma^2, -}] \\ &= \frac{1}{4\sigma^4} (P(y \geq \mu) \mathbb{E}[(w^2\zeta^4)_+] + P(y < \mu) \mathbb{E}[(w^2\zeta^4)_-] - 1). \end{aligned}$$

Notice that:

$$w^2\zeta^4 = \frac{(1 + \eta)^2}{\eta^2} \left( \frac{\eta\zeta^2}{h^2 + \eta\zeta^2} \right)^2 = \frac{(1 + \eta)^2}{\eta^2} \left( \frac{\eta\varepsilon^2}{\sigma^2 h^2 + \eta\varepsilon^2} \right)^2,$$

and evaluating over the positive (negative) semi-support:

$$(w^2\zeta^4)_+ = \frac{(1 + \eta)^2}{\eta^2} \left( \frac{\eta\zeta_+^2}{1 + \eta\zeta_+^2} \right)^2, \quad (w^2\zeta^4)_- = \frac{(1 + \eta)^2}{\eta^2} \left( \frac{\eta\zeta_-^2}{1 + \eta\zeta_-^2} \right)^2.$$

Using [Corollaries 1](#) and [2](#) and [Equation \(B.6\)](#) we have:

$$\mathbb{E}[(w^2\zeta^4)_+] = \mathbb{E}[(w^2\zeta^4)_-] = \frac{(1 + \eta)^2}{\eta^2} \mathbb{E}[b^2] = \frac{3(1 + \eta)}{(1 + 3\eta)} \quad (\text{B.14})$$

Thus,

$$\begin{aligned} \mathcal{I}_{\sigma^2, \sigma^2} &= \frac{1}{4\sigma^2} \left( \frac{3(1 + \eta)}{(1 + 3\eta)} - 1 \right) \\ &= \frac{1}{2\sigma^4(1 + 3\eta)} \end{aligned}$$

$\mathcal{I}_{\varrho, \varrho}$ .

$$\mathcal{I}_{\varrho, \varrho} = \mathbb{E}[\nabla_{\varrho} \nabla'_{\varrho}] = \frac{1}{h^2} \mathbb{E}[w^2\zeta^4].$$

Using the two-piece representation and [Equation \(B.14\)](#) we can write:

$$\begin{aligned} \mathcal{I}_{\varrho, \varrho} &= P(y \geq \mu) \mathbb{E}[\nabla_{\varrho, +} \nabla'_{\varrho, +}] + P(y < \mu) \mathbb{E}[\nabla_{\varrho, -} \nabla'_{\varrho, -}] \\ &= \frac{P(y \geq \mu)}{(1 - \varrho)^2} \mathbb{E}[(w^2\zeta^4)_+] + \frac{P(y < \mu)}{(1 + \varrho)^2} \mathbb{E}[(w^2\zeta^4)_-] \\ &= \frac{3(1 + \eta)}{(1 + 3\eta)(1 - \varrho^2)}. \end{aligned}$$

$\mathcal{I}_{\mu,\varrho}$ .

$$\mathcal{I}_{\mu,\varrho} = \mathbb{E}[\nabla_{\mu} \nabla'_{\varrho}] = -\frac{\text{sgn}(\varepsilon)}{h\sigma} \mathbb{E}[w^2 \zeta^3]$$

Using the two-piece representation we have:

$$\begin{aligned} \mathcal{I}_{\varrho,\mu} &= P(y \geq \mu) \mathbb{E}[\nabla_{\varrho,+} \nabla_{\mu,+}] + P(y < \mu) \mathbb{E}[\nabla_{\varrho,-} \nabla_{\mu,-}] \\ &= -\frac{P(y \geq \mu)}{(1-\varrho)\sigma} \mathbb{E}[(w^2 \zeta^3)_+] + \frac{P(y < \mu)}{(1+\varrho)\sigma} \mathbb{E}[(w^2 \zeta^3)_-] \\ &= -\frac{1}{2\sigma} (\mathbb{E}[(w^2 \zeta^3)_+] - \mathbb{E}[(w^2 \zeta^3)_-]). \end{aligned}$$

Notice that:

$$w^2 \zeta^3 = \frac{(1+\eta)^2}{\eta\sqrt{\eta}} \frac{\eta\zeta^2}{h^2 + \eta\zeta^2} \frac{\sqrt{\eta}\zeta}{h^2 + \eta\zeta^2} = \frac{(1+\eta)^2}{\eta\sqrt{\eta}} \frac{\eta\varepsilon^2}{\sigma^2 h^2 + \eta\varepsilon^2} \frac{\sqrt{\eta}\sigma\varepsilon}{\sigma^2 h^2 + \eta\varepsilon^2}$$

and evaluating over the positive (negative) semi-support:

$$(w^2 \zeta^3)_+ = \frac{1}{(1-\varrho)} \frac{(1+\eta)^2}{\eta\sqrt{\eta}} \frac{\eta\zeta_+^2}{1+\eta\zeta_+^2} \frac{\sqrt{\eta}\zeta_+}{1+\eta\zeta_+^2}, \quad (w^2 \zeta^3)_- = -\frac{1}{(1+\varrho)} \frac{(1+\eta)^2}{\eta\sqrt{\eta}} \frac{\eta\zeta_-^2}{1+\eta\zeta_-^2} \frac{\sqrt{\eta}|\zeta_-|}{1+\eta\zeta_-^2},$$

for  $\zeta_- = -|\zeta_-|$ . Using [Corollaries 1 and 2](#) and [Equation \(B.9\)](#) we get:

$$\mathbb{E}[(w^2 \zeta^3)_+] = \frac{4\mathcal{C}(1+\eta)}{(1-\varrho)(1+3\eta)}, \quad \mathbb{E}[(w^2 \zeta^3)_-] = -\frac{4\mathcal{C}(1+\eta)}{(1+\varrho)(1+3\eta)}; \quad (\text{B.15})$$

therefore,

$$\mathcal{I}_{\varrho,\mu} = -\frac{4\mathcal{C}(1+\eta)}{\sigma(1+3\eta)(1-\varrho^2)}$$

■

$\mathcal{I}_{\mu,\sigma^2}$ .

$$\begin{aligned} \mathcal{I}_{\mu,\sigma^2} &= \mathbb{E}[\nabla_{\mu} \nabla_{\sigma^2}] = \frac{1}{2\sigma^3} \{\mathbb{E}[w^2 \zeta^3] - \mathbb{E}[w\zeta]\} \\ &= \frac{1}{2\sigma^3} \mathbb{E}[w^2 \zeta^3], \end{aligned}$$

as per equation [Equation \(B.11\)](#). Using the two-piece representation and [Equation \(B.15\)](#) we obtain:

$$\begin{aligned} \mathcal{I}_{\mu,\sigma^2} &= P(y \geq \mu) \mathbb{E}[\nabla_{\mu,+} \nabla_{\sigma^2,+}] + P(y < \mu) \mathbb{E}[\nabla_{\mu,+} \nabla_{\sigma^2,-}] \\ &= \frac{1}{2\sigma^3} (P(y \geq \mu) \mathbb{E}[(w^2 \zeta^3)_+] + P(y < \mu) \mathbb{E}[(w^2 \zeta^3)_-]) = 0. \end{aligned}$$

■

$\mathcal{I}_{\varrho,\sigma^2}$ .

$$\mathcal{I}_{\varrho,\sigma^2} = \mathbb{E}[\nabla_{\varrho} \nabla_{\sigma^2}] = -\frac{\text{sgn}(\varepsilon)}{2h\sigma^2} (\mathbb{E}[w^2 \zeta^4] - \mathbb{E}[w\zeta^2]).$$

Using the two-piece representation we get:

$$\mathcal{I}_{\varrho,\sigma^2} = P(y \geq \mu) \mathbb{E}[\nabla_{\varrho,+} \nabla_{\sigma^2,+}] + P(y < \mu) \mathbb{E}[\nabla_{\varrho,-} \nabla_{\sigma^2,-}]$$

$$= -\frac{1}{4\sigma^2} (\mathbb{E} [(w^2\zeta^4)_+] - \mathbb{E} [(w^2\zeta^4)_-]) + \frac{1}{4\sigma^2} (\mathbb{E} [(w\zeta^2)_+] - \mathbb{E} [(w\zeta^2)_-]) = 0,$$

after using [Equation \(B.12\)](#) and [Equation \(B.14\)](#). ■

## B.5 Nonlinear transformation of the parameters

In order to ensure the scale  $\sigma_t$  to be positive and the shape  $\varrho_t$  to lie within the unit circle, we model  $\gamma_t = \log \sigma_t$  and  $\delta_t = \operatorname{arctanh} \varrho_t$ . From a straightforward application of the chain rule for differentiation we have:

$$\frac{\partial \ell_t}{\partial \gamma_t} = \frac{\partial \ell_t}{\partial \sigma_t^2} \frac{\partial \sigma_t^2}{\partial \gamma_t}, \quad \frac{\partial \ell_t}{\partial \delta_t} = \frac{\partial \ell_t}{\partial \varrho_t} \frac{\partial \varrho_t}{\partial \delta_t},$$

where  $\frac{\partial \sigma_t^2}{\partial \gamma_t} = 2\sigma_t^2$ , and  $\frac{\partial \varrho_t}{\partial \delta_t} = (1 - \varrho_t^2)$ . Defining the vector of parameters of interest as  $f_t = [\mu_t, \gamma_t, \delta_t]'$ , we have that  $\frac{\partial \ell_t}{\partial f_t} = J_t' \nabla_t$ , where  $\nabla_t = [\nabla_{\mu,t}, \nabla_{\sigma^2,t}, \nabla_{\varrho,t}]'$ , and the associated Jacobian matrix reads:

$$J_t = \begin{bmatrix} 1 & 0 & 0 \\ 0 & 2\sigma_t^2 & 0 \\ 0 & 0 & 1 - \varrho_t^2 \end{bmatrix}.$$

As for the scaling matrix, we use a smoothed version of the information matrix:

$$\hat{S}_t = (1 - \chi) \hat{S}_{t-1} + \chi (J_t' \operatorname{diag}(\mathcal{I}_t) J_t)^{-\frac{1}{2}},$$

where the smoothing parameter  $0 < \chi < 1$  is estimated together with the other parameters of the model.<sup>5</sup>

Note that without smoothing (for  $\chi = 1$ ), the scaled score  $s_t = (J_t' \operatorname{diag}(\mathcal{I}_t) J_t)^{-\frac{1}{2}} J_t' \nabla_t = \operatorname{diag}(\mathcal{I}_t)^{-\frac{1}{2}} \nabla_t$ , which leads to:

$$\begin{bmatrix} s_{\mu,t} \\ s_{\gamma,t} \\ s_{\delta,t} \end{bmatrix} = \begin{bmatrix} \sqrt{\frac{(1+3\eta)(1-\varrho_t^2)}{(1+\eta)}} w_t \zeta_t \\ \sqrt{\frac{1+3\eta}{2}} (w_t \zeta_t^2 - 1) \\ -\operatorname{sgn}(\varepsilon_t) \sqrt{\frac{(1+3\eta)(1+\operatorname{sgn}(\varepsilon_t)\varrho_t)}{3(1+\eta)(1-\operatorname{sgn}(\varepsilon_t)\varrho_t)}} w_t \zeta_t^2 \end{bmatrix},$$

where  $s_{\delta,t}$  follows noting that  $(1 + \operatorname{sgn}(\varepsilon)\varrho)(1 - \operatorname{sgn}(\varepsilon)\varrho) = (1 - \varrho^2)$ .

## B.6 Robustness to outliers

Here we consider the limiting behaviour of the *Skt* scaled scores. We show that for (standardized) forecast errors approaching positive (negative) infinity, the scaled scores either converge to zero, implying a trimming of the outliers, or converge to a positive (negative) constant, akin to Winsorizing extreme observations (see, e.g., [Caivano and Harvey, 2014](#)). Specifically,

$$\lim_{\zeta \rightarrow \pm\infty} s_{\mu,t} = 0,$$

$$\lim_{\zeta \rightarrow \pm\infty} s_{\gamma,t} = \frac{1 + \eta}{\eta} \sqrt{\frac{1 + 3\eta}{2}},$$

---

<sup>5</sup>It is possible to show that the element of  $\hat{S}_t$  relative to  $\gamma_t$  always converges to  $\sqrt{\frac{2}{1+3\eta}}$ . Therefore, the smoothing the scaling matrix has an impact on  $\mu_t$  and  $\delta_t$  only.

$$\lim_{\zeta \rightarrow \pm\infty} s_{\delta,t} = \mp \frac{1+\eta}{\eta} \sqrt{\frac{(1+3\eta)(1 \pm \varrho_t)}{3(1+\eta)(1 \mp \varrho_t)}}.$$

In line with results for the  $t$  distribution, the scaled score for the location trims outliers, preventing any update of the parameter (Maronna et al., 2019). The limits of the scaled scores for the scale and shape parameter, on the other hand, converge to constant factors. These are functions of the degrees of freedom parameter, as well as of the conditional asymmetry parameter at time  $t$  for the shape.

## B.7 Matrix representation

Given the vector of time-varying parameters,  $f_t$ , we can express the score-driven law of motion of Equation (3) in matrix form.

$$\underbrace{\begin{bmatrix} \bar{\mu}_{t+1} \\ \tilde{\mu}_{t+1} \\ \tilde{\mu}_t \\ \bar{\gamma}_{t+1} \\ \tilde{\gamma}_{t+1} \\ \bar{\delta}_{t+1} \\ \tilde{\delta}_{t+1} \end{bmatrix}}_{f_{t+1}} = \underbrace{\begin{bmatrix} \varsigma_\mu & 0 & 0 \\ \kappa_\mu & 0 & 0 \\ 0 & 0 & 0 \\ 0 & \varsigma_\gamma & 0 \\ 0 & \kappa_\gamma & 0 \\ 0 & 0 & \varsigma_\delta \\ 0 & 0 & \kappa_\delta \end{bmatrix}}_A \underbrace{\begin{bmatrix} s_{\mu t} \\ s_{\gamma t} \\ s_{\delta t} \end{bmatrix}}_{s_t} + \underbrace{\begin{bmatrix} 1 & 0 & 0 & 0 & 0 & 0 & 0 \\ 0 & \phi_{\mu,1} & \phi_{\mu,2} & 0 & 0 & 0 & 0 \\ 0 & 1 & 0 & 0 & 0 & 0 & 0 \\ 0 & 0 & 0 & 1 & 0 & 0 & 0 \\ 0 & 0 & 0 & 0 & \phi_\gamma & 0 & 0 \\ 0 & 0 & 0 & 0 & 0 & 1 & 0 \\ 0 & 0 & 0 & 0 & 0 & 0 & \phi_\delta \end{bmatrix}}_B \underbrace{\begin{bmatrix} \bar{\mu}_t \\ \tilde{\mu}_t \\ \tilde{\mu}_{t-1} \\ \bar{\gamma}_t \\ \tilde{\gamma}_t \\ \bar{\delta}_t \\ \tilde{\delta}_t \end{bmatrix}}_{f_t} + \underbrace{\begin{bmatrix} 0 & 0 \dots 0 \\ \beta_\mu^1 & \beta_\mu^2 \dots \beta_\mu^k \\ 0 & 0 \dots 0 \\ 0 & 0 \dots 0 \\ \beta_\gamma^1 & \beta_\gamma^2 \dots \beta_\gamma^k \\ 0 & 0 \dots 0 \\ \beta_\delta^1 & \beta_\delta^2 \dots \beta_\delta^k \end{bmatrix}}_C X_t,$$

with  $X_t$  being a  $k$ -dimensional vector of predictors, at time  $t$ .

## C On the importance of dynamic conditional moments

In this Section, we consider a restricted specification of the model in line with the work of Plagborg-Møller et al. (2020). As noted in Section 3, when the autoregressive feature of the model is dropped out, and the information content of past prediction errors (condensed into the score) is omitted, our framework collapses to a parametric model for the distribution of GDP growth akin to the one in Plagborg-Møller et al. (2020).<sup>6</sup> Specifically, setting  $\varsigma_\mu = \phi_{\mu,1} = \phi_{\mu,2} = \kappa_\mu = \varsigma_\gamma = \phi_\gamma = \kappa_\gamma = \varsigma_\delta = \phi_\delta = \kappa_\delta = 0$ , we obtain:

$$\mu_{t+1} = \bar{\mu} + \beta'_\mu X_t, \quad (\text{C.1})$$

$$\gamma_{t+1} = \bar{\gamma} + \beta'_\gamma X_t, \quad (\text{C.2})$$

$$\delta_{t+1} = \bar{\delta} + \beta'_\delta X_t, \quad (\text{C.3})$$

so that the parameters' laws of motion become linear functions of predictors only.

We estimate the model above using as predictors the 4 disaggregated components of the NFCI, as well as the factors used in Plagborg-Møller et al. (2020) (including in both cases lagged values of GDP growth).<sup>7</sup> Table C.1 reports the Deviance Information Criterion, the complexity subcomponent, and the log Marginal Likelihood associated to these two specifications. Our baseline model outperforms the two restricted

<sup>6</sup>Note that Plagborg-Møller et al. (2020) consider the Skew- $t$  of Azzalini and Capitanio (2003).

<sup>7</sup>For comparability purposes, we restrict the estimation sample to the 1973-2018 periods, as in Plagborg-Møller et al. (2020).

**Table C.1:** Deviance Information Criterion

| Model  | $DIC$               | $pD$             | $ML$                |
|--|---------------------|------------------|---------------------|
| <i>Skt</i> 4DFI                                | 799.351<br>(13.488) | 9.443<br>(3.458) | -399.048<br>(8.458) |
| Plagborg-Møller et al. (2020) with 4DFI        | 828.937<br>(0.526)  | 7.853<br>(0.262) | -412.925<br>(0.962) |
| Plagborg-Møller et al. (2020) Financial Factor | 813.586<br>(0.536)  | 8.668<br>(0.279) | -406.127<br>(1.178) |

*Note:* The table reports the Deviance Information Criterion ( $DIC$ ) of Spiegelhalter et al. (2002), along with the relative model complexity measure ( $pD$ ), and the log Marginal Likelihood (log  $ML$ ) for the *Skt* -4DFI specification, and the nested version of Plagborg-Møller et al. (2020), with the four disaggregated financial indices and with the global and financial factors.

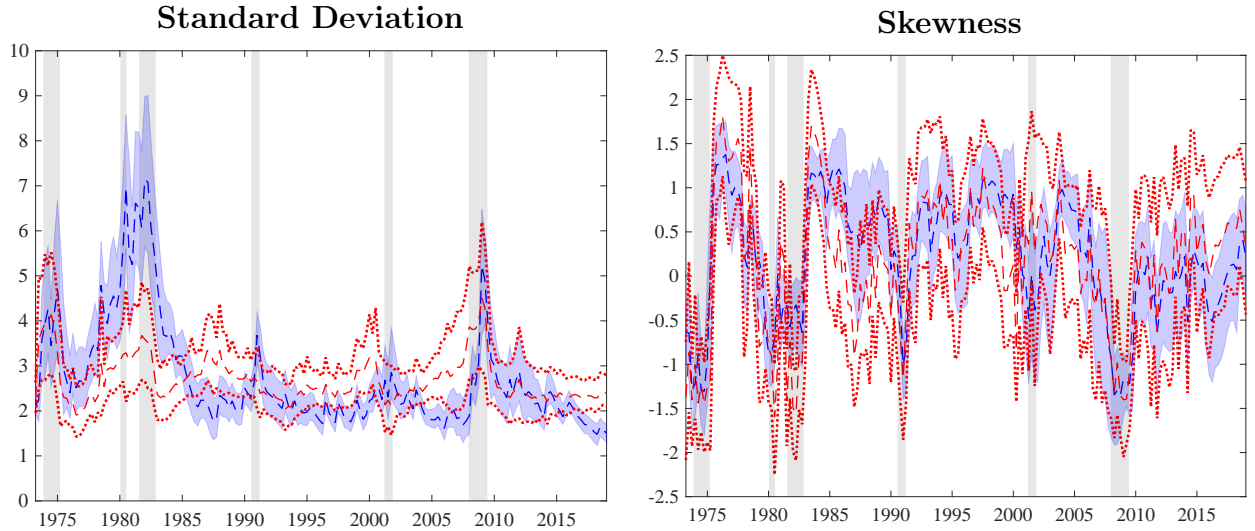
specifications over all criteria. Specifically, it is worth noting that, despite an increase in complexity of about 1% associate with our model, the DIC value is about 5% smaller.

Figure C.1 reports the estimated volatility and skewness from the baseline model (in blue) and the restricted specification (in red). For comparability purposes, both models are estimated using the disaggregated components of the NFCI as predictors.<sup>8</sup> The results of the restricted specification are broadly in line with those reported by Plagborg-Møller et al. (2020). The estimated skewness from their model is cyclical but displays large uncertainty, so that the 90% credible intervals only rarely excludes the zero. Moreover, the simplified specification of the time-varying model does not display the well-known reduction of the volatility occurred during the Great Moderation period.

Overall, comparing the restricted model to the baseline specification highlights the benefits associated with a richer framework, including the score of the predictive likelihood, long-run components, and persistent transitory variations. In terms of volatility estimates, the presence of long-run components, as well as the addition of the score (which for the volatility is a function of the squared prediction errors) as signal for the updating, turn out to be of key importance to track the well-established stylized fact of a substantial decline in volatility from the mid-1980s (McConnell and Perez-Quiros, 2000; Stock and Watson, 2002). The transitory components, on the other hand, allow the model to recover significant variations of the skewness coefficients. This is not surprising, as the unrestricted model implies that the time variation in the parameters reflects current and past discounted variation of the predictors (as well as the information in the scaled score). This implies that high frequency noisy variations of the predictors are averaged out when incorporated into the time-varying dynamics. Moreover, while the skewness from both models set on similar levels at the beginning of the sample and during the 1990s, the asymmetry implied by the restricted specification becomes lower over the mid 1980s, while attaining higher values after the Global Financial Crisis. This pattern supports the addition of secular components, able to track the declining trend of business cycle skewness, as documented by Jensen et al. (2020).

Furthermore, we investigate to what extent our results are affected by the different choice of financial predictors. Re-estimating our baseline model using the two factors employed by Plagborg-Møller et al. (2020), we recover very similar time-varying second and third moments to the ones reported for our baseline specification. Volatility displays a clear countercyclical dynamics, as well as a sharp fall in the mid-1980s. Skewness exhibits pronounced cyclical variation, with recessions characterized by negatively skewed

<sup>8</sup>The mean GDP growth extracted from the two models displays less noticeable differences.



**Figure C.1:** Time-varying moments: *Skt* 4DFI vs. Plagborg-Møller et al. (2020)

*Note:* The plots illustrate the estimated time-varying volatility (left panel) and skewness (right panel) with 90% credible intervals. Results for the *Skt* -4DFI are reported in blue, while red lines report results for the nested version of Plagborg-Møller et al. (2020)'s model. Shaded bands represent NBER recessions.

conditional distributions, and expansions associated with positively skewed distributions. Again, one should not be surprised by these broad similarities. The inclusion of the scaled score as a driver of the time-varying parameters introduces a self-correction mechanism to the model, which allows the parameters to closely track the most pronounced features of the data, regardless of the predictors included in the model. In terms of DIC, the baseline specification with the disaggregated components of the NFCI continues to be preferred with respect to the alternative factors included by Plagborg-Møller et al. (2020).

## D Bayesian estimation

In this Section we outline the Bayesian approach for the estimation of the models. We estimate the vector of static parameters  $\theta$ , and the time-varying parameters  $f_t$ , via an Adaptive Random-Walk Metropolis-Hastings (ARWMH), consisting of the following steps:

- (i) Estimate  $\theta^*$  via Maximum Likelihood to initialize the sampling algorithm;
- (ii) Sample  $\theta^j$  from a random walk candidate density;
- (iii) Compute  $\{f_1, \dots, f_T|\theta^j\}$ , the log-likelihood  $\ell(y|\theta^j)$ , and the posterior  $\pi(\theta^j|y)$ ;
- (iv) Accept or reject  $\theta^j$  according to the MH rule and update the sampling variance;
- (v) Compute the statistics of interest as the percentiles of the empirical distribution function.

In the following subsections, we provide details on the prior specification, including the shrinkage priors and the sparsity step, and we illustrate the steps of the algorithm along with convergence diagnostics.

### D.1 Prior specification

Consider Equations (8), (9), (11), (12), (14) and (15), let  $\phi$  be a generic first-lag partial autocorrelation, while  $\varsigma$  and  $\kappa$  being generic score loadings of the permanent and transitory components, respectively.  $\beta$  is a generic predictor loading,  $\eta$  is the inverse of the Skew-t degrees of freedom, and

$\chi$  is the smoothing parameter of the scaling matrix,  $\mathcal{S}_t$ . The initial values of the permanent components are collected in the vector  $\bar{f}_0 = [\bar{\mu}_0, \bar{\delta}_0, \bar{\gamma}_0]$ . Prior specifications for these parameters read:

$$\phi \sim NID(\mu_\phi, \sigma_\phi) \cdot I_{(\phi \in \Phi)}; \quad (\text{D1}) \quad \beta \sim NID(\mu_\beta, \sigma_\beta); \quad (\text{D2})$$

$$\varsigma, \kappa \sim \mathcal{G}^{-1}(a_j, b_j), \quad j = \varsigma, \kappa; \quad (\text{D3}) \quad \eta \sim \mathcal{G}^{-1}(a_\eta, b_\eta) \cdot I_{(\eta \in \mathcal{H})}; \quad (\text{D4})$$

$$\chi \sim U\left(0, \frac{1}{2}\right); \quad (\text{D5}) \quad \bar{f}_0 \sim \mathcal{N}(\mathbf{m}_0, \mathbf{s}_0). \quad (\text{D6})$$

Prior specification [D1](#) sets the prior distribution for the first autoregressive parameters: we target high persistence, with  $\mu_\phi \lesssim 1$ , with a standard tightness of  $\sigma_\mu = 0.2$ , in line with Bayesian Vector Autoregressive models (see, e.g., [Doan et al., 1984](#); [Sims and Zha, 1998](#)). We restrict the prior distribution to only span the stationary region,  $\Phi$ , by truncating the support, which gives rise to an improper prior distribution as in [Cogley and Sargent \(2005\)](#).<sup>9</sup> We also target the stationarity of the transitory component of the location through a prior on the sum of the autoregressive coefficients ([Sims and Zha, 1998](#)). Let  $\phi^S$  be the sum of two generic autoregressive coefficients,  $\phi^S = \phi^1 + \phi^2$ , we assume  $\phi^S \sim \mathcal{N}(\mu_{\phi^S}, \sigma_{\phi^S}) \cdot I_{(\phi \in \Phi)}$  with  $\mu_{\phi^2} \lesssim 1$  and  $\sigma_{\phi^S} = 0.2$ . Predictor loadings ([D2](#)) are drawn from a Normal distribution with  $\mu_\beta = 0$ , and standard deviations  $\sigma_\beta$  are set to small values of 0.05, 0.2 and 0.1 for the location, scale and shape parameters, respectively. These priors aim at preventing model overfitting, applying an  $L_2$  regularization, akin to the shrinkage induced by a Ridge-type regression. In [D3](#), we set inverse gamma priors for the score loadings, such that they reflect the a priori expectation of small, but positive coefficients, in line with the properties of the score-driven filters (for further discussion, see [Blasques et al., 2014](#)). We set  $a_\varsigma = a_\kappa = 4$ , and  $b_\varsigma = \frac{1}{10}$  and  $b_\kappa = \frac{1}{3}$ , to reflect the properties of the permanent and transitory components. We use an inverse gamma prior for  $\eta$ , the inverse of the degrees of freedom parameter, with  $a_\eta = 2$  and  $b_\eta = 10$  ([D4](#)). In line with [Juárez and Steel \(2010\)](#), these values allow the distribution to explore a wide range of feasible values for  $\nu$ , with a mean of 20 and a median of 10. In order to ensure the existence of, at least, the first three moments, we restrict the support to the  $\mathcal{H} = [0, 0.33]$  set. The prior for the smoothing parameter of the Information matrix is Uniform within the  $[0, 0.5]$  interval ([D5](#)). As per [D6](#), the initial values for the permanent component of time-varying parameters are drawn from a multivariate Gaussian distribution, with mean vector  $\mathbf{m}_0$ , and  $\mathbf{s}_0 = 0.5\mathbf{I}_3$ . The mean vector  $\mathbf{m}_0$  is obtained by matching the moments of the first six years of data.

## D.2 Horseshoe priors and SAVS

Consider the regression model:

$$y_t = b'X_t + e_t, \quad e_t \sim iid(0, \sigma_e^2 I_p) \quad (\text{D7})$$

the Horseshoe (HS) priors of ([Carvalho et al., 2010](#)) posit Ridge-type priors for the coefficients:  $b_i \sim \mathcal{N}(0, \lambda_i \tau)$ , where the hyperparameters  $\lambda_i$  and  $\tau$  control the local (coefficient specific) and the global shrink-

<sup>9</sup>As an alternative to the use of rejection sampling, one can draw the partial autocorrelations to be restricted between 0 and 1 (see, e.g., [Delle Monache and Petrella, 2017](#)). Otherwise, [Planas et al. \(2008\)](#) discuss how to reparametrize the model so as to impose priors on the periodicity and amplitude of an AR(2) cycle with complex roots.



age, respectively. We follow the original paper in setting the hyperpriors as:<sup>10</sup>

$$\lambda_i \sim HC^+(0, 1), \quad \tau \sim HC^+(0, 1), \quad (\text{D8})$$

where  $HC^+(0, 1)$  denotes the standard Half-Cauchy distributions with density function

$$p(z) = \frac{2}{\pi(1+z^2)}, \quad z \in \mathbb{R}^+. \quad (\text{D9})$$

Unlike other common shrinkage priors (e.g. Ridge, Lasso), the HS priors is free of exogenous inputs, implying a fully adaptive shrinkage procedure.

Known pitfalls of shrinkage operators account for parameters not being exactly set to zero (e.g. Ridge), thus increasing parameter uncertainty, or weak selection performances when predictors are correlated (e.g. Lasso). A common remedy to the first pathology is the sparsification of the near-zero elements. Let  $p$  be the number of possible predictors, the sparsification problem can be cast as:

$$b^* = \underset{b}{\operatorname{argmin}} \left[ \frac{1}{2} \|X\hat{b} - Xb\|_2^2 + \sum_{j=1}^p m_j |b_j| \right], \quad (\text{D10})$$

where the sparse coefficients  $b^*$  are obtained minimizing the Euclidean distance between  $Xb$  and the model fit obtained from the shrinkage operator. Additional penalty for the non-zero parameters is controlled by  $m_i$ , which represents a variable specific tuning parameter, generally chosen on the basis of computationally expensive methods (e.g. cross-validation). In their recent contribution, [Ray and Bhattacharya \(2018\)](#) introduce a purely data-driven, and less burdensome solution to the choice of the parameter  $m_i$ , proven to be robust to correlated designs. They suggest to specify the tuning parameter as  $m_i = |\hat{b}_i|^{-2}$  such that the  $j^{\text{th}}$  variable receives a penalization “ranked in inverse-squared order of the magnitude of the corresponding coefficient” ([Ray and Bhattacharya, 2018](#)), an approach similar to the Adaptive Lasso of [Zou \(2006\)](#). The Signal Adaptive Variable Selector (SAVS) algorithm can then be expressed as:

$$b_i^* = \operatorname{sgn}(\hat{b}_i) \|X_i\|^{-2} \max \{ |\hat{b}_i| \cdot \|X_i\|^2 - m_i, 0 \}, \quad (\text{D11})$$

where  $\|\cdot\|$  represents the Euclidean norm of the vector  $X_i$ .

### D.3 Adaptive Metropolis-Hastings

Posterior estimates of the parameters are obtained via simulation by means of the Adaptive Metropolis-Hastings algorithm proposed by [Haario et al. \(1999\)](#). Given that estimated parameters lie in bounded regions of the parameter space, we augment the algorithm with a rejection step to prevent numerical instability due to invalid parameter draws. The algorithm works as follows: given the  $(d \times 1)$  vector of static parameters  $\theta = (\zeta', \kappa', \phi', \bar{f}'_0, \chi, \eta)'$ , we define  $\theta^j$  as the draw of the parameters at the  $j^{\text{th}}$  iteration of the sampler, generated from the random walk kernel:

$$\theta^j = \theta' + \sigma_{j,s} \epsilon \quad \epsilon \sim \mathcal{N}(\mathbf{0}, \Sigma'_H), \quad (\text{D12})$$

---

<sup>10</sup>[Makalic and Schmidt \(2015\)](#) exploit the scale mixture of Inverse Gamma distributions to approximate the Half-Cauchy distributions to propose a tractable framework for posterior simulation via Gibbs sampling. However, this hierarchy features twice as many parameters (auxiliary variables) compared to the original specification.

where  $\sigma_{j,s}$  is a scale parameter that contributes to the stability of the adaptive algorithm.  $\Sigma'_H$  is the covariance matrix of the last  $H$  draws, that is, the covariance matrix updated to reflect the variability of the last  $H$  iterations. Given these two elements, we postulate the following adaptive scheme: we compute the local acceptance rate  $\tilde{\alpha}^s$  each  $s$  iterations; if the acceptance rate is significantly greater (smaller) than the 25-35% target rate, we adjust the scale parameter according to a rescaling function  $r(\tilde{\alpha}^s)$

$$r(\tilde{\alpha}^s) = \begin{cases} \tanh(4\tilde{\alpha}^s + 0.24), & \tilde{\alpha}^s < 0.25 \\ 1, & 0.25 \leq \tilde{\alpha}^s \leq 0.35 \\ 0.88 + \tilde{\alpha}^{s2}, & \tilde{\alpha}^s > 0.35 \end{cases} \quad (\text{D13})$$

such that  $\sigma_{j+1,s} = r(\tilde{\alpha}^s)\sigma_{j,s}$ . **Figure D1** plots the shape of the rescaling function against the admissible range of values for  $\tilde{\alpha}^s$ . Due to the asymmetry of the intervals before and after the 25-35% acceptance

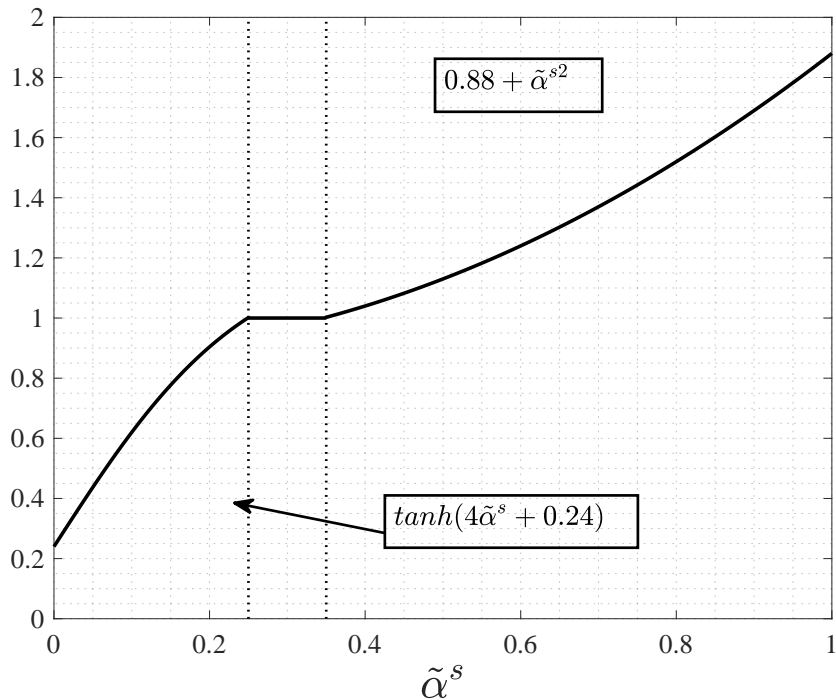


**Figure D1:**  $r(\tilde{\alpha}^s)$  rescaling function

*Note:* The figure plots the rescaling function we apply to the variance of the candidate distribution to target an acceptance rate between 25% and 35%.

region, the two branches of the reshaping function feature different slopes and curvatures.

In addition, every  $U \leq H$  iterations, we use the last  $H$  draws to recalibrate the covariance matrix of the proposal distribution:  $\Sigma'_H = \frac{\tilde{K}}{\sqrt{H-1}}$ , where  $\tilde{K}$  is the  $(H \times d)$  centered matrix of the last  $H$  draws, obtained as  $K - \mathbb{E}[K]$ ; in this process we also reinitialize the scale parameter at the value of  $\frac{2.38}{\sqrt{d}}$ , as suggested by [Gelman et al. \(1996\)](#). According to the Metropolis-Hasting procedure, we accept  $\theta^j$  with probability  $p = \min \{1, \exp(\pi(\theta^j|y) - \pi(\theta^i|y))\}$ , where  $\pi(\theta^j|y) \propto \pi(\theta^j)\ell(y|\theta^j)$  is the posterior distribution conditional on draw  $j$ . Discarded draws are replaced by the latest accepted draw. In order to prevent failures of the algorithm, we discard draws that do not lie in the bounded region of the parameter space, replacing them as specified. We set the number of iterations to 20000, of which we keep the last 40%. We reduce dependence between consecutive draws by “*thinning*” each 2 realizations. Posterior distributions are eventually obtained

from a sample of 4000 iterations. We adjust the scale parameter each hundred iterations ( $s = 100$ ), while the adaptive step takes place every  $U = 1500$  iterations, considering  $H = 2500$  past iterations.<sup>11</sup> The algorithm is rather efficient, and a complete chain from the baseline model in Section 4 can be obtained in less than 3 minutes, whereas for the large data model, a complete chain can be obtained in about 7 minutes.

---

**Algorithm 1:** Adaptive Random-Walk Metropolis-Hastings

---

```

for  $j=1,2,\dots,N$  do
  Generate:  $\theta^j \sim \mathcal{N}(\theta', \sigma_{j,s}^2 \Sigma'_H)$  ;
  if  $\theta^j \in \Theta$  then
    Filtering step
    Compute:  $\{f_1, \dots, f_T | \theta^j\}$ ;
    Evaluate:  $\ell(y | \theta^j)$  and  $\pi(\theta^j | y) \propto \pi(\theta^j) \ell(y | \theta^j)$  ;
    Evaluate:  $p = \min \{1, \exp(\pi(\theta^j | y) - \pi(\theta' | y))\}$  ;
    MH step
    Draw:  $u \sim U[0, 1]$  ;
    if  $u < p$  then
      |  $\theta' = \theta^j, \quad \alpha^j = 1$ ;
    end
  end
  Adaptive step
  if  $j \pmod s = 0$  then
    |  $\sigma_{j+1,s} = \sigma_{j,s} * r(\tilde{\alpha}^s)$ 
  end
  if  $j \pmod U = 0$  then
    |  $\Sigma'_H = Cov(\{\theta^i\}_{i=j-H}^j), \quad \sigma_{j,s} = \frac{2.38}{\sqrt{d}}$ 
  end
end

```

---

*Note:* the notation “ $a \pmod b$ ” represents the modulo operation, while “ $-s$ ” indicates the previous  $s$  draws.

## D.4 MCMC Convergence Diagnostics

Under general, appropriate regularity condition, the (Adaptive) Random-Walk Metropolis-Hastings algorithm is ensured to converge, such that parameters are drawn from their true posterior distribution. Robert and Casella (2004) show that Metropolis-Hastings Markov chains are required to be irreducible (the probability of jumping from a state to another is always positive) and aperiodic (there is a non-zero probability that the chain will not jump) over the parameter space. The aforementioned conditions are weak, and generally hold in practice. Several tools are available to determine the convergence of Markov chains to their ergodic distributions (see, e.g., Gelman et al., 1995; Cowles and Carlin, 1996; Robert and

---

<sup>11</sup>The adaptive process starts when  $j \geq H$ , while the scale updating takes place from the 100<sup>th</sup> iteration

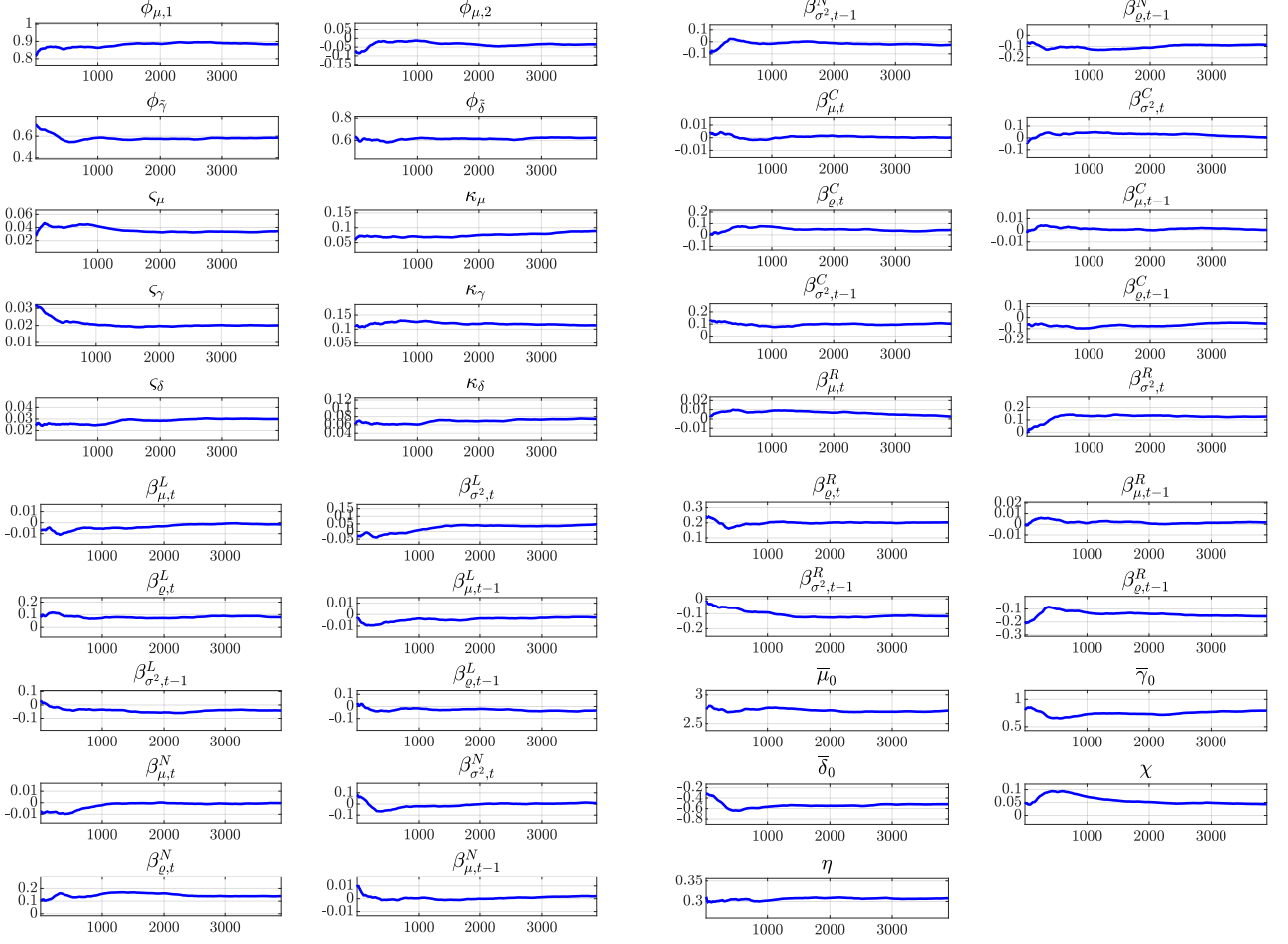


**Figure D2:** Cumulative averages

*Note:* The panels show the cumulative averages of the post burn-in sample.  $\phi$ s are the autoregressive parameters,  $\kappa$ s and  $\varsigma$ s are the smoothing parameters for the transitory and permanent components, respectively,  $\bar{\mu}_0$ ,  $\bar{\gamma}_0$  and  $\bar{\delta}_0$  are the initial values of the permanent components,  $\chi$  is the smoothing parameter of the scaling matrix and  $\eta$  is the inverse of the degrees of freedom.  $\beta$ s are the loadings on the subcomponents of the NCFI: Leverage (L), Nonfinancial Leverage (N), Credit (C) and Risk (R).

Casella, 2004). Here, we consider three types of diagnostics: the graphical inspection of cumulative means, the analysis of variance of several chains, and a test on the ergodic averages. In these exercises we check the convergence of the post burn-in sample,  $\Theta^*$ , for our preferred model specification. We draw  $N = 20000$  replications and we keep the last  $n^* = 4000$  replications, after thinning each two posterior draws to reduce the autocorrelation of the chains.

As a first step, we inspect the cumulative averages of the retained draws. A smooth and stable plot suggests that the chain has converged to the expected value of its invariant distribution. The cumulative averages plotted in Figure D2 appear all smooth and converging to the single value  $\mathbb{E}[\Theta^*]$ , suggesting that the chains have reached convergence.

Next, we turn to analysis of variance techniques, as advocated by Gelman and Rubin (1992). Due to the efficiency of our algorithm, we consider  $m = 100$  parallel chains to compare the dispersion between,  $B$ ,

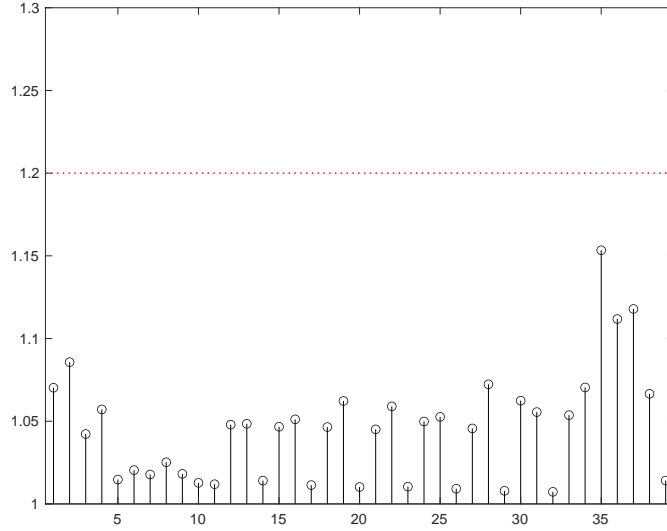


**Figure D3:**  $R$  statistic

*Note:* The plot reports [Gelman and Rubin \(1992\)](#)  $R$  statistic for each parameter of the model. The statistics are computed for  $J=39$  parameters and  $m=100$  chains.

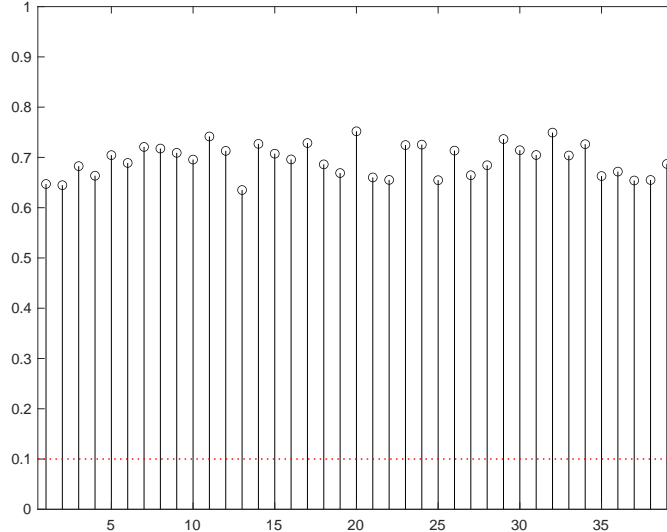


**Figure D4:** p-values for the ergodic averages test

*Note:* The plot reports the p-values for [Geweke \(1992\)](#) test on ergodic averages.

and *within*,  $W$ , chains, and test that the former is greater than the latter. Specifically,

$$B = \frac{n^*}{m-1} \sum_{i=1}^m (\bar{\theta}_i^* - \bar{\theta}^*)^2 \quad \text{and} \quad W = \frac{1}{m(n^* - 1)} \sum_{i=1}^m \sum_{j=1}^J (\theta_{i,j}^* - \bar{\theta}_i^*)^2,$$

where  $\bar{\theta}_i^* = \frac{1}{n^*} \sum_{n=1}^{n^*} \theta_n^*$  and  $\bar{\theta}^* = \sum_{i=1}^m \bar{\theta}_i^*$ . These statistics are used to consistently estimate the marginal posterior variance of  $\theta^*$  as the weighted average of  $W$  and  $B$  as:

$$\hat{\sigma}_{\theta^*}^2 = \frac{n-1}{n} W + \frac{1}{n} B.$$

Convergence can thus be monitored by means of  $\hat{R} = \sqrt{\hat{\sigma}_{\theta^*}^2 W^{-1}} \geq 1$ ; [Gelman \(1995\)](#) suggest that  $R < 1.2$  can be used as an indication to accept the convergence of the MCMC. We report the  $R$  statistics in [Figure D3](#), which make a strong case for the convergence of the chains.

At last, we follow Geweke (1992) and test the ergodic averages of the time series of draws. We split the  $n^*$  draws into a subsample  $B$  of  $n_b^* = 0.1n^*$  and another one  $A$  of  $n_a^* = 0.5n^*$ , and compute

$$\bar{\theta}_b^* = \frac{1}{n_b^*} \sum_{j=1}^{n_b^*} \theta_j^* \quad \text{and} \quad \bar{\theta}_a^* = \frac{1}{n_a^*} \sum_{j=n_a^*}^{n^*} \theta_j^*.$$

As we only consider the post burn-in sample,  $\bar{\theta}_b^*$  and  $\bar{\theta}_a^*$  are the ergodic averages at the beginning and at the end of the convergence sample, and should therefore behave similarly. This can be tested by means of a simple  $t$ -test on the standardized difference between  $\bar{\theta}_b^*$  and  $\bar{\theta}_a^*$

$$z_G = \frac{\bar{\theta}_a^* - \bar{\theta}_b^*}{\sqrt{\hat{V}(\bar{\theta}_a^*) + \hat{V}(\bar{\theta}_b^*)}} \sim N(0, 1).$$

We report the p-values for the tests in Figure D4. We do not reject the null hypothesis for any of the parameters.

## D.5 Sensitivity to priors

In Section 3.2 we have emphasized the role played by the priors choice when estimating a highly parametrized model on a relatively small sample of data. A relevant question to ask at this point is to what extent our results, in particular those regarding the cyclical and low frequency variations of the conditional distribution of GDP growth, are affected by our choice for the priors. To answer this question, in Figure D5 we report the location, log-scale and shape parameters that one would retrieve by sampling the static parameters,  $\theta$ , directly from their prior distribution,  $\pi(\theta)$ . The priors encode some feature of the model parameters which one would expect ‘a priori’ to hold in the model estimates. Specifically, we target a relatively small time variation of the permanent components, and larger and persistent variation of the transitory components of the parameters. These priors are reflected into smaller ‘a priori’ credible intervals for the permanent components of the time-varying parameters, as opposed to the transitory components’. Yet, these priors do not translate directly into any particular pattern for the time variation of the location, (log-) scale and shape of the distribution. In fact, the green plots in Figure D5 highlight that our priors remain quite agnostic about the values of the time varying parameters and their dynamics over time. We overlay in the panels the posterior median and credible intervals for the same parameters; the latter show distinct patterns in terms of cyclicity and trends, which reflect the information content of the data. As a second check, we ask ourselves to what extent the results are sensitive to the exact specification of the prior we chose. In this respect, there is a multitude of exercises one could perform. Here we focus mainly on the sensitivity of the results with respect to the prior of the smoothing coefficients ( $\varsigma_i$  and  $\kappa_i$ , where  $i = \{\mu, \gamma, \delta\}$ ), due to the importance of these parameters for the estimated time variation of the parameters (of any observation-driven model). Figure D6 reports the posterior estimates of the time-varying parameters for alternative prior choices: we vary the scale of the inverse gamma priors for the smoothing coefficients scaling them by a factor  $c = \{0.5, 1.5, 1.75\}$ , but preserving their relative proportions. In each panel we confront the posterior estimates obtained with the alternative priors against the baseline one.<sup>12</sup> Small variation of the priors do not meaningfully affect the estimates of the time-varying parameters.

<sup>12</sup>We have repeated the same exercise also varying the tightness of the priors of the autoregressive coefficients of the model. The results of this exercise are virtually identical to the one reported in Figure D6.

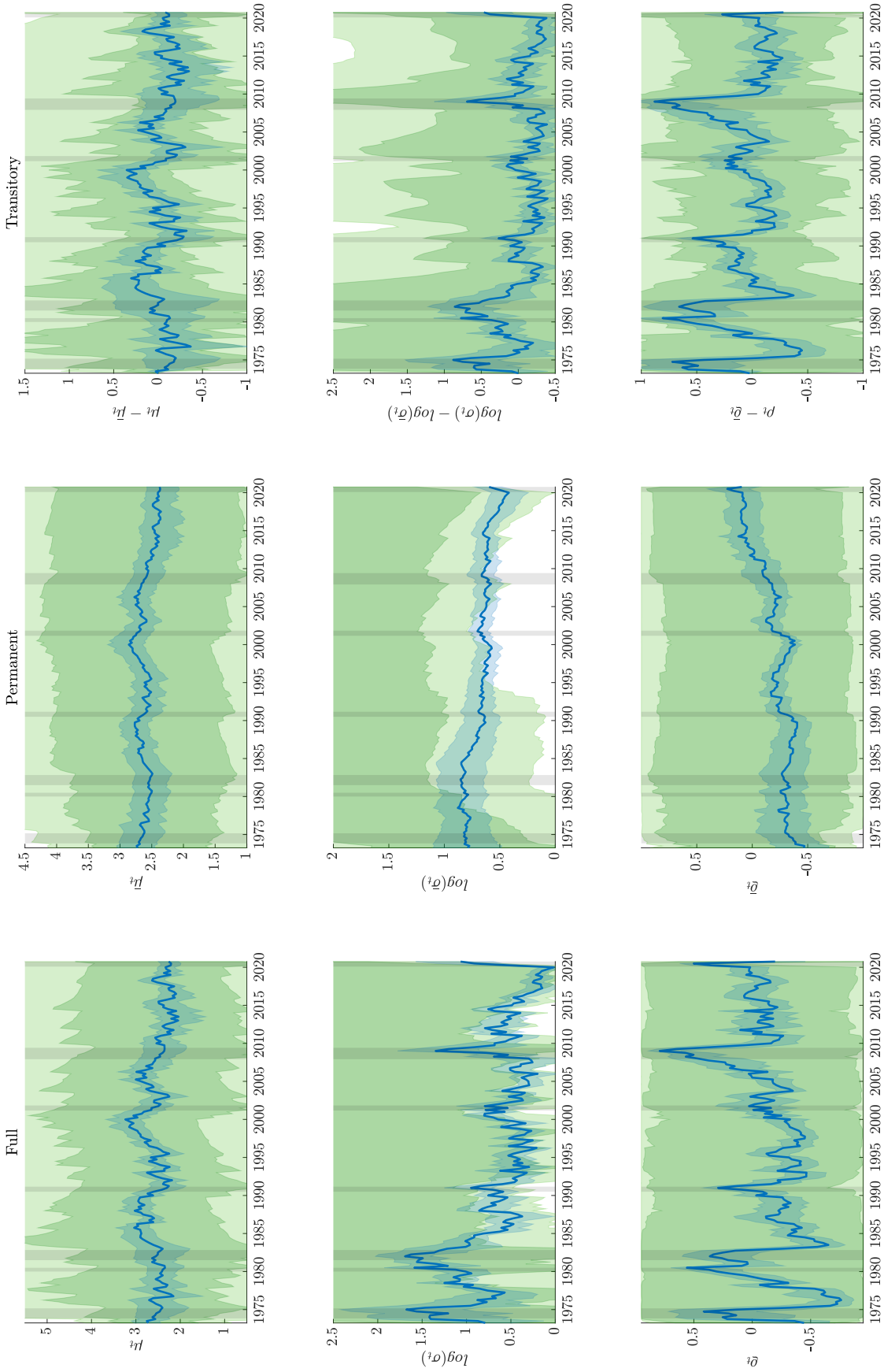


**Figure D5:** Sampling from the prior distribution

*Note:* The figure reports the 90/99% credible sets for the time-varying parameters estimated by sampling from the prior distribution of the static parameters of the model,  $\theta$ . We also separately report the permanent and the transitory components for each parameter. In blue we report the time-varying parameters estimated by sampling from the posterior distribution of the static parameters,  $\theta$ , along with the 90% credible set. Shaded bands represent NBER recessions.

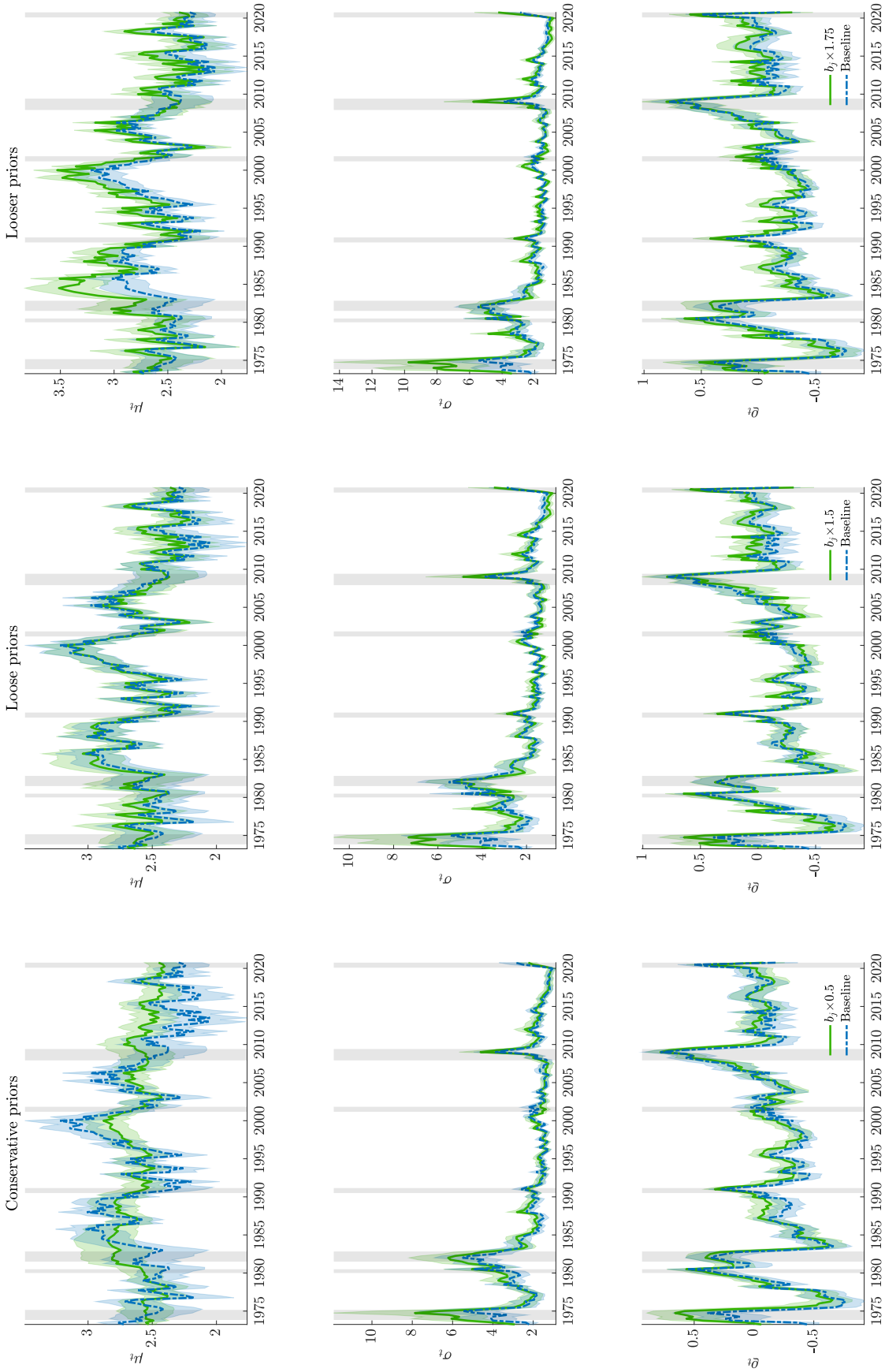


**Figure D6:** Smoothing parameters prior sensitivity

*Note:* The panels report the parameters, and the associated 90% credible sets, estimated from specifications featuring different scales,  $b_j$  (where  $j = \{\varsigma_i, \kappa_i\}$  and  $i = \{\mu, \gamma, \delta\}$ ), of the prior distribution of the smoothing coefficients. In each column we report the posterior estimate associated with priors set to  $c \times b_j$ . Each panel column corresponds to a different value of the scaling constant  $c$ : conservative ( $c = 0.5$ ), loose ( $c = 1.5$ ), and looser ( $c = 1.75$ ). Shaded bands represent NBER recessions.



## E Monte Carlo Exercise

In this Section we outline a Monte Carlo exercise with the aim of illustrating the small-sample properties of the Skew-t model described in [Section 3](#). We are interested in the reliability of the estimates of the asymmetry parameter and, in particular, whether the model is able to correctly disentangle the movements in the asymmetry parameter from the movements in the location and scale parameters.

We simulate  $T=250$  observations for the parameters of location,  $\mu_t$ , scale,  $\sigma_t$ , and asymmetry,  $\varrho_t$ , for every period  $t$  from the  $Sk_{t\nu}(\mu_t, \sigma_t, \varrho_t)$  to obtain the series  $\{y_t\}_{t=1}^T$ , then used to estimate the model discussed in [Section 3](#) (excluding explanatory variables). Therefore, regardless of the DGP considered we always estimate a two component specification for all the three time-varying parameters. This approach mimics the true estimation process carried out on real data, to approximate the conditional distribution of the underlying GDP growth. We first consider ad-hoc specifications for the location and scale parameters (AR(2) and AR(1), respectively). Then, we turn to DGPs that replicate closely the dynamic properties of the time-varying parameters we estimate from the data (and in particular replicate the correlation between the location and scale parameter that we observe in the data). For the shape parameter, we consider a number of different DGPs, including no asymmetry, constant asymmetry, a single break in the asymmetry, and cyclical asymmetry.

In the first DGP, data are simulated from a specification featuring symmetric distributions, with independent, time-varying location and volatility, therefore aiming at checking that the model does not pick up any asymmetry when this is not a feature of the data. The second DGP considers the case in which the asymmetry parameter experiences a jump, from 0 to 0.5 after 100 observations, hence implying negatively skewed distributions in the second part of the sample. This case sheds light on the adaptiveness of the model, and provides a clear framework for illustrating the distinctive role played by the secular and transitory components. The third and fourth DGPs consider a specification for the location and scale parameter that replicate the basic features of the estimated location and scale parameters, e.g. a mildly negative correlation, whereas the shape parameter is constant, either at zero or at a positive value.<sup>13</sup> In the last DGP, the asymmetry parameter varies over time, with cyclical fluctuations. To ensure that we replicate the transitory variation in the parameters, we simulate the three parameters from a VAR(1), with the system parameters estimated on the time-varying parameters obtained from the  $Sk_{t\nu}$ -4DFI specification. For each DGP we perform  $N=500$  replications and we estimate the parameters of the two-component model using the estimation approach introduced in the main text, and detailed in [Appendix D](#).

We simulate  $\mu_t$ ,  $\gamma_t = \log(\sigma_t)$ , and  $\delta_t = \text{arctanh}(\varrho_t)$  from the following processes:

### DGP1: (No asymmetry)

$$\mu_t = 0.125 + 1.2\mu_{t-1} - 0.25\mu_{t-2} + \epsilon_t, \quad \epsilon_t \sim N(0, 0.05);$$

$$\gamma_t = 0.95\gamma_{t-1} + \epsilon_t, \quad \epsilon_t \sim N(0, 0.025);$$

$$\delta_t = 0.$$

---

<sup>13</sup>Specifically, we fit a VAR(1) to the location and log-scale parameters estimated from the data, and use these estimates for the DGPs.

**DGP2: (Single break)**

$$\mu_t = 0.125 + 1.2\mu_{t-1} - 0.25\mu_{t-2} + \epsilon_t, \quad \epsilon_t \sim N(0, 0.05);$$

$$\gamma_t = 0.95\gamma_{t-1} + \epsilon_t, \quad \epsilon_t \sim N(0, 0.025);$$

$$\delta_t = \begin{cases} 0, & t \leq 100 \\ 0.5, & t > 100 \end{cases}.$$

**DGP3: (Correlated location, scale and no asymmetry)**

$$\begin{bmatrix} \mu_t \\ \gamma_t \end{bmatrix} = \begin{bmatrix} 0.29 \\ -0.12 \end{bmatrix} + \begin{bmatrix} 0.89 & 0.01 \\ 0.06 & 0.94 \end{bmatrix} \begin{bmatrix} \mu_{t-1} \\ \gamma_{t-1} \end{bmatrix} + \epsilon_t, \quad \epsilon_t \sim N(\mathbf{0}, \Omega),$$

where

$$\Omega = \begin{bmatrix} 0.008 & -0.001 \\ -0.001 & 0.015 \end{bmatrix}$$

and  $\delta_t = 0, \forall t$ .

**DGP4: (Correlated location, scale and constant asymmetry)**

$$\begin{bmatrix} \mu_t \\ \gamma_t \end{bmatrix} = \begin{bmatrix} 0.29 \\ -0.12 \end{bmatrix} + \begin{bmatrix} 0.89 & 0.01 \\ 0.06 & 0.94 \end{bmatrix} \begin{bmatrix} \mu_{t-1} \\ \gamma_{t-1} \end{bmatrix} + \epsilon_t, \quad \epsilon_t \sim N(\mathbf{0}, \Omega),$$

where

$$\Omega = \begin{bmatrix} 0.008 & -0.001 \\ -0.001 & 0.015 \end{bmatrix}$$

and  $\delta_t = 0.5, \forall t$ .

**DGP5: (Cyclical asymmetry)**

$$\begin{bmatrix} \mu_t \\ \gamma_t \\ \delta_t \end{bmatrix} = \begin{bmatrix} 0.40 \\ -0.38 \\ -0.33 \end{bmatrix} + \begin{bmatrix} 0.85 & 0.03 & -0.06 \\ 0.17 & 0.88 & 0.13 \\ 0.14 & -0.09 & 0.95 \end{bmatrix} \begin{bmatrix} \mu_{t-1} \\ \gamma_{t-1} \\ \delta_{t-1} \end{bmatrix} + \epsilon_t, \quad \epsilon_t \sim N(\mathbf{0}, \Omega),$$

where

$$\Omega = \begin{bmatrix} 0.008 & -0.001 & -0.007 \\ -0.001 & 0.015 & 0.008 \\ -0.007 & 0.008 & 0.025 \end{bmatrix}$$

For all the DGPs, the model correctly picks up the time variation in the location and scale with great precision, and the degrees of freedom are estimated without bias. These results are not reported in the interest of brevity, but are available upon request. Hence, in what follows we comment on the ability of the model to track the underlying asymmetry of the distribution. For the first four DGPs, we report the true asymmetry parameter and the 99, 95, 90 and 75 confidence bands for the estimated counterpart. For the fifth DGP we consider the median difference between the estimated and the simulated parameters.

[Figures E1](#) and [E4](#) show that when the distribution is symmetric, the estimated median parameter, and the associated confidence bands, remain close to zero with small variability. Therefore, the model clearly

captures the symmetry of the underlying data generating process, and correctly disentangles the time variations of the volatility from changes in the asymmetry of the distribution in simple settings (DGP1), as well as when location and scale are correlated (DGP3). The filter is also able to detect the case with constant negative skewness (DGP4), in spite of the dynamic correlation between location and scale. The model does not confound variations of the first two moments of the data with variation of the asymmetry (Figure E5). Interestingly, for all the cases where the asymmetry parameter is fixed at a positive value, the transitory components are always estimated to be approximately zero, suggesting that no variation at all is captured. Whereas, the secular components show minimal variation, always fluctuating around the true value.<sup>14</sup> For this case we also investigate what happens when the initialization of the filter is away from the true parameter. The filter neatly discovers the true level of asymmetry relatively quickly (i.e. after roughly 20 observations), and the parameter sets around the true value.

In Figure E2 we report the results for the case of a single break in the asymmetry parameter. Until the jump takes place, the estimated asymmetry remains centered around zero, while it timely reacts to the jump occurring on the 100<sup>th</sup> observation. Furthermore, due to the presence of a slow-moving trend component, the model fully captures the extent of the asymmetry in the second part of the sample in just 50 observations. Within this case, we also investigate to what extent the model is able to recognize the persistent nature of the shift in the asymmetry. Figure E3 reports the estimated permanent and transitory components, respectively. The permanent component picks up the jump in a timely manner, and contributes to most of the variability of the estimated parameter. In addition, the first few observations after the jump are partly captured by the model as short-lived movements, reverting to zero soon after.

Lastly, we report in Figure E6 the difference, and the associate confidence set, between the simulated and the estimated parameters. Despite co-movements in the location, scale and asymmetry parameters, the model clearly captures the transitory variations of the latter, reported in red. The estimated parameter converges to the correct values after few observations, with small deviations, as suggested by the narrow bounds. Key for the identification of parameters' variation is that, as discussed in Section 4, shifts in the shape parameter map into a time-varying correlation between the first and second moments of the data. Therefore, in spite of the (dynamic) interaction between the key parameters of the distribution, the model correctly identifies, in a timely manner, movements in the asymmetry of the distribution.

---

<sup>14</sup>These results are not reported but available upon request.

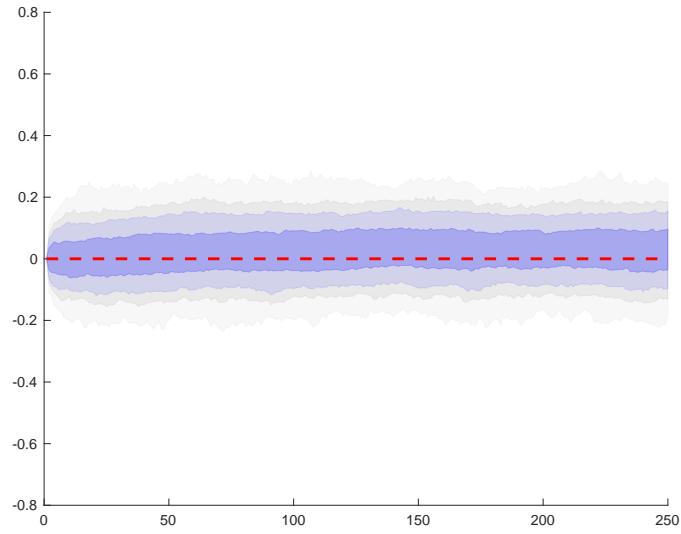


**Figure E1: DGP1 - No asymmetry.**

*Note:* The median simulated parameter is reported in red, while shades of blue represent the 99<sup>th</sup>, 95<sup>th</sup>, 90<sup>th</sup>, 75<sup>th</sup>, 25<sup>th</sup>, 10<sup>th</sup>, 5<sup>th</sup> and 1<sup>st</sup> percentiles of the empirical distribution of the estimated parameter.

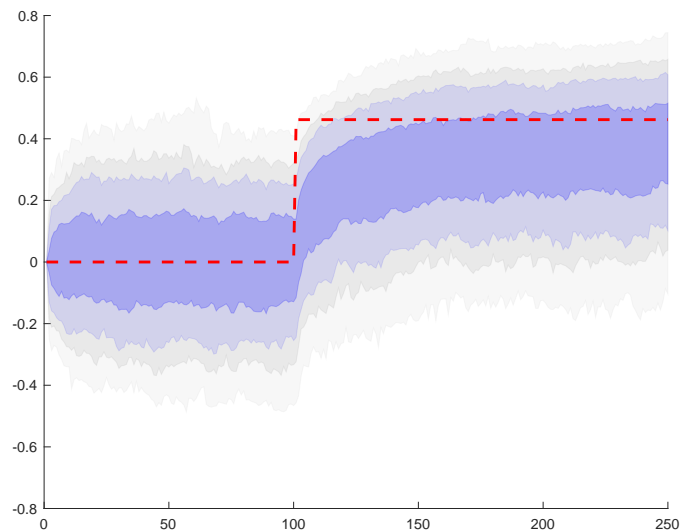


**Figure E2: DGP2 - Single break in asymmetry.**

*Note:* The median simulated parameter is reported in red, while shades of blue represent the 99<sup>th</sup>, 95<sup>th</sup>, 90<sup>th</sup>, 75<sup>th</sup>, 25<sup>th</sup>, 10<sup>th</sup>, 5<sup>th</sup> and 1<sup>st</sup> percentiles of the empirical distribution of the estimated parameter.

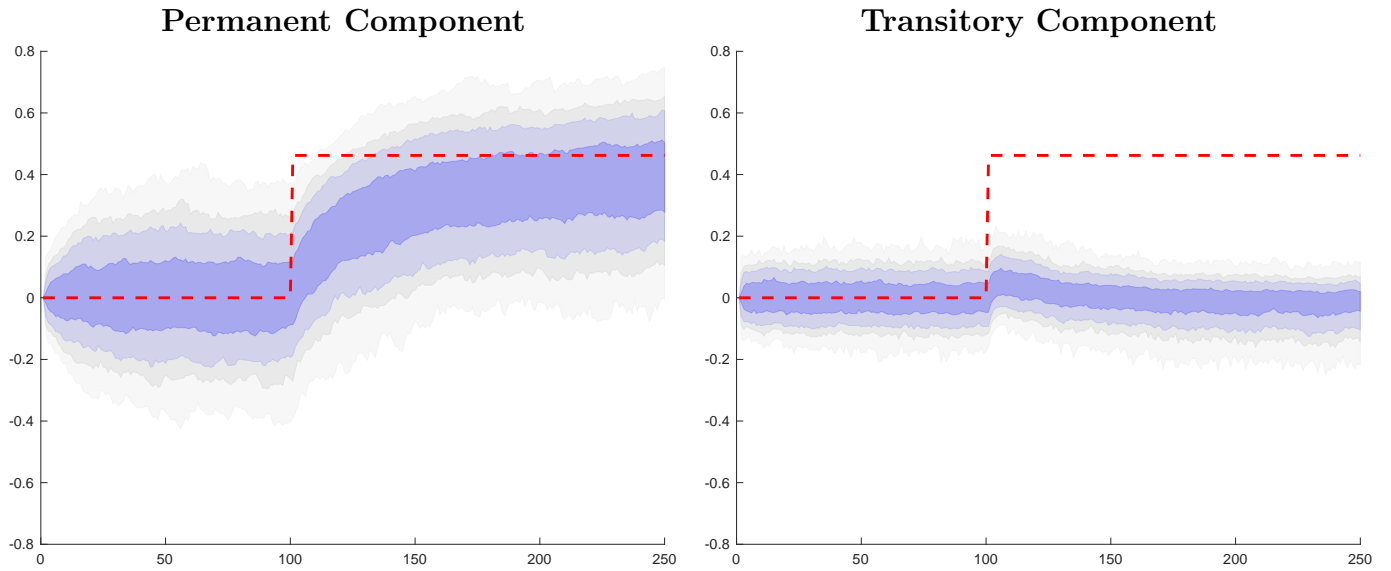


**Figure E3:** Permanent and transitory components for the **DGP2** case.

*Note:* The median simulated parameter is reported in red, while shades of blue represent the 99<sup>th</sup>, 95<sup>th</sup>, 90<sup>th</sup>, 75<sup>th</sup>, 25<sup>th</sup>, 10<sup>th</sup>, 5<sup>th</sup> and 1<sup>st</sup> percentiles of the empirical distribution of the estimated parameter.

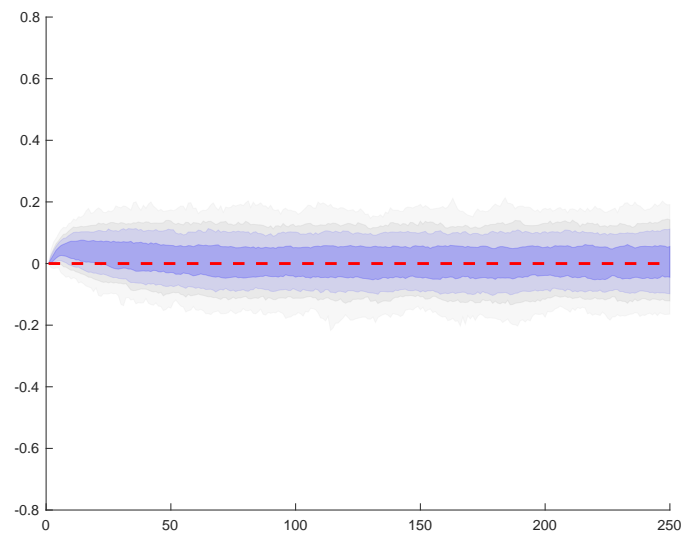


**Figure E4:** **DGP3** - Correlated location, scale and no asymmetry.

*Note:* The median simulated parameter is reported in red, while shades of blue represent the 99<sup>th</sup>, 95<sup>th</sup>, 90<sup>th</sup>, 75<sup>th</sup>, 25<sup>th</sup>, 10<sup>th</sup>, 5<sup>th</sup> and 1<sup>st</sup> percentiles of the empirical distribution of the estimated parameter.

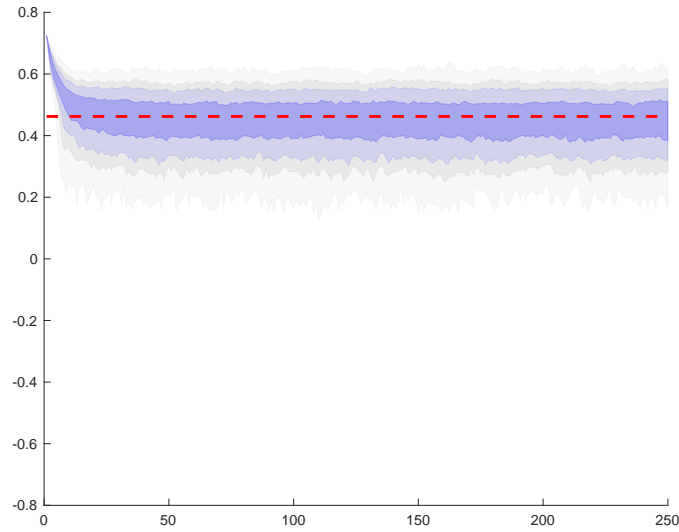


**Figure E5: DGP4** - Correlated location, scale and constant negative skewness.

*Note:* The original parameter is reported in red, while shades of blue represent the 99<sup>th</sup>, 95<sup>th</sup>, 90<sup>th</sup>, 75<sup>th</sup>, 25<sup>th</sup>, 10<sup>th</sup>, 5<sup>th</sup> and 1<sup>st</sup> percentiles of the empirical distribution of the estimated parameter. The initial point for the estimation is set to 0.75.

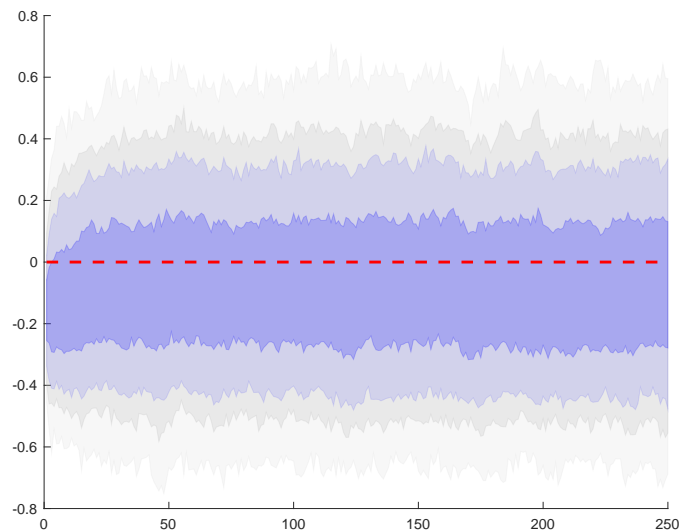


**Figure E6: DGP5** - Cyclical asymmetry.

*Note:* The plot reports the dispersion round the difference between the simulated and estimated skewness. The red dashed line represents the perfect match while shades of blue represent the 99<sup>th</sup>, 95<sup>th</sup>, 90<sup>th</sup>, 75<sup>th</sup>, 25<sup>th</sup>, 10<sup>th</sup>, 5<sup>th</sup> and 1<sup>st</sup> percentiles of the empirical distribution of such difference.

## F Data

In this Appendix we provide additional details on the data sources. We focus on (real) GDP growth in the US, and we measure financial conditions using the Chicago FED National Financial Condition Index (NFCI), and its subcomponents (Brave and Butters, 2011). The NFCI is a weekly index tracking the status of money markets, debt and equity markets, and the banking sector (comprehensive of the “shadow” banking sector). The contribution of these sectors maps into three subindices, each of which gauges financial conditions in terms of risk, leverage, and credit (refer to Brave and Butters, 2012, for further details). We use quarterly data on economic activity and financial conditions over the period 1973Q1 to 2018Q4, where the starting date for the analysis is dictated by the availability of the NFCI.

As new information is available, these indices are standardized. Thus, when an index takes a value of 1 (-1), it signals that the financial conditions are one standard deviation tighter (looser) than their historical average. Consistently with the concept of financial tightening, the measure relating to the risk subcomponent positively contributes to the NFCI, reflecting increasing risk premia. In contrast, measures of leverage and credit receive negative weights in response to lower asset values and declining liquidity in the financial sector. The top panel of Figure F1 plots the NFCI against GDP growth, whereas the bottom panels report the NFCI subcomponents. The NFCI (and its three subcomponents) spikes during recessions, as indicated by the gray-shaded bands, and displays a clear negative correlation with GDP growth, suggesting that periods of financial overheating coincide with severe economic troughs, as documented by Adrian et al. (2019). The NFCI closely tracks the risk subcomponent, due to high weights being attached to some of the risk variables, such as the VIX index. This is consistent with the observation that volatility of the stock market is an accurate predictor of financial instability (see, e.g. Bekaert and Hoerova, 2014). The leverage component shows strong procyclicality, and tends to pick up on high values before other indices, consistently with the findings of Adrian and Shin (2010) and Jordà et al. (2013). Lastly, measures of credit spread and credit risk are contained in the risk and credit components (Krishnamurthy and Muir, 2017).

Alongside these subindices, the Chicago FED also produces the nonfinancial leverage (NFL) index (bottom right panel of Figure F1). This series tracks developments in the nonfinancial credit market using data on household and nonfinancial business leverage. Household data receive weights roughly 1.5 times higher than the latter. Mian and Sufi (2010) argue that the build up of financial instability leading to the Great Recession was mainly due to an “over-leveraged” household sector. Similarly, Jensen et al. (2020) observe that increasing households and firms leverage anticipates a deepening of business cycle skewness. A closer examination of the panel suggests that the massive deleveraging started in the early 2008 coincides with the beginning of the recession in the same year. This measure can thus be intended as an “early-warning” signal for economic downturns. In addition, this index is a clear leading indicator of the HP-filtered credit-to-GDP ratio measure, frequently considered as a leading signal of financial distress (Drehmann et al., 2010; Jordà et al., 2017).<sup>15</sup>

**Real-time data.** In Sections 5 and 6 we evaluate the performance of our models, and compare them to a number of alternatives, considering both an in- and out-of-sample forecasting exercise. For these exercises, we use real time data on GDP, provided by the Philadelphia FED’s Real Time Data Research

---

<sup>15</sup>Hasenzagl et al. (2020) extensively investigate the relation between the Nonfinancial leverage index and the Credit-to-GDP ratio index for forecasting purposes.

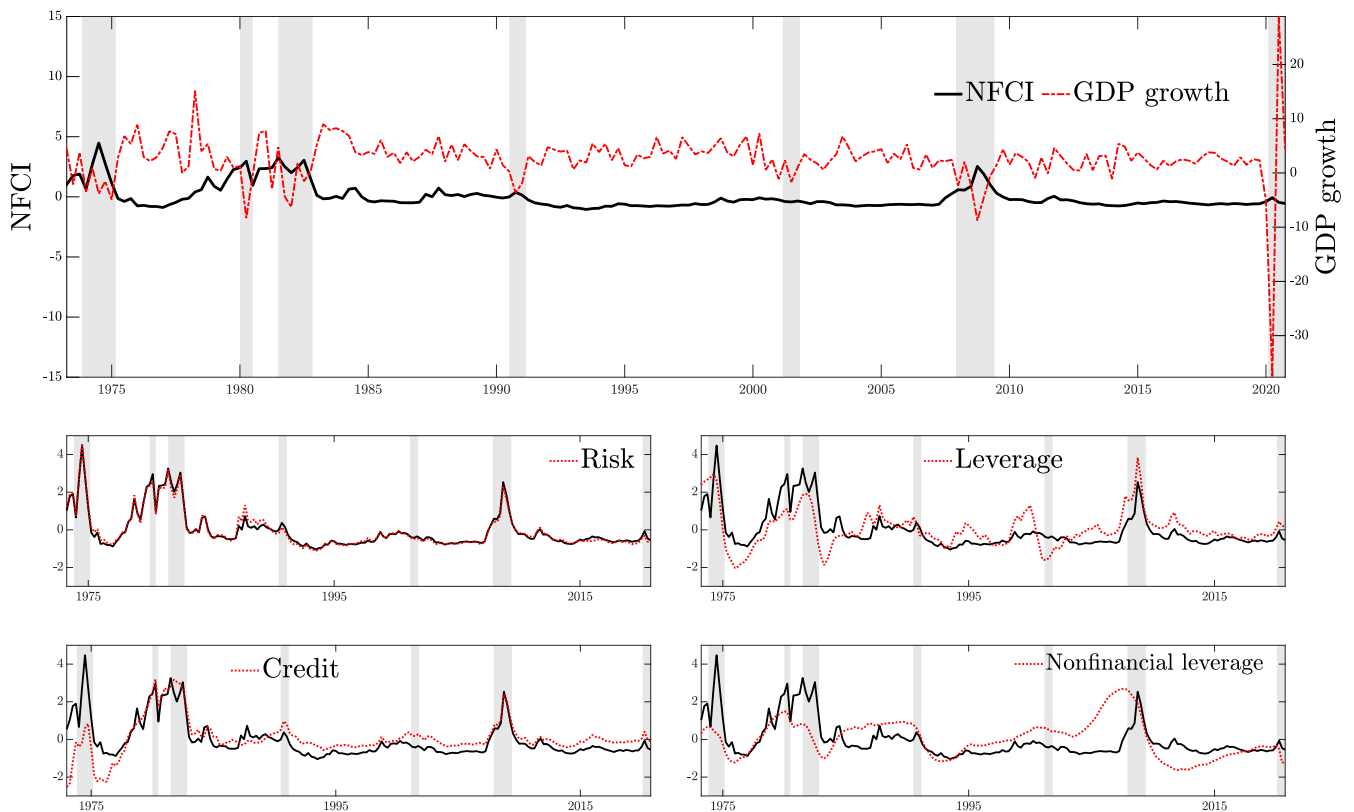


**Figure F1:** National Financial Condition Index and subcomponents

*Note:* The top panel illustrates the evolution of the NFCI and of GDP growth. Lower panels plot the risk, leverage, credit and nonfinancial leverage subcomponents, respectively. Shaded bands represent NBER recessions.

Center. This dataset contains GDP observations available at a particular vintage date, that is, GDP values available in the second week of the middle month of each quarter, as described in [Croushore and Stark \(2001\)](#). GDP growth undergoes substantial revisions, in particular over the first releases, and even more so around turning points (see, e.g. [Croushore, 2011](#)). Despite there is no consensus on what releases to use as “actual” data for forecast evaluation ([Croushore, 2006](#)), we evaluate models using the latest release.<sup>16</sup>

While real time data are available for GDP, the same is not true for the NFCI and its subcomponents. These are common factors in a broad panel of financial indicators, extracted using state-space methods. As such, these indicators are always revised at any point in time, when new information arrives. To this extent, we can only use a pseudo real-time dataset for the NFCI and its subcomponents. In Section 6, we use the disaggregated contributions of all financial indicators which form the basis of the NFCI, as illustrated in [Brave and Butters \(2012\)](#).<sup>17</sup> As GDP data are released about 45 days after the end of the reference quarter, we assume that it is at that point in time that the forecaster estimates the model and produces the forecasts. The weekly nature of these data allows us to include all the available information, by averaging all the weeks within the reference quarter, meaning that we can use all the information made available within the reference quarter. Despite not being real-time, this method comes the closest to mimic the available information set at the time of the forecasts.

<sup>16</sup>This choice implies that the forecast error produced by our models also accounts for a “measurement error” component, induced by possible GDP measurement redefinitions, that took place over the considered forecast sample (for further discussion, see [Stark and Croushore, 2002](#)). The results of our forecast exercise would be qualitatively similar to the ones reported if we were to target the ‘advanced’ (i.e. third) revision of GDP growth.

<sup>17</sup>We are grateful to the authors and the Chicago FED for making the full panel of weighted contribution of the financial indicators available for this work.



## F.1 Main data sources and mnemonics

Data on quarterly real economic activity come from the Federal Reserve Bank of St. Louis FRED dataset (mnemonic; GDPC1). The NFCI and the relative risk, leverage, nonfinancial leverage and credit subcomponents are downloaded from the same source (mnemonic: NFCI, NFCIRISK, NFCILEVERAGE, NFCINONFINLEVERAGE and NFCICREDIT). These latter are available at the weekly frequency, and they are converted into quarterly figures by taking the quarterly average. Overlapping weeks are accounted for in the averaging process: weekly values are computed in only one of the quarterly variables.<sup>18</sup>

## F.2 Additional details on the disaggregated financial indicators

We are grateful to Scot Brave and the Federal Reserve Bank of Chicago for sharing the weighted individual contribution to the NFCI. The dataset contains weekly time series of financial indicators that feed into the factor model generating both the NFCI and its subcomponents, as illustrated by [Brave and Butters \(2012\)](#). In Tables F1–F4 we report all the indicators, their mnemonic, and the date they become available for the index. [Figure F2](#) provides a graphical illustration of the time schedule of the availability of the predictors. The y-axis reports the years considered in our work in an ascending order (e.g. most recent times are closer to the origins).

---

<sup>18</sup>See <https://fredhelp.stlouisfed.org/fred/data/understanding-the-data/how-are-data-aggregated-when-periods-overlap/>

**Table F1:** Risk subindex components

| Mnemonic  | Financial Indicator  | Starting date |
|-----------|--|---------------|
| ABCP      | 1-mo. Asset-backed/Financial commercial paper spread                         | 05/01/2001    |
| ABSSPREAD | BofAML Home Equity ABS/MBS yield spread                                      | 05/07/1991    |
| CBILL     | 3-mo. Financial commercial paper/Treasury bill spread                        | 08/01/1971    |
| CG        | Commercial Paper Outstanding   | 10/11/1995    |
| CMBS      | BofAML 3-5 yr AAA CMBS OAS spread  | 02/01/1998    |
| CPR       | Counterparty Risk Index (formerly maintained by Credit Derivatives Research) | 13/09/2002    |
| CTABS     | FTSE Russell US Global Markets ABS/5-yr Treasury yield spread                | 01/02/1991    |
| CTERM     | 3-mo./1-wk AA Financial commercial paper spread                              | 10/01/1997    |
| CTF       | FTSE Russell US Global Markets Financial/Corporate Credit bond spread        | 31/01/1997    |
| CTMBS     | FTSE Russell US Global Markets MBS/10-year Treasury yield spread             | 27/01/1989    |
| FAILS     | Treasury Repo Delivery Fails Rate  | 07/10/1994    |
| FAILSA    | Agency Repo Delivery Failures Rate   | 07/10/1994    |
| FAILSC    | Corporate Securities Repo Delivery Failures Rate                             | 05/10/2001    |
| FAILSMBS  | Agency MBS Repo Delivery Failures Rate                                       | 07/10/1994    |
| GVL       | FDIC Volatile Bank Liabilities   | 01/07/1994    |
| LIBID     | 3-mo. Eurodollar spread (LIBID-Treasury)                                     | 08/01/1971    |
| MLIQ10    | On-the-run vs. Off-the-run 10-yr Treasury liquidity premium                  | 04/01/1985    |
| MMF       | Total Money Market Mutual Fund Assets/Total Long-term Fund Assets            | 28/12/1984    |
| REPO      | Fed Funds/Overnight Treasury Repo rate spread                                | 24/05/1991    |
| REPOA     | Fed Funds/Overnight Agency Repo rate spread                                  | 24/05/1991    |
| REPOGR    | Repo Market Volume (Repurchases+Reverse Repurchases of primary dealers)      | 07/10/1994    |
| REPOMORT  | Fed Funds/Overnight MBS Repo rate spread                                     | 24/05/1991    |
| RTERM     | 3-mo./1-wk Treasury Repo spread  | 24/05/1991    |
| SPR210    | 10-yr/2-yr Treasury yield spread   | 20/08/1971    |
| SPR23M    | 2-yr/3-mo. Treasury yield spread   | 08/01/1971    |
| SWAP10    | 10-yr Interest Rate Swap/Treasury yield spread                               | 03/04/1987    |
| SWAP2     | 2-yr Interest Rate Swap/Treasury yield spread                                | 03/04/1987    |
| SWAP3M    | 3-mo. Overnight Indexed Swap (OIS)/Treasury yield spread                     | 19/09/2003    |
| TED       | 3-mo. TED spread (LIBOR-Treasury)  | 06/06/1980    |
| TERM      | 1-yr/1-mo. LIBOR spread  | 10/01/1986    |
| USD       | Advanced Foreign Economies Trade-weighted US Dollar Value Index              | 12/01/1973    |
| VIX       | CBOE Market Volatility Index VIX   | 05/01/1990    |
| VOL1      | 1-mo. BofAML Option Volatility Estimate Index                                | 08/04/1988    |
| VOL3      | 3-mo. BofAML Swaption Volatility Estimate Index                              | 06/12/1996    |

**Table F2:** Leverage subindex components

| Mnemonic  | Financial Indicator  | Starting date |
|-----------|--|---------------|
| ABSI      | Nonmortgage ABS Issuance (Relative to 12-mo. MA)                             | 29/12/2000    |
| BDG       | Broker-dealer Debit Balances in Margin Accounts                              | 29/01/1971    |
| BONDGR    | New US Corporate Debt Issuance (Relative to 12-mo. MA)                       | 01/01/1988    |
| CITA      | Commercial Bank C&I Loans/Total Assets                                       | 02/03/1973    |
| CMBSI     | CMBS Issuance (Relative to 12-mo. MA)  | 28/12/1990    |
| COMMODLIQ | COMEX Gold/NYMEX WTI Futures Market Depth                                    | 04/01/2008    |
| CONTA     | Commercial Bank Consumer Loans/Total Assets                                  | 02/03/1973    |
| CPH       | FRB Commercial Property Price Index  | 02/04/1971    |
| D10       | 10-yr Constant Maturity Treasury yield                                       | 08/01/1971    |
| DCOMM     | Commercial Bank Total Unused C&I Loan Commitments/Total Assets               | 29/06/1990    |
| DNET      | Net Notional Value of Credit Derivatives                                     | 07/11/2008    |
| EQUITYLIQ | CME E-mini S&P Futures Market Depth  | 04/01/2008    |
| FC        | Total Assets of Finance Companies/GDP  | 02/04/1971    |
| FCORP     | Total Assets of Funding Corporations/GDP                                     | 02/04/1971    |
| FINS      | S&P 500 Financials/S&P 500 Price Index (Relative to 2-yr MA)                 | 06/09/1991    |
| GSE       | Total Agency and GSE Assets/GDP  | 30/12/1983    |
| INS       | Total Assets of Insurance Companies/GDP                                      | 02/04/1971    |
| ITA       | Fed funds and Reverse Repurchase Agreements/Total Assets of Commercial Banks | 30/03/1973    |
| LPH       | CoreLogic National House Price Index   | 02/04/1976    |
| MBONDGR   | New State & Local Government Debt Issues (Relative to 12-mo.h MA)            | 27/02/2004    |
| MBSI      | Total MBS Issuance (Relative to 12-mo. MA)                                   | 29/12/2000    |
| MCAP      | S&P 500, NASDAQ, and NYSE Market Capitalization/GDP                          | 28/06/1985    |
| OEQ       | S&P 500, S&P 500 mini, NASDAQ 100, NASDAQ mini Open Interest                 | 24/09/1999    |
| OINT      | 3-mo. Eurodollar, 10-yr/3-mo. swap, 2-yr and 10-yr Treasury Open Interest    | 23/06/1995    |
| PENS      | Total Assets of Pension Funds/GDP  | 02/04/1971    |
| RATELIQ   | CME Eurodollar/CBOT T-Note Futures Market Depth                              | 01/02/2008    |
| REIT      | Total REIT Assets/GDP  | 02/04/1971    |
| RTA       | Commercial Bank Real Estate Loans/Total Assets                               | 02/03/1973    |
| SBD       | Total Assets of Broker-dealers/GDP   | 02/04/1971    |
| STA       | Commercial Bank Securities in Bank Credit/Total Assets                       | 02/03/1973    |
| STKGR     | New US Corporate Equity Issuance (Relative to 12-mo. MA)                     | 01/01/1988    |
| STLOC     | Federal, state, and local debt outstanding/GDP                               | 02/04/1971    |
| TABS      | Total Assets of ABS issuers/GDP  | 30/12/1983    |
| W500      | Wilshire 5000 Stock Price Index  | 29/01/1971    |

**Table F3:** Nonfinancial Leverage subindex components

| Mnemonic | Financial Indicator  | Starting date |
|----------|--|---------------|
| HH       | Household debt outstanding/PCE Durables and Residential Investment | 02/04/1971    |
| NFC      | Nonfinancial business debt outstanding/GDP                         | 02/04/1971    |

**Table F4:** Credit subindex components

| Mnemonic   | Financial Indicator   | Starting date |
|------------|---|---------------|
| A2P2       | 1-mo. Nonfinancial commercial paper A2P2/AA credit spread               | 10/01/1997    |
| BAA        | Moody's Baa corporate bond/10-yr Treasury yield spread                  | 03/01/1986    |
| CARSPREAD  | UM Household Survey: Auto Credit Conditions Good/Bad spread             | 24/02/1978    |
| CBCAR      | Commercial Bank 48-mo. New Car Loan/2-yr Treasury yield spread          | 05/05/1972    |
| CBPER      | Commercial Bank 24-mo. Personal Loan/2-yr Treasury yield spread         | 05/05/1972    |
| CCDQ       | S&P US Bankcard Credit Card: 3-mo. Delinquency Rate                     | 28/02/1992    |
| CCG        | Consumer Credit Outstanding   | 29/01/1971    |
| CCINC      | S&P US Bankcard Credit Card: Excess Rate Spread                         | 31/01/1992    |
| CILARGE    | FRB Senior Loan Officer Survey: Tightening Standards on Large C&I Loans | 13/07/1990    |
| CISMAIL    | FRB Senior Loan Officer Survey: Tightening Standards on Small C&I Loans | 13/07/1990    |
| CRE        | FRB Senior Loan Officer Survey: Tightening Standards on CRE Loans       | 12/10/1990    |
| CRG        | S&P US Bankcard Credit Card: Receivables Outstanding                    | 28/02/1992    |
| CWILL      | FRB Senior Loan Officer Survey: Willingness to Lend to Consumers        | 15/01/1971    |
| DBC        | ABA Value of Delinquent Bank Card Credit Loans/Total Loans              | 26/02/1999    |
| DCLOSE     | ABA Value of Delinquent Consumer Loans/Total Loans                      | 26/02/1999    |
| DHE        | ABA Value of Delinquent Home Equity Loans/Total Loans                   | 26/02/1999    |
| DOTH       | ABA Value of Delinquent Noncard Revolving Credit Loans/Total Loans      | 26/02/1999    |
| DURSPREAD  | UM Household Survey: Durable Goods Credit Conditions Good/Bad spread    | 27/01/1978    |
| FG         | Finance Company Owned & Managed Receivables                             | 29/01/1971    |
| HOUSSPREAD | UM Household Survey: Mortgage Credit Conditions Good/Bad spread         | 24/02/1978    |
| HY         | BofAML High Yield/Moody's Baa corporate bond yield spread               | 07/11/1986    |
| JINC       | 30-yr Jumbo/Conforming fixed rate mortgage spread                       | 12/06/1998    |
| LHY        | Markit High Yield (HY) 5-yr Senior CDS Index                            | 07/01/2005    |
| LIG        | Markit Investment Grade (IG) 5-yr Senior CDS Index                      | 01/10/2004    |
| MBOND      | 20-yr Treasury/State & Local Government 20-yr GO bond spread            | 08/01/1971    |
| MDQ        | MBA Serious Delinquencies   | 30/06/1972    |
| MG         | Money Stock: MZM  | 01/03/1974    |
| MINC       | 30-yr Conforming Mortgage/10-yr Treasury yield spread                   | 02/04/1971    |
| MSWAP      | Bond Market Association Municipal Swap/20-yr Treasury yield spread      | 07/07/1989    |
| NACMM      | NACM Survey of Credit Managers: Credit Manager's Index                  | 15/02/2002    |
| NCL        | Commercial Bank Noncurrent/Total Loans                                  | 28/06/1985    |
| RRE        | FRB Senior Loan Officer Survey: Tightening Standards on RRE Loans       | 12/10/1990    |
| SMALL      | NFIB Survey: Credit Harder to Get                                       | 02/11/1973    |
| SPCILARGE  | FRB Senior Loan Officer Survey: Increasing spreads on Large C&I Loans   | 13/07/1990    |
| SPCISMAIL  | FRB Senior Loan Officer Survey: Increasing spreads on Small C&I Loans   | 13/07/1990    |

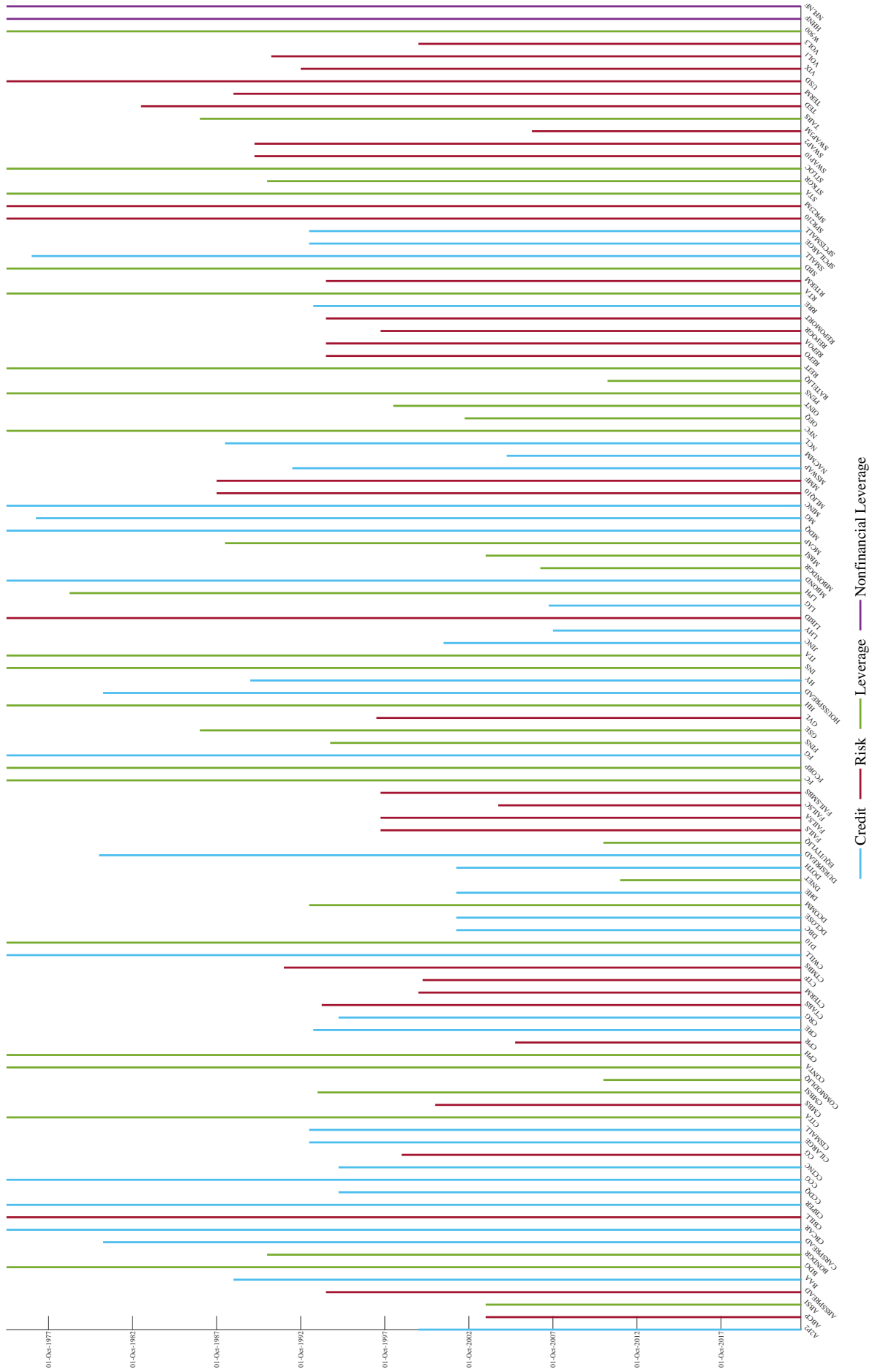


**Figure F2:** Timetable of predictors

*Note:* The chart reports the availability of the 105 predictors over time, during the period 1973Q1 to 2018Q4.

## G Model fit diagnostics

In this Appendix we detail the computation methodology for different measures of model fit, and we report some selected, additional results about the model specification.

### G.1 Deviance Information Criterion and Marginal Likelihood

We compare different models by means of the Deviance Information Criterion (*DIC*, Spiegelhalter et al., 2002), and the log Marginal Likelihood (*logML*), both discussed in detail by Chan and Grant (2016a,b).

**Deviance Information Criterion** Model fit can be summarized by the *deviance* measure, defined as

$$D(\theta) = -2 \log p(y|\theta) + 2 \log h(y),$$

where  $h(y)$  is a standardizing term, function of the sole data; for practical purposes we set  $h(y) = 1$ . A measure of model complexity can then be defined:

$$pD = \overline{D(\theta)} - D(\tilde{\theta}),$$

where  $\overline{D(\theta)}$  is the posterior mean deviance, defined as  $\overline{D(\theta)} = -2 \mathbb{E}_\theta[\log p(y|\theta)]$ , and  $D(\tilde{\theta})$  is the deviance computed at the mean estimate of  $\theta$ . The DIC is then a measure trading-off the fit of the model against the complexity:

$$\begin{aligned} DIC &= \overline{D(\theta)} + pD \\ &= -4 \mathbb{E}_\theta[\log p(y|\theta)] + 2 \log p(y|\tilde{\theta}), \end{aligned}$$

being the sum of a Bayesian measure of adequacy and the effective number of parameters.

**Marginal Likelihood** Another measure commonly used in Bayesian statistics to compare models is the Marginal Likelihood ( $\pi(y_t)$ ), that is the normalizing constant from the Bayes theorem:

$$\pi(\theta^j|y) = \frac{\pi(\theta^j) \log p(y|\theta^j)}{\pi(y)}.$$

Amongst the several ways available to compute this measure (see, e.g., Gamerman and Lopes, 2006), we opt for the *harmonic mean estimator* of Newton and Raftery (1994):

$$\pi(y) = \left[ \frac{1}{n^*} \sum_{j=1}^{n^*} \frac{1}{\log p(y|\theta^j)} \right]^{-1},$$

that is a special case of the importance sampling estimator in which the importance density  $g(\theta) = \pi(\theta)$ .

### G.2 Model fit diagnostics

Table G1 investigates the goodness of fit of alternative models. In this comparison, we consider three main specifications: AR(2) models with Gaussian and *Skt* innovations, one-component *Skt* models, featuring a constant, unconditional drift for each parameter (e.g.  $\varsigma = 0, \forall f$ ), and two-component *Skt* specifica-

**Table G1:** Model fit

|  | $DIC$              | $pD$             | $\log ML$           |
|--|--------------------|------------------|---------------------|
| Gaussian AR(2) + GARCH(1,1)                  | 908.976<br>(0.008) | 3.548<br>(0.004) | -456.952<br>(0.013) |
| Skew-t AR(2) + GAS(1,1) with $\varrho$ fixed | 883.939<br>(0.017) | 4.503<br>(0.015) | -444.821<br>(0.016) |
| One-Component Skew-t                         | 895.974<br>(0.005) | 6.162<br>(0.002) | -448.013<br>(0.010) |
| One-Component Skew-t with NFCI               | 932.717<br>(2.789) | 3.110<br>(1.355) | -475.868<br>(1.310) |
| One-Component Skew-t with 4DFI               | 937.180<br>(0.106) | 7.185<br>(0.042) | -471.049<br>(0.055) |
| Two-Component Skew-t                         | 898.415<br>(0.006) | 5.067<br>(0.003) | -449.190<br>(0.006) |
| Two-Component Skew-t with NFCI               | 882.963<br>(0.009) | 6.558<br>(0.004) | -442.051<br>(0.013) |
| Two-Component Skew-t with 4DFI               | 882.364<br>(0.021) | 8.830<br>(0.007) | -440.780<br>(0.018) |

*Note:* The table reports the Deviance Information Criterion ( $DIC$ ) of Spiegelhalter et al. (2002) along with the relative model complexity measure ( $pD$ ), and the log Marginal Likelihood ( $\log ML$ ) for different model specifications. Numerical standard errors are reported in parentheses. We consider two AR(2) specifications, one with Gaussian GARCH(1,1) volatility and one with Skew-t GAS(1,1) volatility with constant asymmetry. Next, we consider three specifications of the one-component and the two-component models: no predictors, lags of the NFCI and lags of the four disaggregated financial indices. In the one-component models the long-run components are kept fixed over time; in the two-component models the long-run components are modelled as unit root processes, as described in Section 3. Appendix D provides additional information about the computation of the  $DIC$  and the  $\log ML$  quantities.

tions, that allow for a permanent and transitory component for each time-varying parameter as described in Section 3. Table G1 reports the  $DIC$ , the model complexity component ( $pD$ ) of the  $DIC$ , and the  $\log ML$  with numerical standard errors in parentheses.

A simple Gaussian AR(2) model with time-varying volatility underperforms with respect to models featuring unconditional skewness and fat tails, despite a slight increase in complexity, highlighting the importance of modeling the non-Gaussian features of GDP growth. Inducing time-variation in the asymmetry component leads to different results: when secular trends are omitted  $DIC$  and  $\log ML$  increase compared to the model with unconditional skewness, due to the increasing complexity of the specifications. Adding two lags of financial variables further deteriorates the performance. Differently, modeling the time variation of secular trends improves model fit by lowering  $DIC$  and  $\log ML$ , despite the higher level of complexity. In this case, adding financial predictors delivers additional benefits. Therefore, the best specification is the two-component  $Sk_t$  model including two lags of the subcomponents of the NFCI. We label this specification as  $Sk_t -4DFI$ , and we treat it as the baseline specification throughout Section 4.

## H Additional forecast results

In this Appendix we report a number of additional results related to the forecast exercise we described in [Section 5](#).

### H.1 Comparison with Adrian et al. (2019)



**Figure H1:** Predictive densities

*Note:* The figure shows the predictive densities from the *Skt* -4DFI specification and the model of [Adrian et al. \(2019\)](#). The plots report the 5<sup>th</sup>, 50<sup>th</sup> and 95<sup>th</sup> quantities of the predictive densities. Shaded bands represent NBER recessions.



## H.2 Additional details on density forecast calibration

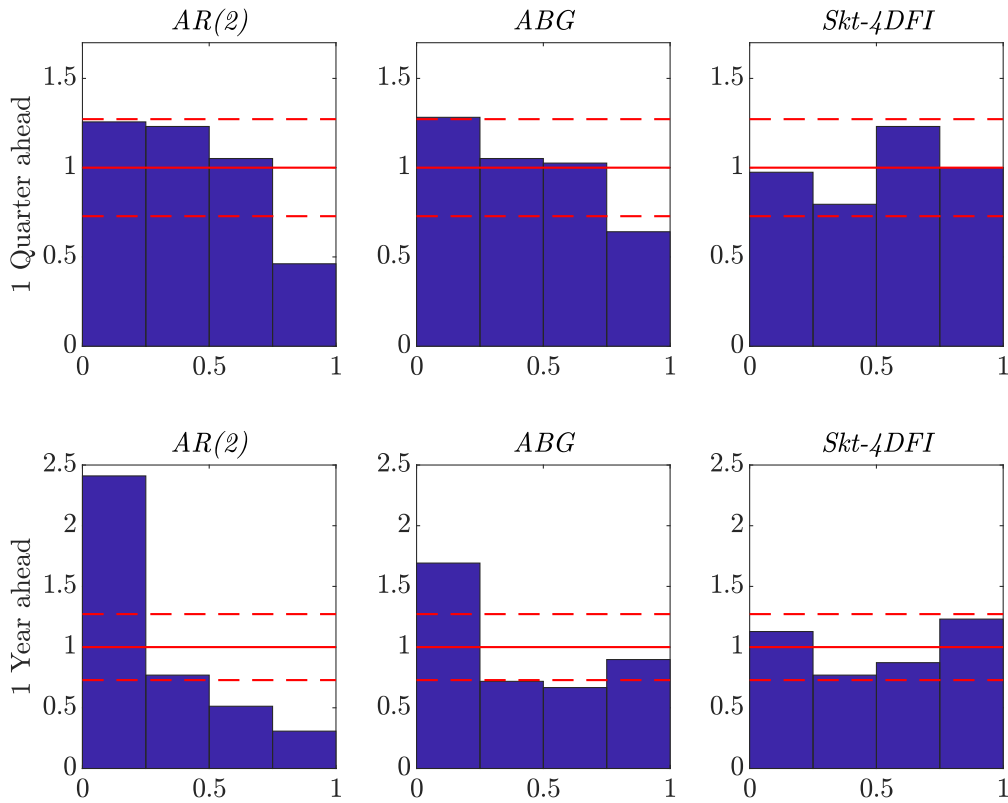


**Figure H2:** Probability density function of PITs

*Note:* The plots report the density functions of the normalized PITs for the  $AR(2)$ ,  $ABG$  and  $Skt-4DFI$  specifications, for 1-quarter and 1-year-ahead. The dashed lines represent 95% confidence levels, obtained as in [Diebold et al. \(1998\)](#)

## H.3 Lagged GDP growth as additional predictor

In this Section we show that adding past lags of the observable to the  $Skt$  specifications does not lead to any substantial gains in the forecasting accuracy of the models.

**Table H1:** Forecast performance with respect to 4DFI,Y

|                 | <i>One-quarter ahead</i> |                   |                         |                         | <i>One-year ahead</i>   |                         |                  |                         |
|-----------------|--------------------------|-------------------|-------------------------|-------------------------|-------------------------|-------------------------|------------------|-------------------------|
|                 | MSFE                     | logS              | CRPS                    | wQS                     | MSFE                    | logS                    | CRPS             | wQS                     |
| <i>Full</i>     | <b>0.957</b><br>(0.004)  | -0.018<br>(0.784) | <b>0.971</b><br>(0.032) | 0.987<br>(0.243)        | <b>0.740</b><br>(0.000) | <b>0.104</b><br>(0.010) | 0.988<br>(0.265) | <b>0.938</b><br>(0.048) |
| <i>Post '00</i> | <b>0.959</b><br>(0.000)  | -0.008<br>(0.617) | <b>0.972</b><br>(0.006) | <b>0.983</b><br>(0.097) | <b>0.918</b><br>(0.009) | 0.010<br>(0.412)        | 0.984<br>(0.178) | 0.999<br>(0.480)        |
| <i>Rec.</i>     | <b>0.969</b><br>(0.039)  | -0.004<br>(0.524) | <b>0.967</b><br>(0.085) | 0.969<br>(0.180)        | <b>0.680</b><br>(0.006) | 0.052<br>(0.301)        | 0.992<br>(0.429) | 0.912<br>(0.147)        |

*Note:* The table reports the average forecast metrics from the  $Skt-4DFI$  model relative to  $Skt-4DFI,Y$ . We use ratios for the MSFE, CRPS and wQS, and differences for the logS. Ratios smaller than 1, and positive values of the log-score differences indicate that the  $Skt-4DFI$  model performs better than  $Skt-4DFI,Y$ . The p-values for [Diebold and Mariano \(1995\)](#) tests, augmented with the small sample correction of [Harvey et al. \(1997\)](#), are in parentheses. Values in **bold** are significant at the 10% level; gray shaded cells highlight the best score.

## H.4 How important is parameters' uncertainty?

In the following Tables we compare forecasts generated with and without taking into account parameter uncertainty.

**Table H2:** Forecast performance - Parameter uncertainty

|                  | <i>One-quarter ahead</i> |                         | <i>One-year ahead</i>   |                         |
|------------------|--------------------------|-------------------------|-------------------------|-------------------------|
|                  | MSFE                     | logS                    | MSFE                    | logS                    |
| <i>Full</i>      | <b>0.965</b><br>(0.000)  | -0.001<br>(0.510)       | <b>0.845</b><br>(0.000) | <b>0.105</b><br>(0.017) |
| <i>Post '00.</i> | <b>0.850</b><br>(0.004)  | 0.011<br>(0.445)        | <b>0.680</b><br>(0.006) | <b>0.314</b><br>(0.052) |
| <i>Rec.</i>      | <b>0.959</b><br>(0.000)  | <b>0.046</b><br>(0.058) | <b>0.770</b><br>(0.000) | <b>0.073</b><br>(0.079) |
|                  | CRPS                     | wQS                     | CRSP                    | wQS                     |
|                  |                          |                         |                         |                         |
| <i>Full</i>      | <b>0.983</b><br>(0.039)  | <b>0.986</b><br>(0.095) | 1.010<br>(0.753)        | 1.023<br>(0.859)        |
| <i>Post '00.</i> | <b>0.942</b><br>(0.048)  | <b>0.931</b><br>(0.064) | 1.005<br>(0.552)        | 0.941<br>(0.109)        |
| <i>Rec.</i>      | <b>0.964</b><br>(0.000)  | <b>0.955</b><br>(0.000) | 1.005<br>(0.599)        | <b>0.950</b><br>(0.014) |

*Note:* In this table we compare the forecast metrics of the baseline model, *Skt* 4FDI, against a version of the same model that does not account for parameter uncertainty (*w/o P.U.*). The table reports the average forecast metrics relative to the *w/o P.U.* model. We use ratios for the MSFE, CRSP and wQS, and differences for the logS. Ratios smaller than 1, and positive values of the log-score differences indicate that the baseline model (which allows for uncertainty) performs better than the model without parameters uncertainty. The p-values for [Diebold and Mariano \(1995\)](#) tests, augmented with the small sample correction of [Harvey et al. \(1997\)](#), are in parentheses.

**Table H3:** Density calibration tests - Parameter uncertainty

|           | <i>w/ PU</i>             | <i>w/o PU</i> | <i>w/ PU</i>          | <i>w/o PU</i> |
|-----------|--------------------------|---------------|-----------------------|---------------|
|           | <i>One-quarter ahead</i> |               | <i>One-year ahead</i> |               |
| Dist.     | 0.883                    | 0.763         | 1.162                 | 1.217         |
| Left tail | 0.501                    | 0.615         | 1.162                 | 1.217         |

*Note:* The table reports the test statistics for the [Rossi and Sekhposyan \(2019\)](#) tests, based on the Cramér-von Mises type tests. The left tail score is computed over the support  $[0, 0.25]$ . Values in **bold** indicate the rejection of the null hypothesis of correct specification of the density forecast, at the 10% confidence level. Critical values are obtained by 1000 bootstrap simulations. Gray shaded cells indicate lowest value of the statistic.

## H.5 Excluding 2020 from the forecast evaluation sample

In [Sections 5.1](#) and [5.2](#), we excluded the 2020 quarters from the forecast evaluation of the recession subsample. In this Appendix we report the results for the full and the post-2000s samples excluding the pandemic period.

**Table H4:** Forecasting performance

|                          | <i>Skt</i>              | <i>Skt</i><br><i>NFCI</i> | <i>Skt</i><br><i>4DFI</i> | <i>Skt</i>              | <i>Skt</i><br><i>NFCI</i> | <i>Skt</i><br><i>4DFI</i> |
|--------------------------|-------------------------|---------------------------|---------------------------|-------------------------|---------------------------|---------------------------|
| <i>One-quarter ahead</i> |                         |                           |                           |                         |                           |                           |
|                          | <b>MSFE</b>             |                           |                           | <b>logS</b>             |                           |                           |
| <i>Full</i>              | 0.951<br>(0.120)        | <b>0.847</b><br>(0.002)   | <b>0.862</b><br>(0.004)   | <b>0.123</b><br>(0.000) | <b>0.148</b><br>(0.000)   | <b>0.074</b><br>(0.032)   |
| <i>Post '00</i>          | <b>0.881</b><br>(0.000) | <b>0.795</b><br>(0.000)   | <b>0.795</b><br>(0.000)   | <b>0.186</b><br>(0.000) | <b>0.231</b><br>(0.000)   | <b>0.200</b><br>(0.000)   |
|                          | <b>CRPS</b>             |                           |                           | <b>wQS</b>              |                           |                           |
| <i>Full</i>              | <b>0.964</b><br>(0.088) | <b>0.934</b><br>(0.009)   | <b>0.952</b><br>(0.043)   | 0.984<br>(0.290)        | <b>0.936</b><br>(0.016)   | <b>0.941</b><br>(0.028)   |
| <i>Post '00</i>          | <b>0.913</b><br>(0.001) | <b>0.875</b><br>(0.000)   | <b>0.890</b><br>(0.001)   | <b>0.935</b><br>(0.037) | <b>0.888</b><br>(0.001)   | <b>0.894</b><br>(0.006)   |
| <i>One-year ahead</i>    |                         |                           |                           |                         |                           |                           |
|                          | <b>MSFE</b>             |                           |                           | <b>logS</b>             |                           |                           |
| <i>Full</i>              | <b>0.720</b><br>(0.000) | <b>0.716</b><br>(0.002)   | <b>0.693</b><br>(0.004)   | <b>0.463</b><br>(0.000) | <b>0.561</b><br>(0.000)   | <b>0.502</b><br>(0.002)   |
| <i>Post '00</i>          | <b>0.719</b><br>(0.000) | <b>0.694</b><br>(0.000)   | <b>0.718</b><br>(0.003)   | <b>0.807</b><br>(0.000) | <b>0.937</b><br>(0.000)   | <b>0.942</b><br>(0.000)   |
|                          | <b>CRPS</b>             |                           |                           | <b>wQS</b>              |                           |                           |
| <i>Full</i>              | <b>0.913</b><br>(0.003) | <b>0.902</b><br>(0.002)   | <b>0.883</b><br>(0.003)   | <b>0.779</b><br>(0.001) | <b>0.746</b><br>(0.001)   | <b>0.765</b><br>(0.006)   |
| <i>Post '00</i>          | <b>0.841</b><br>(0.000) | <b>0.824</b><br>(0.000)   | <b>0.817</b><br>(0.000)   | <b>0.722</b><br>(0.000) | <b>0.698</b><br>(0.000)   | <b>0.707</b><br>(0.001)   |

*Note:* The table reports the average forecast metrics relative to the Gaussian model over the 1973-2019 sample. We use ratios for the MSFE, CRSP and wQS, and differences for the logS. Ratios smaller than 1, and positive values of the log-score differences indicate that the column-specific model performs better than the Gaussian benchmark. The p-values for Diebold and Mariano (1995) tests, augmented with the small sample correction of Harvey et al. (1997), are in parentheses. Values in **bold** are significant at the 10% level; gray shaded cells highlight the best score.

**Table H5:** Forecast performance with respect to Adrian et al. (2019)

|                 | <i>One-quarter ahead</i> |                         |                         |                         | <i>One-year ahead</i> |                         |                         |                  |
|-----------------|--------------------------|-------------------------|-------------------------|-------------------------|-----------------------|-------------------------|-------------------------|------------------|
|                 | MSFE                     | logS                    | CRPS                    | wQS                     | MSFE                  | logS                    | CRPS                    | wQS              |
| <i>Full</i>     | 1.073<br>(0.944)         | <b>0.212</b><br>(0.000) | 1.021<br>(0.766)        | 1.043<br>(0.940)        | 1.024<br>(0.604)      | <b>0.560</b><br>(0.000) | 0.994<br>(0.456)        | 1.032<br>(0.697) |
| <i>Post '00</i> | <b>0.905</b><br>(0.004)  | <b>0.078</b><br>(0.027) | <b>0.951</b><br>(0.065) | <b>0.962</b><br>(0.095) | 0.903<br>(0.123)      | <b>0.414</b><br>(0.001) | <b>0.906</b><br>(0.060) | 0.948<br>(0.257) |

*Note:* The table reports the average forecast metrics from the *Skt* -4DFI model relative to Adrian et al. (2019) over the 1973-2019 sample. We use ratios for the MSFE, CRSP and wQS, and differences for the logS. Ratios smaller than 1, and positive values of the log-score differences indicate that the *Skt* 4DFI model performs better than Adrian et al. (2019). The p-values for Diebold and Mariano (1995) tests, augmented with the small sample correction of Harvey et al. (1997), are in parentheses. Values in **bold** are significant at the 10% level; gray shaded cells highlight the best score.

**Table H6:** Forecast performance with respect to 4DFI,Y

|                 | <i>One-quarter ahead</i> |                         |                         |                  | <i>One-year ahead</i>   |                         |                  |                         |
|-----------------|--------------------------|-------------------------|-------------------------|------------------|-------------------------|-------------------------|------------------|-------------------------|
|                 | MSFE                     | logS                    | CRPS                    | wQS              | MSFE                    | logS                    | CRPS             | wQS                     |
| <i>Full</i>     | 0.958<br>(0.104)         | 0.002<br>(0.467)        | <b>0.974</b><br>(0.085) | 0.991<br>(0.319) | <b>0.737</b><br>(0.000) | <b>0.124</b><br>(0.004) | 0.985<br>(0.235) | <b>0.931</b><br>(0.035) |
| <i>Post '00</i> | 0.977<br>(0.202)         | <b>0.032</b><br>(0.085) | <b>0.979</b><br>(0.093) | 0.989<br>(0.271) | <b>0.922</b><br>(0.016) | 0.049<br>(0.154)        | 0.979<br>(0.121) | 0.987<br>(0.326)        |

*Note:* The table reports the average forecast metrics from the *Skt* -4DFI model relative to *Skt* -4DFI,Y over the 1973-2019 sample. We use ratios for the MSFE, CRSP and wQS, and differences for the logS. Ratios smaller than 1, and positive values of the log-score differences indicate that the *Skt* 4DFI model performs better than *Skt* -4DFI,Y. The p-values for Diebold and Mariano (1995) tests, augmented with the small sample correction of Harvey et al. (1997), are in parentheses. Values in **bold** are significant at the 10% level; gray shaded cells highlight the best score.

## H.6 Conditional vs. unconditional skewness

In this Section we assess the impact of accounting for unconditional skewness in the benchmark model. Specifically, we assume an AR(2) model for GDP growth with  $Sk_t$   $\nu$  innovations with fixed shape parameter.

**Table H7:** Forecasting performance against  $Sk_t$  -fix

|                          | $\mathcal{N}$<br>AR     | $Sk_t$                  | $Sk_t$<br>NFCI          | $Sk_t$<br>4DFI          | $\mathcal{N}$<br>AR | $Sk_t$                  | $Sk_t$<br>NFCI          | $Sk_t$<br>4DFI          |
|--------------------------|-------------------------|-------------------------|-------------------------|-------------------------|---------------------|-------------------------|-------------------------|-------------------------|
| <i>One-quarter ahead</i> |                         |                         |                         |                         |                     |                         |                         |                         |
|                          | MSFE                    |                         |                         |                         | logS                |                         |                         |                         |
| <i>Full</i>              | <b>0.958</b><br>(0.000) | <b>0.807</b><br>(0.000) | <b>0.783</b><br>(0.000) | <b>0.778</b><br>(0.000) | -0.119<br>(1.000)   | 0.002<br>(0.464)        | 0.021<br>(0.230)        | -0.059<br>(0.937)       |
| <i>Post '00</i>          | <b>0.951</b><br>(0.000) | <b>0.770</b><br>(0.000) | <b>0.764</b><br>(0.000) | <b>0.754</b><br>(0.000) | -0.125<br>(1.000)   | <b>0.056</b><br>(0.054) | <b>0.087</b><br>(0.004) | 0.042<br>(0.155)        |
| <i>Rec.</i>              | <b>0.952</b><br>(0.004) | <b>0.791</b><br>(0.000) | <b>0.769</b><br>(0.000) | <b>0.757</b><br>(0.000) | -0.226<br>(0.948)   | 0.001<br>(0.492)        | 0.038<br>(0.241)        | -0.078<br>(0.805)       |
|                          | CRPS                    |                         |                         |                         | wQS                 |                         |                         |                         |
| <i>Full</i>              | <b>0.982</b><br>(0.032) | <b>0.947</b><br>(0.001) | <b>0.924</b><br>(0.000) | <b>0.935</b><br>(0.001) | 1.010<br>(0.820)    | <b>0.969</b><br>(0.052) | <b>0.935</b><br>(0.000) | <b>0.935</b><br>(0.002) |
| <i>Post '00</i>          | <b>0.977</b><br>(0.002) | <b>0.913</b><br>(0.000) | <b>0.891</b><br>(0.000) | <b>0.897</b><br>(0.000) | 1.034<br>(0.999)    | <b>0.951</b><br>(0.001) | <b>0.925</b><br>(0.000) | <b>0.921</b><br>(0.002) |
| <i>Rec.</i>              | <b>0.957</b><br>(0.042) | <b>0.920</b><br>(0.004) | <b>0.904</b><br>(0.005) | <b>0.898</b><br>(0.008) | 1.028<br>(0.913)    | <b>0.950</b><br>(0.064) | <b>0.932</b><br>(0.035) | <b>0.892</b><br>(0.019) |
| <i>One-year ahead</i>    |                         |                         |                         |                         |                     |                         |                         |                         |
|                          | MSFE                    |                         |                         |                         | logS                |                         |                         |                         |
| <i>Full</i>              | 1.095<br>(0.999)        | <b>0.789</b><br>(0.003) | <b>0.785</b><br>(0.012) | <b>0.760</b><br>(0.009) | -0.232<br>(1.000)   | <b>0.254</b><br>(0.005) | <b>0.352</b><br>(0.000) | <b>0.286</b><br>(0.009) |
| <i>Post '00</i>          | 1.022<br>(0.974)        | <b>0.736</b><br>(0.000) | <b>0.711</b><br>(0.000) | <b>0.734</b><br>(0.005) | -0.323<br>(1.000)   | <b>0.526</b><br>(0.000) | <b>0.656</b><br>(0.000) | <b>0.647</b><br>(0.000) |
| <i>Rec.</i>              | 1.119<br>(0.864)        | 0.832<br>(0.130)        | 0.855<br>(0.218)        | <b>0.734</b><br>(0.051) | -0.704<br>(0.996)   | <b>0.367</b><br>(0.033) | <b>0.505</b><br>(0.035) | <b>0.533</b><br>(0.065) |
|                          | CRPS                    |                         |                         |                         | wQS                 |                         |                         |                         |
| <i>Full</i>              | 1.016<br>(0.853)        | <b>0.927</b><br>(0.003) | <b>0.917</b><br>(0.001) | <b>0.897</b><br>(0.003) | 1.080<br>(1.000)    | <b>0.841</b><br>(0.008) | <b>0.807</b><br>(0.002) | <b>0.828</b><br>(0.014) |
| <i>Post '00</i>          | 1.046<br>(1.000)        | <b>0.882</b><br>(0.000) | <b>0.864</b><br>(0.000) | <b>0.857</b><br>(0.000) | 1.072<br>(1.000)    | <b>0.777</b><br>(0.000) | <b>0.754</b><br>(0.000) | <b>0.762</b><br>(0.004) |
| <i>Rec.</i>              | 0.985<br>(0.384)        | <b>0.928</b><br>(0.035) | 0.943<br>(0.176)        | <b>0.877</b><br>(0.043) | 1.099<br>(0.983)    | <b>0.797</b><br>(0.022) | <b>0.810</b><br>(0.055) | <b>0.734</b><br>(0.036) |

*Note:* The table reports the average forecast metrics relative to the Gaussian model. We use ratios for the MSFE, CRPS and wQS, and differences for the logS. Ratios smaller than 1, and positive values of the log-score differences indicate that the column-specific model performs better than the Gaussian benchmark. The p-values for [Diebold and Mariano \(1995\)](#) tests, augmented with the small sample correction of [Harvey et al. \(1997\)](#), are in parentheses. Values in **bold** are significant at the 10% level; gray shaded cells highlight the best score.

**Table H8:** Downside risk scores against *Skt* -fix

|                 | <i>Skt</i><br><i>no-X</i> | <i>Skt</i><br><i>4DFI</i> | <i>Skt</i><br><i>no-X</i> | <i>Skt</i><br><i>4DFI</i> | <i>Skt</i><br><i>no-X</i> | <i>Skt</i><br><i>4DFI</i> |
|-----------------|---------------------------|---------------------------|---------------------------|---------------------------|---------------------------|---------------------------|
|                 | FZG                       |                           | ALS                       |                           | TLF                       |                           |
|                 | <i>One-quarter ahead</i>  |                           |                           |                           |                           |                           |
| <i>Full</i>     | 0.831<br>(1.000)          | 0.819<br>(0.913)          | <b>0.959</b><br>(0.000)   | <b>0.948</b><br>(0.002)   | 0.978<br>(0.702)          | <b>0.900</b><br>(0.001)   |
| <i>Post '00</i> | 0.693<br>(0.994)          | 0.720<br>(0.934)          | <b>0.912</b><br>(0.000)   | <b>0.926</b><br>(0.001)   | 0.943<br>(0.508)          | 0.915<br>(0.164)          |
| <i>Rec.</i>     | 0.741<br>(0.265)          | <b>0.651</b><br>(0.018)   | <b>0.880</b><br>(0.000)   | <b>0.850</b><br>(0.001)   | 0.925<br>(0.200)          | <b>0.821</b><br>(0.008)   |
|                 | <i>One-year ahead</i>     |                           |                           |                           |                           |                           |
| <i>Full</i>     | <b>0.241</b><br>(0.001)   | <b>0.310</b><br>(0.002)   | <b>0.397</b><br>(0.000)   | <b>0.424</b><br>(0.002)   | <b>0.692</b><br>(0.010)   | <b>0.622</b><br>(0.010)   |
| <i>Post '00</i> | <b>0.246</b><br>(0.002)   | <b>0.371</b><br>(0.010)   | <b>0.361</b><br>(0.000)   | <b>0.398</b><br>(0.008)   | <b>0.727</b><br>(0.018)   | <b>0.600</b><br>(0.010)   |
| <i>Rec.</i>     | <b>0.192</b><br>(0.000)   | <b>0.300</b><br>(0.002)   | <b>0.263</b><br>(0.000)   | <b>0.308</b><br>(0.003)   | <b>0.551</b><br>(0.000)   | <b>0.495</b><br>(0.006)   |

*Note:* The table reports the average downside risk test scores, expressed as ratios relative to the *Skt* -fix model. Ratios smaller than 1 indicate that the column-specific model performs better than the benchmark. The p-values for Diebold and Mariano (1995) tests, augmented with the small sample correction of Harvey et al. (1997), are reported in parentheses. Values in **bold** are significant at the 10% level; gray shaded cells highlight the best score. FZG: Fissler et al. (2016) loss function; ALS: Taylor (2019) loss function; TLF: Giacomini and Komunjer (2005) tick loss function.

## H.7 Predicting GDP vintage releases

In this Section we show that adding past lags of the observable to the *Skt* specifications does not lead to any substantial gains in the forecasting accuracy of the models.

**Table H9:** Forecasting performance - first vintage

|                          | <i>Skt</i>              | <i>Skt</i><br><i>NFCI</i> | <i>Skt</i><br><i>ΔDFI</i> | <i>Skt</i>              | <i>Skt</i><br><i>NFCI</i> | <i>Skt</i><br><i>ΔDFI</i> |
|--------------------------|-------------------------|---------------------------|---------------------------|-------------------------|---------------------------|---------------------------|
| <i>One-quarter ahead</i> |                         |                           |                           |                         |                           |                           |
|                          | MSFE                    |                           |                           | logS                    |                           |                           |
| <i>Full</i>              | <b>0.787</b><br>(0.000) | <b>0.760</b><br>(0.000)   | <b>0.758</b><br>(0.000)   | <b>0.117</b><br>(0.000) | <b>0.136</b><br>(0.000)   | <b>0.117</b><br>(0.000)   |
| <i>Post '00</i>          | <b>0.779</b><br>(0.000) | <b>0.774</b><br>(0.000)   | <b>0.767</b><br>(0.000)   | <b>0.091</b><br>(0.006) | <b>0.117</b><br>(0.000)   | <b>0.098</b><br>(0.004)   |
| <i>Rec.</i>              | <b>0.795</b><br>(0.000) | <b>0.767</b><br>(0.000)   | <b>0.759</b><br>(0.000)   | 0.079<br>(0.150)        | <b>0.141</b><br>(0.066)   | 0.068<br>(0.311)          |
|                          | CRPS                    |                           |                           | wQS                     |                           |                           |
| <i>Full</i>              | <b>0.922</b><br>(0.000) | <b>0.896</b><br>(0.000)   | <b>0.903</b><br>(0.000)   | <b>0.934</b><br>(0.004) | <b>0.897</b><br>(0.000)   | <b>0.896</b><br>(0.000)   |
| <i>Post '00</i>          | <b>0.940</b><br>(0.002) | <b>0.910</b><br>(0.000)   | <b>0.927</b><br>(0.001)   | <b>0.933</b><br>(0.001) | <b>0.897</b><br>(0.000)   | <b>0.903</b><br>(0.001)   |
| <i>Rec.</i>              | 0.960<br>(0.162)        | <b>0.930</b><br>(0.071)   | <b>0.928</b><br>(0.085)   | <b>0.920</b><br>(0.037) | <b>0.896</b><br>(0.022)   | <b>0.871</b><br>(0.026)   |
| <i>One-year ahead</i>    |                         |                           |                           |                         |                           |                           |
|                          | MSFE                    |                           |                           | logS                    |                           |                           |
| <i>Full</i>              | <b>0.408</b><br>(0.000) | <b>0.486</b><br>(0.000)   | <b>0.464</b><br>(0.000)   | <b>2.994</b><br>(0.000) | <b>2.584</b><br>(0.000)   | <b>2.583</b><br>(0.000)   |
| <i>Post '00</i>          | <b>0.599</b><br>(0.000) | <b>0.642</b><br>(0.000)   | <b>0.688</b><br>(0.000)   | <b>3.384</b><br>(0.000) | <b>3.055</b><br>(0.000)   | <b>2.977</b><br>(0.000)   |
| <i>Rec.</i>              | <b>0.518</b><br>(0.000) | <b>0.555</b><br>(0.001)   | <b>0.483</b><br>(0.000)   | <b>4.019</b><br>(0.000) | <b>3.735</b><br>(0.000)   | <b>4.208</b><br>(0.000)   |
|                          | CRPS                    |                           |                           | wQS                     |                           |                           |
| <i>Full</i>              | <b>0.724</b><br>(0.000) | <b>0.752</b><br>(0.000)   | <b>0.739</b><br>(0.000)   | <b>0.451</b><br>(0.000) | <b>0.571</b><br>(0.000)   | <b>0.553</b><br>(0.000)   |
| <i>Post '00</i>          | <b>0.779</b><br>(0.000) | <b>0.793</b><br>(0.000)   | <b>0.817</b><br>(0.000)   | <b>0.556</b><br>(0.000) | <b>0.618</b><br>(0.000)   | <b>0.655</b><br>(0.000)   |
| <i>Rec.</i>              | <b>0.814</b><br>(0.000) | <b>0.832</b><br>(0.000)   | <b>0.743</b><br>(0.000)   | <b>0.583</b><br>(0.000) | <b>0.670</b><br>(0.000)   | <b>0.559</b><br>(0.000)   |

*Note:* The table reports the average forecast metrics relative to the Gaussian model. The target variable is the first vintage of GDP growth. We use ratios for the MSFE, CRSP and wQS, and differences for the logS. Ratios smaller than 1, and positive values of the log-score differences indicate that the column-specific model performs better than the Gaussian benchmark. The p-values for [Diebold and Mariano \(1995\)](#) tests, augmented with the small sample correction of [Harvey et al. \(1997\)](#), are in parentheses. Values in **bold** are significant at the 10% level; gray shaded cells highlight the best score.

**Table H10:** Forecasting performance - second vintage

|                          | <i>Skt</i>              | <i>Skt</i><br><i>NFCI</i> | <i>Skt</i><br><i>ΔDFI</i> | <i>Skt</i>              | <i>Skt</i><br><i>NFCI</i> | <i>Skt</i><br><i>ΔDFI</i> |
|--------------------------|-------------------------|---------------------------|---------------------------|-------------------------|---------------------------|---------------------------|
| <i>One-quarter ahead</i> |                         |                           |                           |                         |                           |                           |
|                          | MSFE                    |                           |                           | logS                    |                           |                           |
| <i>Full</i>              | <b>0.789</b><br>(0.000) | <b>0.765</b><br>(0.000)   | <b>0.763</b><br>(0.000)   | <b>0.117</b><br>(0.000) | <b>0.117</b><br>(0.000)   | <b>0.069</b><br>(0.032)   |
| <i>Post '00</i>          | <b>0.778</b><br>(0.000) | <b>0.773</b><br>(0.000)   | <b>0.768</b><br>(0.000)   | <b>0.100</b><br>(0.005) | <b>0.102</b><br>(0.006)   | <b>0.066</b><br>(0.084)   |
| <i>Rec.</i>              | <b>0.791</b><br>(0.000) | <b>0.765</b><br>(0.000)   | <b>0.757</b><br>(0.000)   | <b>0.135</b><br>(0.099) | 0.110<br>(0.136)          | -0.001<br>(0.505)         |
|                          | CRPS                    |                           |                           | wQS                     |                           |                           |
| <i>Full</i>              | <b>0.933</b><br>(0.000) | <b>0.912</b><br>(0.000)   | <b>0.918</b><br>(0.001)   | <b>0.936</b><br>(0.008) | <b>0.906</b><br>(0.001)   | <b>0.904</b><br>(0.000)   |
| <i>Post '00</i>          | <b>0.953</b><br>(0.008) | <b>0.927</b><br>(0.000)   | <b>0.944</b><br>(0.003)   | <b>0.940</b><br>(0.001) | <b>0.910</b><br>(0.001)   | <b>0.916</b><br>(0.006)   |
| <i>Rec.</i>              | 0.960<br>(0.161)        | 0.935<br>(0.115)          | 0.932<br>(0.118)          | <b>0.918</b><br>(0.034) | <b>0.897</b><br>(0.025)   | <b>0.868</b><br>(0.025)   |
| <i>One-year ahead</i>    |                         |                           |                           |                         |                           |                           |
|                          | MSFE                    |                           |                           | logS                    |                           |                           |
| <i>Full</i>              | <b>0.409</b><br>(0.000) | <b>0.487</b><br>(0.000)   | <b>0.464</b><br>(0.000)   | <b>2.984</b><br>(0.000) | <b>2.572</b><br>(0.000)   | <b>2.562</b><br>(0.000)   |
| <i>Post '00</i>          | <b>0.598</b><br>(0.000) | <b>0.641</b><br>(0.000)   | <b>0.684</b><br>(0.000)   | <b>3.456</b><br>(0.000) | <b>3.096</b><br>(0.000)   | <b>2.984</b><br>(0.000)   |
| <i>Rec.</i>              | <b>0.521</b><br>(0.000) | <b>0.557</b><br>(0.001)   | <b>0.485</b><br>(0.000)   | <b>4.134</b><br>(0.000) | <b>3.746</b><br>(0.000)   | <b>4.216</b><br>(0.000)   |
|                          | CRPS                    |                           |                           | wQS                     |                           |                           |
| <i>Full</i>              | <b>0.725</b><br>(0.000) | <b>0.754</b><br>(0.000)   | <b>0.740</b><br>(0.000)   | <b>0.454</b><br>(0.000) | <b>0.572</b><br>(0.000)   | <b>0.553</b><br>(0.000)   |
| <i>Post '00</i>          | <b>0.780</b><br>(0.000) | <b>0.792</b><br>(0.000)   | <b>0.815</b><br>(0.000)   | <b>0.555</b><br>(0.000) | <b>0.616</b><br>(0.000)   | <b>0.652</b><br>(0.000)   |
| <i>Rec.</i>              | <b>0.817</b><br>(0.000) | <b>0.836</b><br>(0.001)   | <b>0.746</b><br>(0.000)   | <b>0.588</b><br>(0.000) | <b>0.673</b><br>(0.000)   | <b>0.561</b><br>(0.000)   |

*Note:* The table reports the average forecast metrics relative to the Gaussian model. The target variable is the second vintage of GDP growth. We use ratios for the MSFE, CRSP and wQS, and differences for the logS. Ratios smaller than 1, and positive values of the log-score differences indicate that the column-specific model performs better than the Gaussian benchmark. The p-values for [Diebold and Mariano \(1995\)](#) tests, augmented with the small sample correction of [Harvey et al. \(1997\)](#), are in parentheses. Values in **bold** are significant at the 10% level; gray shaded cells highlight the best score.

## H.8 NFCI: last vintage vs. real time data

Here, we evaluate the difference in forecasting performance associated with the availability of real-time vintages of the NFCI and its four subcomponents.

**Table H11:** Forecast comparison with real-time NFCI

|           | <i>Sk</i><br>NFCI       | <i>Sk</i><br>4DFI       | <i>Sk</i><br>NFCI       | <i>Sk</i><br>4DFI       | <i>Sk</i><br>NFCI       | <i>Sk</i><br>4DFI       | <i>Sk</i><br>NFCI       | <i>Sk</i><br>4DFI |
|-----------|-------------------------|-------------------------|-------------------------|-------------------------|-------------------------|-------------------------|-------------------------|-------------------|
|           | One-quarter ahead       |                         |                         |                         | One-year ahead          |                         |                         |                   |
|           | MSFE                    |                         | logS                    |                         | MSFE                    |                         | logS                    |                   |
| 2013-2020 | <b>1.010</b><br>(0.019) | <b>0.984</b><br>(0.000) | 0.005<br>(0.945)        | -0.085<br>(0.241)       | <b>0.942</b><br>(0.032) | <b>1.030</b><br>(0.000) | 0.056<br>(0.336)        | -0.058<br>(0.250) |
| 2013-2019 | 0.900<br>(0.365)        | 0.985<br>(0.664)        | 0.067<br>(0.165)        | -0.006<br>(0.782)       | <b>0.956</b><br>(0.025) | <b>1.034</b><br>(0.000) | 0.059<br>(0.378)        | -0.041<br>(0.458) |
|           | CRPS                    |                         | wQS                     |                         | CRPS                    |                         | wQS                     |                   |
| 2013-2020 | 0.979<br>(0.149)        | <b>0.986</b><br>(0.014) | <b>0.968</b><br>(0.023) | <b>0.976</b><br>(0.000) | <b>0.949</b><br>(0.056) | 1.012<br>(0.327)        | <b>0.937</b><br>(0.013) | 1.011<br>(0.260)  |
| 2013-2019 | 0.921<br>(0.182)        | 0.991<br>(0.557)        | 0.962<br>(0.327)        | 0.973<br>(0.146)        | 0.960<br>(0.112)        | 1.015<br>(0.256)        | <b>0.943</b><br>(0.069) | 1.017<br>(0.232)  |

*Note:* The table compares forecast produced with real time vintages of the NFCI and its subindices. Average forecast metrics are reported relative to the forecasts using the last release of the NFCI. The sample spans the period from 2013Q1 to 2020Q4 to match the availability of real-time observations. We evaluate forecasts for the full sample ('13-'20) and for a subsample excluding the pandemic ('13-'19). We use ratios for the MSFE, CRSP and wQS, and differences for the logS. Ratios smaller than 1, and positive values of the log-score differences indicate that using real-time NFCI observations improves forecasts' accuracy. The p-values for [Diebold and Mariano \(1995\)](#) tests, augmented with the small sample correction of [Harvey et al. \(1997\)](#), are in parentheses. Values in **bold** are significant at the 10% level.

## I Additional results on the *Sparse* model

In this Appendix we report additional results concerning the *sparse* model introduced in [Section 6](#).

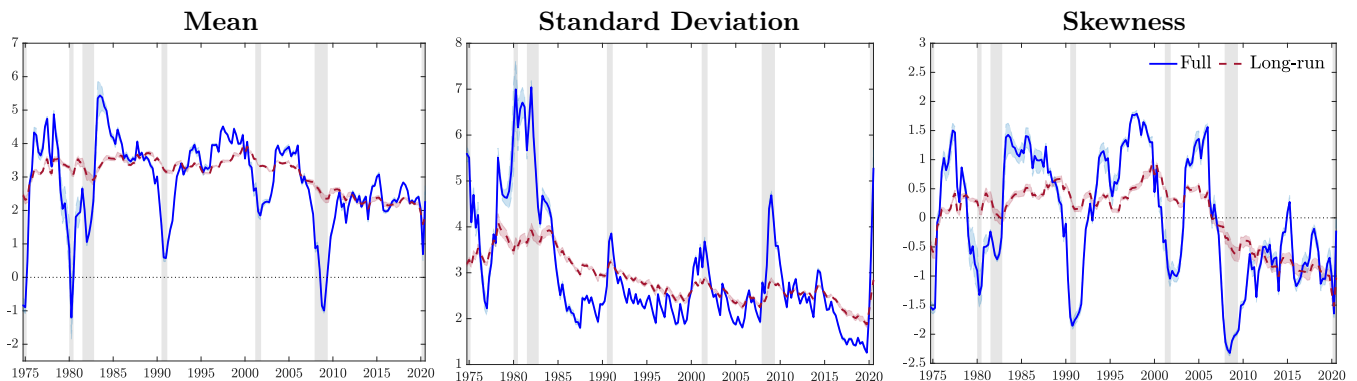


**Figure I1:** Time-varying moments

*Note:* The panels show the time-varying mean, volatility and skewness (in blue), along with the respective long-run components (in red), produced by the *sparse* model. shadings correspond to 90% credible intervals. Shaded bands represent NBER recessions.

[Figure I1](#) reports the (in-sample) estimates of the mean, volatility and skewness of the conditional distribution of GDP growth, along with the relative long-run components. Overall, the model reproduces



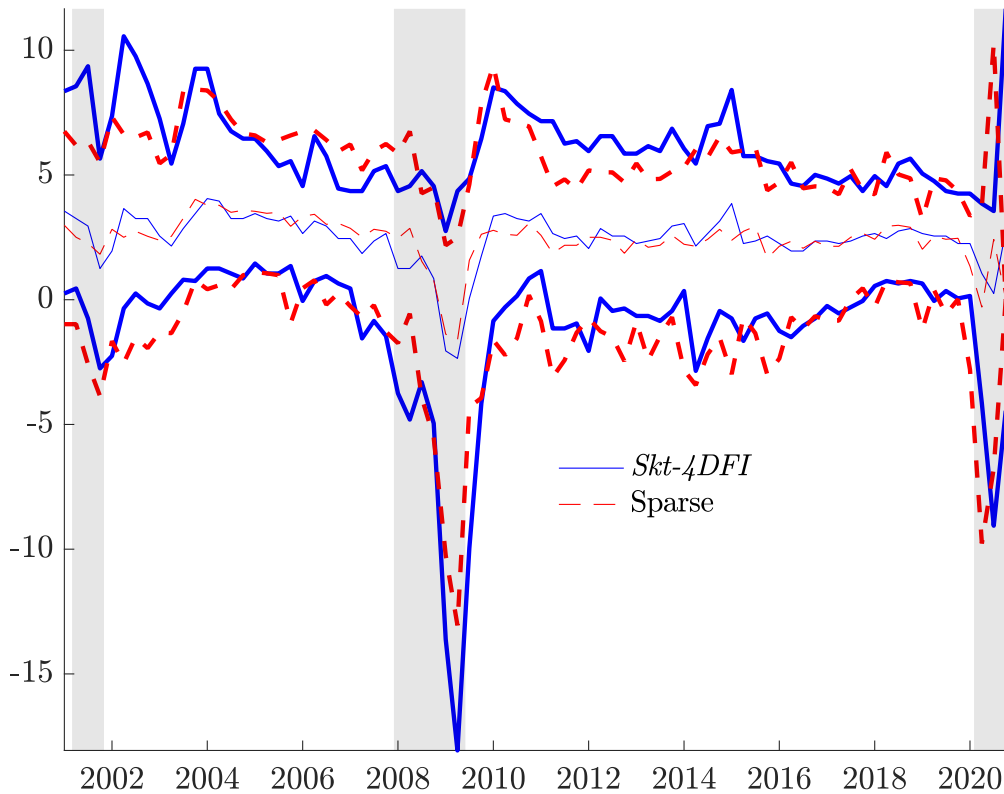


**Figure I2:** Time-varying densities for baseline and sparse models

*Note:* The plots report the time series of the 5<sup>th</sup>, 50<sup>th</sup> and 95<sup>th</sup> quantiles of the one-quarter-ahead predictive densities for our baseline model *Skt -4DFI* (blue) and the sparse mode *Skt -sparse* (red).

the same features discussed in Section 4. In particular, the skewness presents an evident downward trend and displays strong procyclicality. The long-run component of the volatility displays a reduction in the second since the mid 80s, whereas the overall volatility is markedly countercyclical. Compared to the estimates from the baseline *Skt -4DFI* model, reported in Figure 2, the estimated moments from the *sparse* model are smoother and sharper. These differences reflect the fact that the sparsification step drastically reduces the number of predictors used for the estimation, whereas the Horseshoe prior severely shrink the coefficients of the variables kept into the model. Noticeably, the *sparse* model estimates a pronounced long-run downside risk to US economic growth in the aftermath of the Global Financial Crisis.

Figure I2 compares the out-of-sample predictions of the competing models. As for the in-sample results, the (one-quarter ahead) conditional predictive distributions of the *Skt -4DFI* and the *sparse* models do not show major differences, and the *sparse* model produces smoother variations in the predictive densities. Interestingly, around the GFC, the baseline model is more timely in picking up an increase in downside risk with respect to the *sparse* model. On the other hand, the baseline model fails to timely capture the large fall in GDP in 2020Q2, whereas the *sparse* model is quick to pick up the increase in downside risk at the beginning of the sample and the quick turnaround in the last quarter of the sample.

Figure I3 reports the cumulative differences in the forecast loss for the four predictive accuracy measures, focusing on the one-quarter ahead forecast. We compute the relative measures as the difference between the *sparse* metrics and *Skt -4DFI*'s; therefore, downward (upward) trends in the MSFE, CRPS and wQS (logScore) imply a superior performance of the *sparse* over the *Skt -4DFI* model. The *sparse* model almost always improve upon our baseline model. Major improvements occur during recessive periods, with the

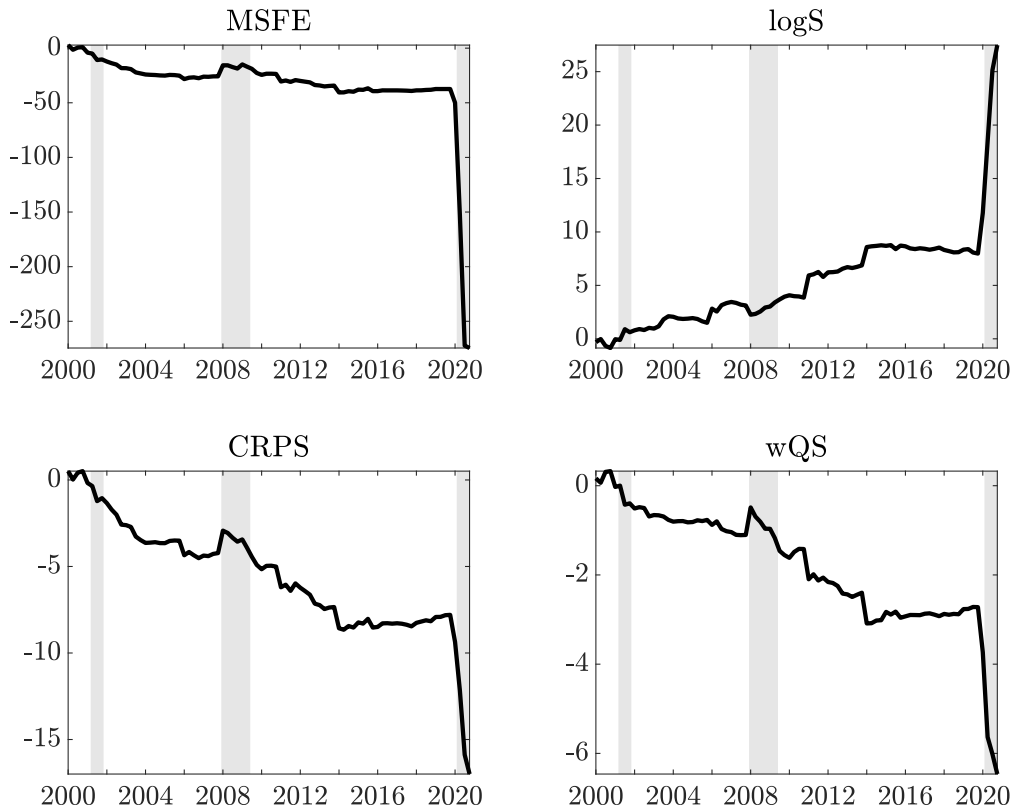


**Figure I3:** Forecast scoring functions

*Note:* The plots report the cumulative sum of the relative forecast loss functions, computed as the difference between the sparse model and baseline model,  $Skt - 4DFI$ .

exception of the of first quarters of the 2007 recession where the delay in picking up an increase in downside risk of the *sparse* model is associated with larger losses. Noticeably, the ability of the *sparse* model to pick up the turn in the events in 2020 is associated with massive gains in the forecast performance (based on all metrics considered).

Last, we evaluate the importance of allowing for a *sparse* specification when using a large number of predictions. [Table I1](#) compares a *sparse* model and a *dense* specification, where the sparsity step is omitted. The results highlight the importance of the sparsity: the *sparse* model is associated with very large (and always significant) gains in forecasting, for all the metrics considered, for one-quarter and one-year ahead forecasts.

**Table I1:** *Sparse* against *dense* forecast performance

|                 | <i>One-quarter ahead</i> |                          |                         |                         | <i>One-year ahead</i>   |                          |                         |                         |
|-----------------|--------------------------|--------------------------|-------------------------|-------------------------|-------------------------|--------------------------|-------------------------|-------------------------|
|                 | MSFE                     | logS                     | CRPS                    | wQS                     | MSFE                    | logS                     | CRPS                    | wQS                     |
| <i>Full</i>     | <b>1.376</b><br>(0.000)  | <b>-1.070</b><br>(0.000) | <b>1.544</b><br>(0.000) | <b>1.574</b><br>(0.000) | <b>2.088</b><br>(0.000) | <b>-1.911</b><br>(0.000) | <b>1.838</b><br>(0.000) | <b>2.251</b><br>(0.000) |
| <i>Pre-2020</i> | <b>2.797</b><br>(0.000)  | <b>-1.094</b><br>(0.000) | <b>1.880</b><br>(0.000) | <b>1.925</b><br>(0.000) | <b>5.838</b><br>(0.000) | <b>-1.952</b><br>(0.000) | <b>2.071</b><br>(0.000) | <b>2.764</b><br>(0.000) |
| <i>Rec.</i>     | <b>1.287</b><br>(0.000)  | <b>-1.576</b><br>(0.000) | <b>1.428</b><br>(0.000) | <b>1.512</b><br>(0.000) | <b>3.687</b><br>(0.000) | <b>-1.386</b><br>(0.010) | <b>1.342</b><br>(0.001) | <b>1.536</b><br>(0.001) |

*Note:* The table reports the average forecast metrics from the *dense* model relative to the *sparse* specification. We use ratios for the MSFE, CRSP and wQS, and differences for the logS. Ratios smaller than 1, and positive values of the log-score differences indicate that the *dense* model performs better than the *sparse* one. The p-values for [Diebold and Mariano \(1995\)](#) tests, augmented with the small sample correction of [Harvey et al., 1997](#), are in parentheses. Values in **bold** are significant at the 10% level.

# J Additional material

## J.1 Additional tables

**Table J1:** Static parameters

|                   | $\mu_y$                | $\mu_\sigma$           | $\phi_{y,1}$           | $\phi_{y,2}$           | $\phi_{\mu,1}$         | $\phi_{\mu,2}$            | $\phi_\gamma$          | $\phi_\delta$          |
|-------------------|------------------------|------------------------|------------------------|------------------------|------------------------|---------------------------|------------------------|------------------------|
| <i>AR</i> (2)     | 2.150<br>[2.024,2.282] | 0.015<br>[0.013,0.017] | 0.386<br>[0.330,0.440] | 0.066<br>[0.019,0.120] |                        |                           | 0.977<br>[0.971,0.983] |                        |
| <i>Sk</i> t -No-X |                        |                        |                        |                        | 1.027<br>[0.914,1.155] | -0.227<br>[-0.366,-0.096] | 0.728<br>[0.641,0.811] | 0.770<br>[0.689,0.834] |
| <i>Sk</i> t -NFCI |                        |                        |                        |                        | 0.960<br>[0.846,1.085] | -0.127<br>[-0.257,0.001]  | 0.662<br>[0.571,0.744] | 0.719<br>[0.612,0.806] |
| <i>Sk</i> t -4DFI |                        |                        |                        |                        | 0.885<br>[0.840,0.927] | -0.032<br>[-0.079,0.011]  | 0.588<br>[0.521,0.654] | 0.621<br>[0.565,0.684] |
|                   | $\varsigma_\mu$        | $\kappa_\mu$           | $\varsigma_\gamma$     | $\kappa_\gamma$        | $\varsigma_\delta$     | $\kappa_\delta$           | $\chi$                 | $\eta$                 |
| <i>AR</i> (2)     |                        |                        |                        | 0.108<br>[0.099,0.121] |                        |                           | 0.267<br>[0.166,0.362] |                        |
| <i>Sk</i> t -No-X | 0.025<br>[0.019,0.034] | 0.081<br>[0.058,0.111] | 0.027<br>[0.020,0.039] | 0.148<br>[0.110,0.198] | 0.027<br>[0.021,0.037] | 0.091<br>[0.072,0.118]    | 0.283<br>[0.147,0.395] | 0.301<br>[0.273,0.321] |
| <i>Sk</i> t -NFCI | 0.025<br>[0.018,0.035] | 0.089<br>[0.063,0.131] | 0.028<br>[0.020,0.040] | 0.117<br>[0.084,0.158] | 0.026<br>[0.020,0.032] | 0.064<br>[0.051,0.080]    | 0.229<br>[0.109,0.372] | 0.300<br>[0.269,0.321] |
| <i>Sk</i> t -4DFI | 0.032<br>[0.021,0.046] | 0.083<br>[0.063,0.111] | 0.019<br>[0.015,0.024] | 0.110<br>[0.086,0.136] | 0.029<br>[0.023,0.036] | 0.070<br>[0.055,0.091]    | 0.031<br>[0.014,0.064] | 0.312<br>[0.294,0.327] |

*Note:* The table reports the estimates of the static parameters for all the models: the Gaussian *AR*(2), the *Sk*t no-X without predictors, with lags of the NFCI (*Sk*t NFCI) and with lags of the subcomponents of the index (*Sk*t 4DFI). Credible intervals at the 68% level are in brackets.

**Table J2:** Predictor loadings

|              |              | <i>Sk</i> t<br>NFCI       | <i>Sk</i> t<br>4DFI      |                           |                          |                           |
|--------------|--------------|---------------------------|--------------------------|---------------------------|--------------------------|---------------------------|
|              |              | NFCI                      | Leverage                 | NF Leverage               | Risk                     | Credit                    |
| <i>t</i>     | $\mu_t$      | 0.001<br>[-0.006,0.007]   | -0.001<br>[-0.008,0.005] | -0.000<br>[-0.006,0.005]  | 0.000<br>[-0.005,0.006]  | 0.003<br>[-0.005,0.010]   |
|              | $\sigma_t^2$ | 0.118<br>[0.041,0.178]    | 0.051<br>[-0.001,0.098]  | 0.013<br>[-0.047,0.074]   | -0.002<br>[-0.060,0.068] | 0.126<br>[0.074,0.178]    |
|              | $\varrho_t$  | 0.260<br>[0.198,0.324]    | 0.079<br>[0.037,0.125]   | 0.141<br>[0.087,0.195]    | 0.040<br>[-0.016,0.100]  | 0.206<br>[0.163,0.249]    |
| <i>t</i> - 1 | $\mu_t$      | 0.003<br>[-0.004,0.010]   | -0.002<br>[-0.008,0.003] | 0.002<br>[-0.003,0.007]   | -0.000<br>[-0.006,0.005] | 0.002<br>[-0.005,0.008]   |
|              | $\sigma_t^2$ | -0.028<br>[-0.103,0.043]  | -0.040<br>[-0.088,0.003] | -0.024<br>[-0.088,0.033]  | 0.106<br>[0.050,0.160]   | -0.116<br>[-0.163,-0.068] |
|              | $\varrho_t$  | -0.209<br>[-0.278,-0.137] | -0.035<br>[-0.090,0.021] | -0.081<br>[-0.147,-0.028] | -0.054<br>[-0.110,0.006] | -0.163<br>[-0.206,-0.114] |

*Note:* 90% credible intervals are reported in brackets.

## J.2 Additional plots

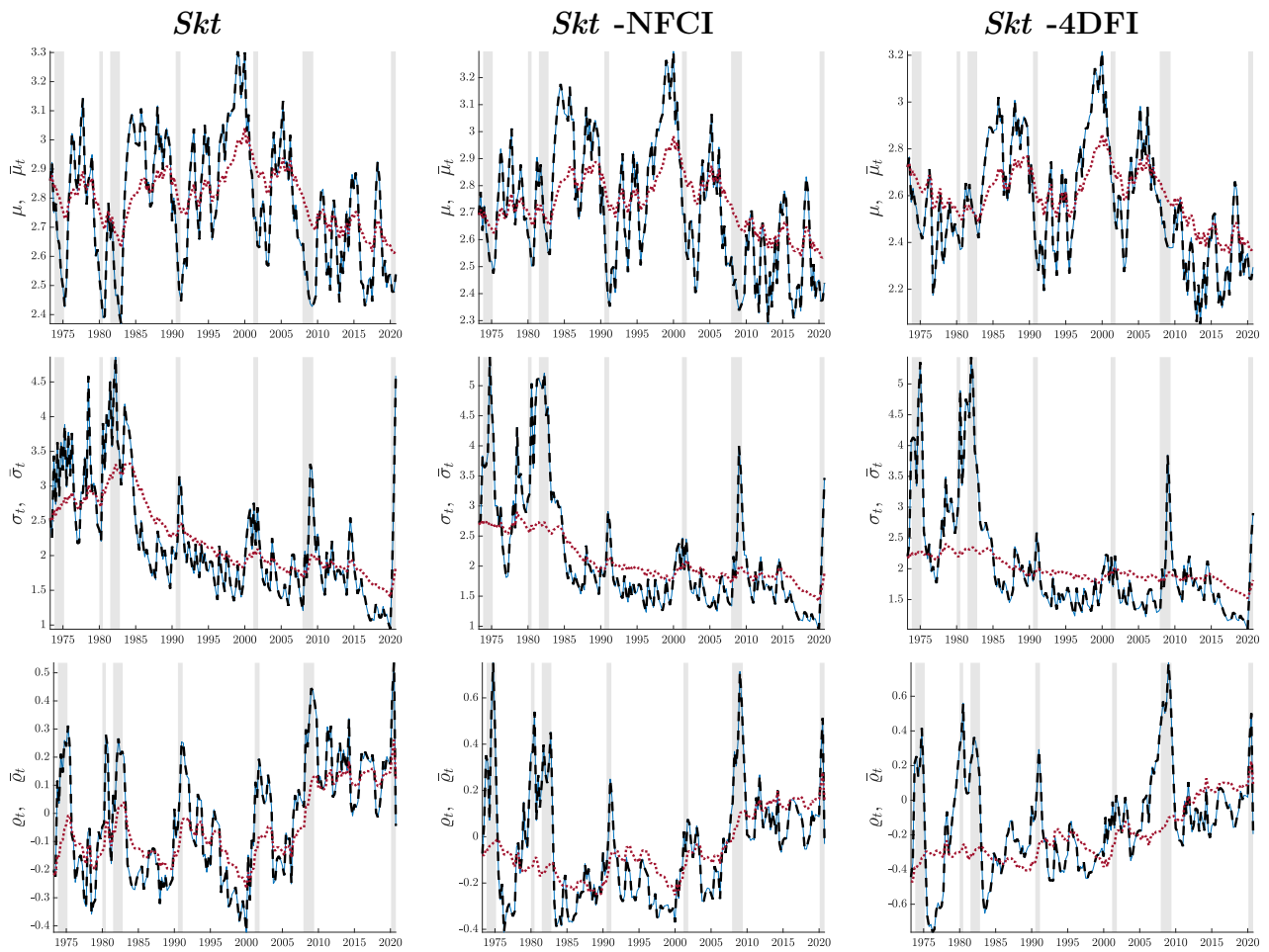


**Figure J1:** Time-varying parameters

*Note:* The plots illustrate the estimated time-varying parameters (black) for the three model specifications. Permanent components are reported in red (right scale). Shaded bands represent NBER recessions.

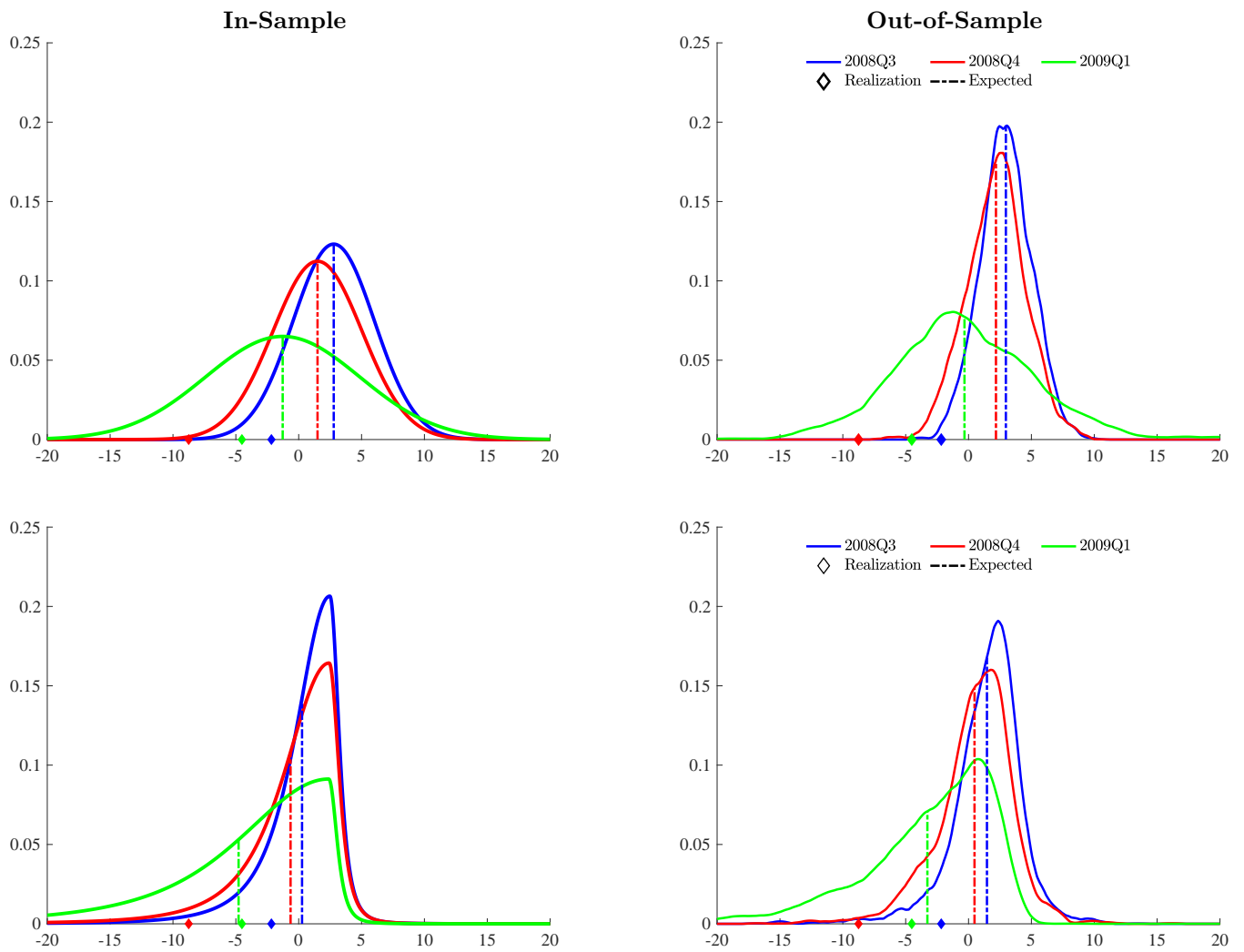


**Figure J2:** Predictive densities around the GFC

*Note:* The panels show the predictive densities for 2008Q3 (blue), 2008Q4 (red) and 2009Q1 (green) from the Gaussian AR(2) model (top panels) and from the *Skt*-4DFI specification (bottom panel). In-sample densities are in the right panels, out-of-sample densities are in the left ones. Realizations of economic growth are denoted by diamonds, dot-dashed lines report expected values.

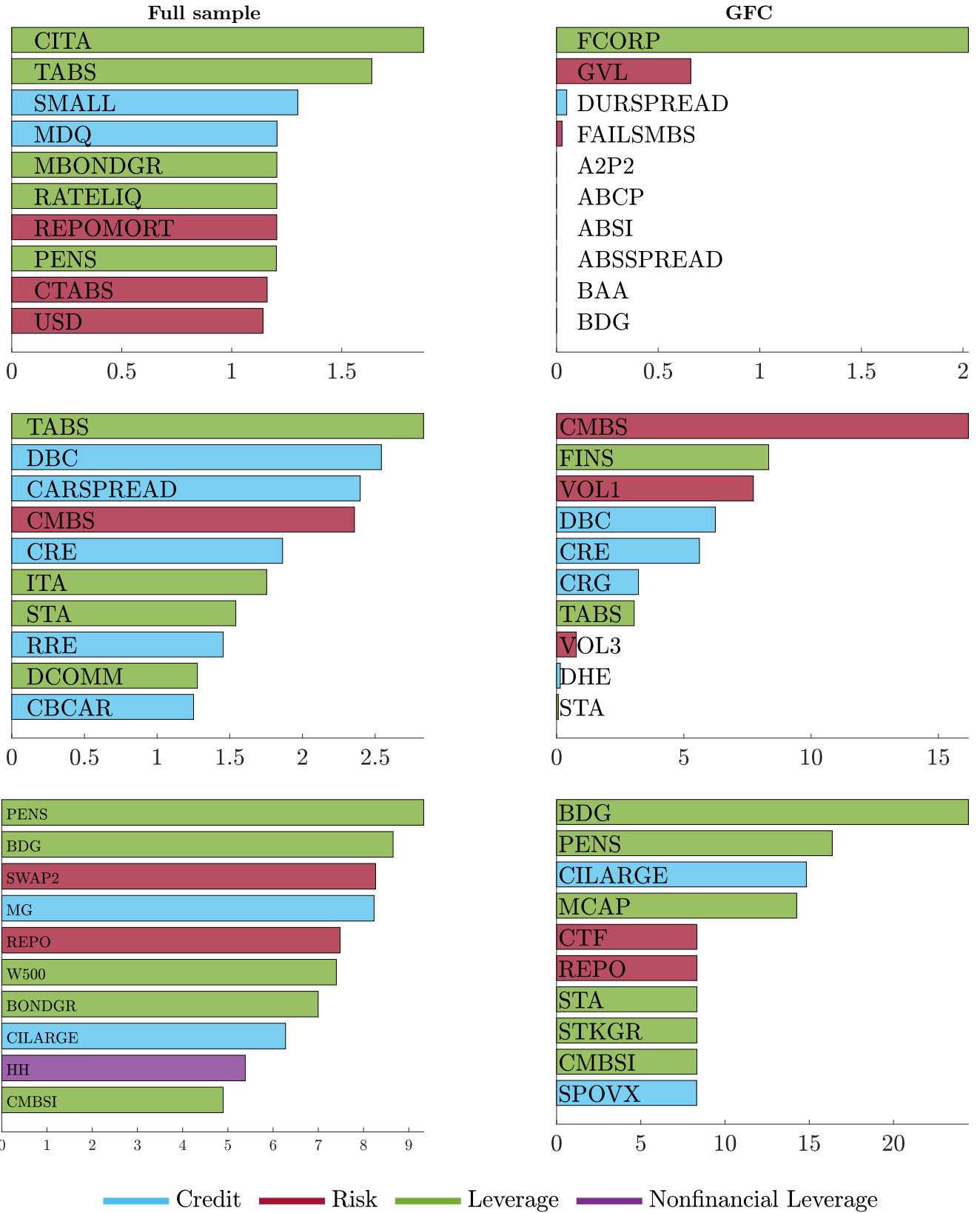


**Figure J3:** Top 10 predictors

*Note:* The bar plots report the top 10 predictors for the location, scale and shape parameters, over the forecasting sample and during the quarters of the Great Recession of 2008. The *x-axis* reports average posterior probability of inclusion, expressed in percentage terms.

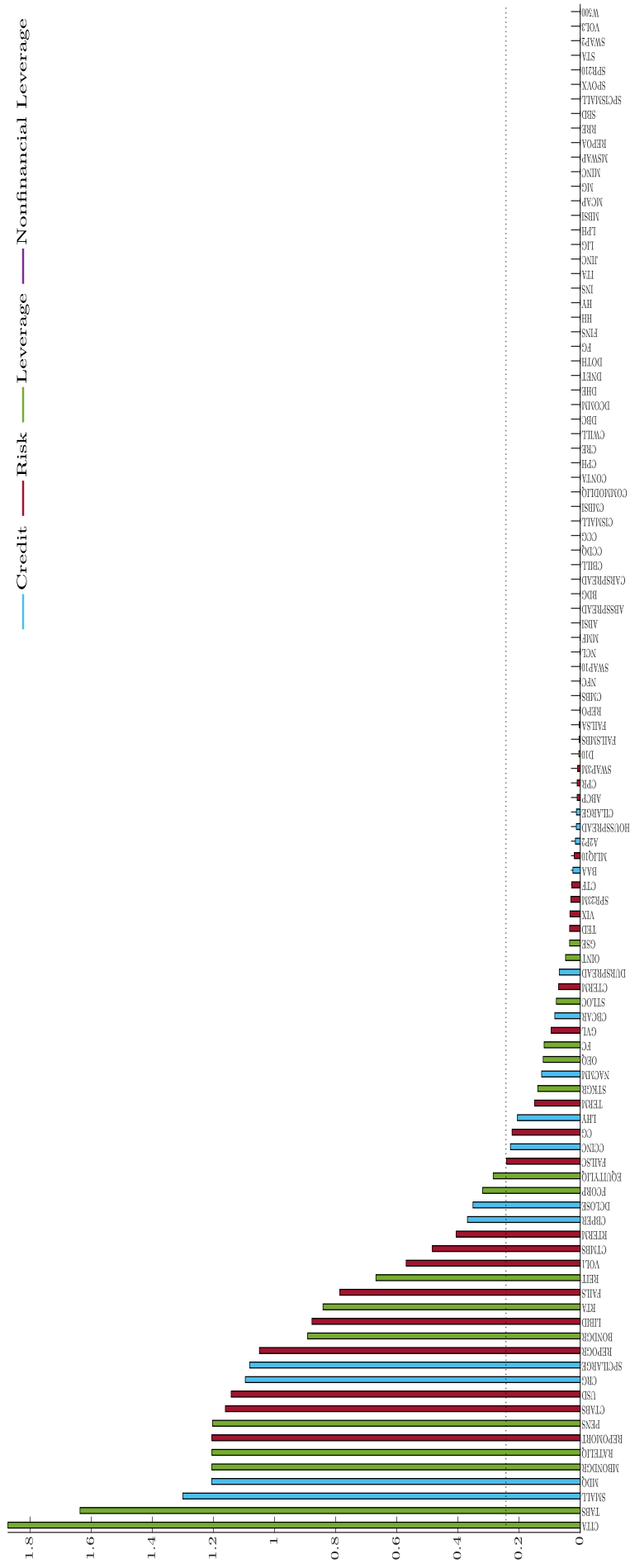


Figure J4: Predictors - Location

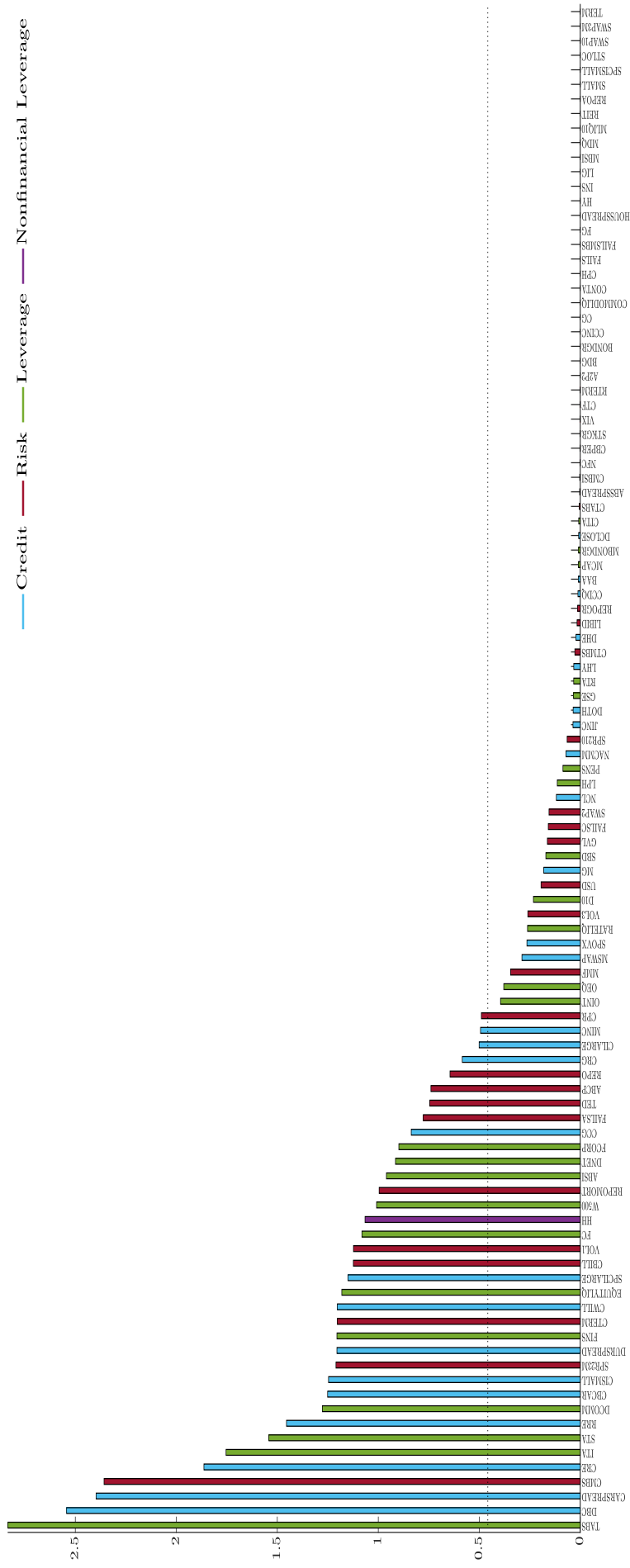


Figure J5: Predictors - Scale



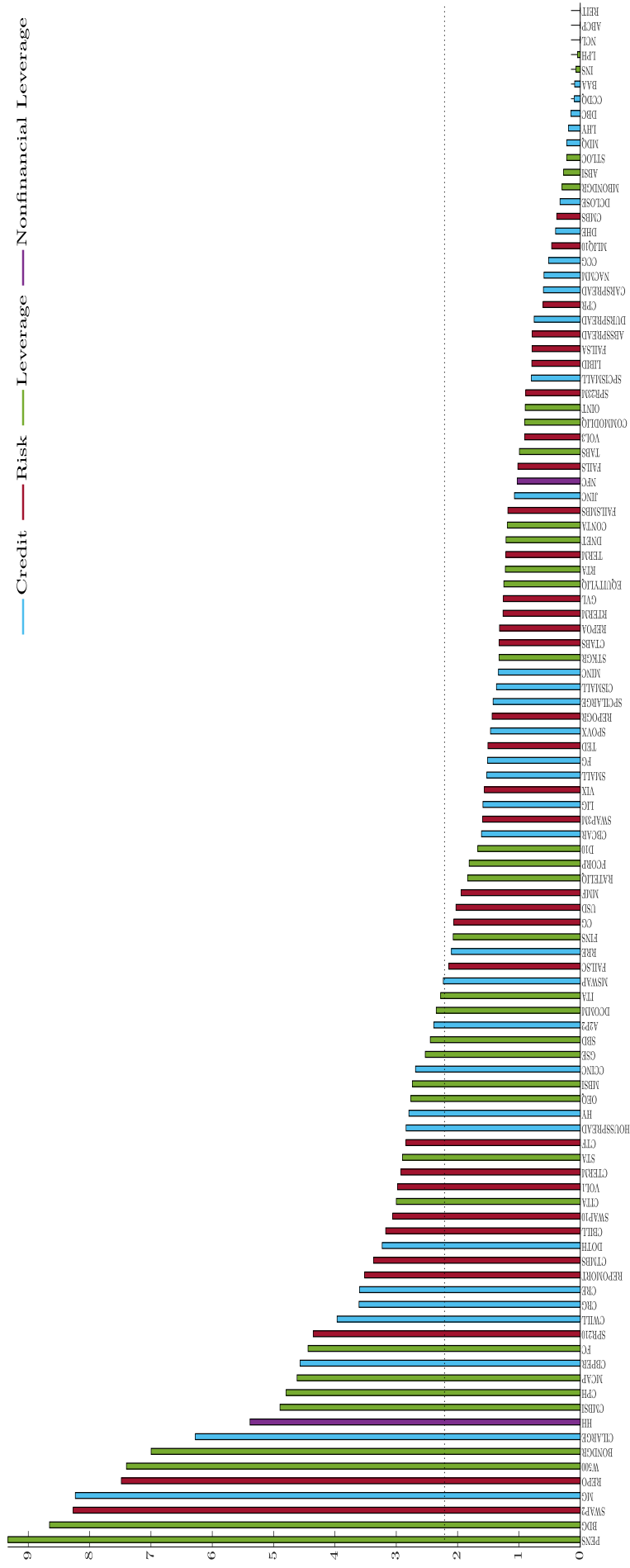


Figure J6: Predictors - Asymmetry

## References

- ADRIAN, T., N. BOYARCHENKO, AND D. GIANNONE (2019): “Vulnerable Growth,” *American Economic Review*, 109, 1263–89.
- ADRIAN, T. AND H. S. SHIN (2010): “Liquidity and leverage,” *Journal of Financial Intermediation*, 19, 418–437.
- ARELLANO-VALLE, R. B., H. W. GÓMEZ, AND F. A. QUINTANA (2005): “Statistical inference for a general class of asymmetric distributions,” *Journal of Statistical Planning and Inference*, 128, 427–443.
- AZZALINI, A. AND A. CAPITANIO (2003): “Distributions generated by perturbation of symmetry with emphasis on a multivariate skew t-distribution,” *Journal of the Royal Statistical Society: Series B (Statistical Methodology)*, 65, 367–389.
- BAI, J. AND S. NG (2005): “Tests for skewness, kurtosis, and normality for time series data,” *Journal of Business & Economic Statistics*, 23, 49–60.
- BEKAERT, G. AND M. HOEROVA (2014): “The VIX, the variance premium and stock market volatility,” *Journal of Econometrics*, 183, 181–192.
- BLASQUES, F., S. J. KOOPMAN, AND A. LUCAS (2014): “Stationarity and ergodicity of univariate generalized autoregressive score processes,” *Electronic Journal of Statistics*, 8, 1088–1112.
- BRAVE, S. AND R. A. BUTTERS (2012): “Diagnosing the Financial System: Financial Conditions and Financial Stress,” *International Journal of Central Banking*, 8, 191–239.
- BRAVE, S. A. AND R. BUTTERS (2011): “Monitoring financial stability: A financial conditions index approach,” *Economic Perspectives*, 35, 22.
- CAIVANO, M. AND A. HARVEY (2014): “Time-series models with an EGB2 conditional distribution,” *Journal of Time Series Analysis*, 35, 558–571.
- CALVORI, F., D. CREAL, S. J. KOOPMAN, AND A. LUCAS (2017): “Testing for parameter instability across different modeling frameworks,” *Journal of Financial Econometrics*, 15, 223–246.
- CARVALHO, C. M., N. G. POLSON, AND J. G. SCOTT (2010): “The horseshoe estimator for sparse signals,” *Biometrika*, 97, 465–480.
- CHAN, J. C. AND A. L. GRANT (2016a): “Fast computation of the deviance information criterion for latent variable models,” *Computational Statistics & Data Analysis*, 100, 847–859.
- (2016b): “On the observed-data deviance information criterion for volatility modeling,” *Journal of Financial Econometrics*, 14, 772–802.
- COGLEY, T. AND T. J. SARGENT (2005): “Drifts and volatilities: monetary policies and outcomes in the post WWII US,” *Review of Economic Dynamics*, 8, 262–302.
- COWLES, M. K. AND B. P. CARLIN (1996): “Markov Chain Monte Carlo Convergence Diagnostics: A Comparative Review,” *Journal of the American Statistical Association*, 91, 883–904.
- CROUSHORE, D. (2006): “Forecasting with real-time macroeconomic data,” *Handbook of Economic Forecasting*, 1, 961–982.
- (2011): “Frontiers of real-time data analysis,” *Journal of Economic Literature*, 49, 72–100.
- CROUSHORE, D. AND T. STARK (2001): “A real-time data set for macroeconomists,” *Journal of Econometrics*, 105, 111–130.

- DELLE MONACHE, D. AND I. PETRELLA (2017): “Adaptive models and heavy tails with an application to inflation forecasting,” *International Journal of Forecasting*, 33, 482–501.
- DIEBOLD, F. X., T. A. GUNTHER, AND A. TAY (1998): “Evaluating density forecasts, with Applications to Financial Risk Management,” *International Economic Review*, 39, 863–883.
- DOAN, T., R. LITTERMAN, AND C. SIMS (1984): “Forecasting and conditional projection using realistic prior distributions,” *Econometric Reviews*, 3, 1–100.
- DREHMANN, M., C. E. BORIO, L. GAMBACORTA, G. JIMENEZ, AND C. TRUCHARTE (2010): “Counter-cyclical capital buffers: exploring options,” Working Paper 317, Bank for International Settlement.
- ESCANCIANO, J. C. AND I. N. LOBATO (2009): “An automatic portmanteau test for serial correlation,” *Journal of Econometrics*, 151, 140–149.
- FERNÁNDEZ, C. AND M. F. STEEL (1998): “On Bayesian modeling of fat tails and skewness,” *Journal of the American Statistical Association*, 93, 359–371.
- GAMERMAN, D. AND H. F. LOPES (2006): *Markov chain Monte Carlo: stochastic simulation for Bayesian inference*, CRC Press.
- GELMAN, A. (1995): “Inference and monitoring,” *Markov chain Monte Carlo in practice*, 131.
- GELMAN, A., J. B. CARLIN, H. S. STERN, AND D. B. RUBIN (1995): *Bayesian data analysis*, Chapman and Hall/CRC.
- GELMAN, A., G. O. ROBERTS, W. R. GILKS, ET AL. (1996): “Efficient Metropolis jumping rules,” *Bayesian Statistics*, 5, 42.
- GELMAN, A. AND D. B. RUBIN (1992): “Inference from iterative simulation using multiple sequences,” *Statistical science*, 7, 457–472.
- GEWEKE, J. F. (1992): “Evaluating the accuracy of sampling-based approaches to the calculation of posterior moments,” Staff report, Federal Reserve Bank of Minneapolis.
- GÓMEZ, H. W., F. J. TORRES, AND H. BOLFARINE (2007): “Large-sample inference for the epsilon-skew-t distribution,” *Communications in Statistics—Theory and Methods*, 36, 73–81.
- HAARIO, H., E. SAKSMAN, AND J. TAMMINEN (1999): “Adaptive proposal distribution for random walk Metropolis algorithm,” *Computational Statistics*, 14, 375–396.
- HARVEY, A. AND M. STREIBEL (1998): “Testing for a slowly changing level with special reference to stochastic volatility,” *Journal of Econometrics*, 87, 167–189.
- HARVEY, A. AND S. THIELE (2016): “Testing against changing correlation,” *Journal of Empirical Finance*, 38, 575–589.
- HARVEY, A. C. (2013): *Dynamic models for volatility and heavy tails: with applications to financial and economic time series*, vol. 52, Cambridge University Press.
- HASENZAGL, T., L. REICHLIN, AND G. RICCO (2020): “Financial Variables as Predictors of Real Growth Vulnerability,” Discussion Paper DP14322, CEPR.
- HORSWELL, R. AND S. LOONEY (1993): “Diagnostic limitations of skewness coefficients in assessing departures from univariate and multivariate normality: Diagnostic limitations of skewness coefficients,” *Communications in statistics-simulation and computation*, 22, 437–459.
- JENSEN, H., I. PETRELLA, S. H. RAVN, AND E. SANTORO (2020): “Leverage and Deepening Business-Cycle Skewness,” *American Economic Journal: Macroeconomics*, 12, 245–81.

- JOHNSON, N. L., S. KOTZ, AND N. BALAKRISHNAN (1995): *Continuous univariate distributions, volume 2*, vol. 289, John Wiley & Sons.
- JORDÀ, Ò., M. SCHULARICK, AND A. M. TAYLOR (2013): “When credit bites back,” *Journal of Money, Credit and Banking*, 45, 3–28.
- (2017): “Macrofinancial history and the new business cycle facts,” *NBER Macroeconomics Annual Report*, 31, 213–263.
- JUÁREZ, M. A. AND M. F. STEEL (2010): “Model-based clustering of non-Gaussian panel data based on skew-t distributions,” *Journal of Business & Economic Statistics*, 28, 52–66.
- KRISHNAMURTHY, A. AND T. MUIR (2017): “How credit cycles across a financial crisis,” Working Paper 23850, National Bureau of Economic Research.
- MAKALIC, E. AND D. F. SCHMIDT (2015): “A simple sampler for the horseshoe estimator,” *IEEE Signal Processing Letters*, 23, 179–182.
- MARONNA, R. A., R. D. MARTIN, V. J. YOHAI, AND M. SALIBIÁN-BARRERA (2019): *Robust statistics: theory and methods (with R)*, John Wiley & Sons.
- MCCONNELL, M. M. AND G. PEREZ-QUIROS (2000): “Output fluctuations in the United States: What has changed since the early 1980’s?” *American Economic Review*, 90, 1464–1476.
- MIAN, A. AND A. SUFI (2010): “Household Leverage and the Recession of 2007–09,” *IMF Economic Review*, 58, 74–117.
- NEWTON, M. A. AND A. E. RAFTERY (1994): “Approximate Bayesian inference with the weighted likelihood bootstrap,” *Journal of the Royal Statistical Society: Series B (Methodological)*, 56, 3–26.
- NYBLOM, J. (1989): “Testing for the constancy of parameters over time,” *Journal of the American Statistical Association*, 84, 223–230.
- PLAGBORG-MØLLER, M., L. REICHLIN, G. RICCO, AND T. HASENZAGL (2020): “When is Growth at Risk?” *Brookings Papers on Economic Activity*, 2020, 167–229.
- PLANAS, C., A. ROSSI, AND G. FIORENTINI (2008): “Bayesian Analysis of the Output Gap,” *Journal of Business & Economic Statistics*, 26, 18–32.
- PSARAKIS, S. AND J. PANARETOES (1990): “The folded t distribution,” *Communications in Statistics-Theory and Methods*, 19, 2717–2734.
- RAY, P. AND A. BHATTACHARYA (2018): “Signal Adaptive Variable Selector for the Horseshoe Prior,” *arXiv preprint arXiv:1810.09004*.
- ROBERT, C. P. AND G. CASELLA (2004): *Monte Carlo statistical methods*, vol. 2, Springer.
- SIMS, C. A. AND T. ZHA (1998): “Bayesian methods for dynamic multivariate models,” *International Economic Review*, 949–968.
- SPIEGELHALTER, D. J., N. G. BEST, B. P. CARLIN, AND A. VAN DER LINDE (2002): “Bayesian measures of model complexity and fit,” *Journal of the Royal Statistical Society: Series B (Statistical Methodology)*, 64, 583–639.
- STARK, T. AND D. CROUSHORE (2002): “Forecasting with a real-time data set for macroeconomists,” *Journal of Macroeconomics*, 24, 507–531.
- STOCK, J. H. AND M. W. WATSON (2002): “Has the business cycle changed and why?” *NBER Macroeconomics Annual Report*, 17, 159–218.
- ZOU, H. (2006): “The adaptive lasso and its oracle properties,” *Journal of the American Statistical Association*, 101, 1418–1429.